

2003

# Effects of Strand Geometry on Selected Properties of Long-Stand Structural Composite Lumber Made from Northeastern Hardwoods

Russell Edgar

Follow this and additional works at: <http://digitalcommons.library.umaine.edu/etd>



Part of the [Bioresource and Agricultural Engineering Commons](#), and the [Forest Sciences Commons](#)

---

## Recommended Citation

Edgar, Russell, "Effects of Strand Geometry on Selected Properties of Long-Stand Structural Composite Lumber Made from Northeastern Hardwoods" (2003). *Electronic Theses and Dissertations*. 459.  
<http://digitalcommons.library.umaine.edu/etd/459>

This Open-Access Thesis is brought to you for free and open access by DigitalCommons@UMaine. It has been accepted for inclusion in Electronic Theses and Dissertations by an authorized administrator of DigitalCommons@UMaine.

**EFFECTS OF STRAND GEOMETRY ON SELECTED PROPERTIES OF  
LONG-STRAND STRUCTURAL COMPOSITE LUMBER  
MADE FROM NORTHEASTERN HARDWOODS**

By

Russell A. Edgar

B.A. University of Massachusetts Amherst, 1992

B.S. University of Massachusetts Amherst, 2002

A THESIS

Submitted in Partial Fulfillment of the

Requirements for the Degree of

Master of Science

(in Forestry)

The Graduate School

The University of Maine

December, 2003

Advisory Committee:

Stephen M. Shaler, Professor of Wood Science & Technology, Advisor

Habib J. Dagher, Professor of Civil Engineering

Douglas J. Gardner, Professor of Wood Science & Technology

© 2003 Russell A. Edgar  
All Rights Reserved

## **LIBRARY RIGHTS STATEMENT**

In presenting this thesis in partial fulfillment of the requirements for an advanced degree at The University of Maine, I agree that the Library shall make it freely available for inspection. I further agree that permission for “fair use” copying of this thesis for scholarly purposes may be granted by the Librarian. It is understood that any copying or publication of this thesis for financial gain shall not be allowed without my written permission.

Signature:

Date:

**EFFECTS OF STRAND GEOMETRY ON SELECTED PROPERTIES OF  
LONG-STRAND STRUCTURAL COMPOSITE LUMBER  
MADE FROM NORTHEASTERN HARDWOODS**

By Russell A. Edgar

Thesis Advisor: Dr. Stephen M. Shaler

An Abstract of the Thesis Presented  
in Partial Fulfillment of the Requirements for the  
Degree of Master of Science  
(in Forestry)  
December, 2003

Structural composite lumber (SCL) products often possess significantly higher design values than the top grades of solid lumber, making it a popular choice for both residential and commercial applications. The enhanced mechanical properties of SCL are mainly due to defect randomization and densification of the wood fiber, both largely functions of the size, shape and composition (species) of the wood element. Traditionally, SCL manufacturers have used thin, rectangular elements produced from either moderate density softwoods or low density hardwoods. Higher density hardwood species have been avoided, as they require higher pressures to adequately densify and consolidate the wood furnish. These higher pressures can lead to increased manufacturing costs, damage to the wood fiber and/or a product that is too dense, making it heavy and unreceptive to common mechanical fastening techniques.

In the northeastern United States high density, diffuse-porous hardwoods (such as maple, beech and birch) are abundant. Use of these species as primary furnish for a SCL product may allow for a competitive advantage in terms of resource cost against products that rely on veneer grade logs. Proximity to this abundant and relatively inexpensive resource may facilitate entry of SCL production facilities in the northeastern United States, where currently none exist. However, modifications to current strand sizes, geometries or production techniques will likely be required to allow for use of these species.

A new SCL product concept has been invented allowing for use of these high density hardwoods. The product, referred to as long-strand structural composite lumber (LSSCL), uses strands of significantly larger cross sectional areas and volumes than existing SCL products. In spite of the large strand size, satisfactory consolidation is achieved without excessive densification of the wood fiber through use of a symmetrical strand geometric cross-section. LSSCL density is similar to that of existing SCL products, but is due mainly to the inherent density of the species, rather than through densification.

An experiment was designed and conducted producing LSSCL from both large (7/16") and small (1/4") strands, of both square and triangular geometric cross sections. Testing results indicate that the large, triangular strands produce LSSCL beams with projected design values of: Modulus of elasticity ( $MOE_{app}$ ) – 1,750,000 psi; Allowable bending stress ( $F_b$ ) – 2750 psi; Allowable shear stress ( $F_v$ ) – 260 psi. Several modifications are recommended which may lead to improvement of these values, likely allowing for competition against existing SCL products.

## DEDICATION

For Cynthia and Jonah

*The king lost his way in a jungle and was required to spend the night in a tree.*

*The next day he told some fellow traveler that the total number  
of leaves on the tree were “so many” (an actual number was stated).*

*On being challenged as to whether he counted all the leaves he replied,*

*“No, but I counted the leaves on a few branches of the tree  
and I know the science of die throwing”.*

From the ancient Indian epic Mahabharat (Nala-Damayanti Akhyân)

*Facts, or what a man believes to be facts, are delightful...*

*Get your facts first, and then you can distort them as much as you please.*

Mark Twain

Quotes from Misused Statistics, Straight Talk for Twisted Numbers (Jaffe and Spirer, 1987)

## ACKNOWLEDGMENTS

Funding for this project was provided by the United States Department of Agriculture (USDA) Wood Utilization Research (WUR) program, and the Federal Highway Administration (FHWA).

In addition to these agencies, much appreciation is extended to the following people and companies, all of whom provided significant support over the past two years.

Alan Marra, Professor Emeritus, University of Massachusetts, Amherst, MA.

Borden Chemical Inc.

Calley & Courier, Patten, ME.

Chuck Simpson, Forester, University of Maine

Dana Hodgkin, Progress Engineering, Manchester, ME.

Douglas Gardner, Professor of Wood Science and Technology, University of Maine

Greg Porter, Professor, University of Maine.

Jon Fiutak, Engineered Materials of Maine, Bangor, ME.

My folks, in-laws, entire family and friends

Nyle Dry Kiln Corp., Brewer, ME.

Scott McEntire, Borden Chemical Inc.

Staff and friends at the Advanced Engineered Wood Composite Center, University of Maine

Student workers: Stig Callahan, Nick Walters, Trapper Clark

Thermex-Thermatron Inc., Louisville, KY.

Vernon Darling, Lab Operations Manager, AEW, University of Maine.

William Halteman, Professor and Statistician, University of Maine.

Special thanks are given to my advisor, Dr. Stephen Shaler, as well as the Director of the Advanced Engineered Wood Composite (AEWC) Center at the University of Maine, Dr. Habib Dagher, both of whom have provided tremendous support over the past two years.

## TABLE OF CONTENTS

DEDICATION .....	iii
ACKNOWLEDGMENTS.....	iv
LIST OF TABLES .....	x
LIST OF FIGURES.....	xiv
Chapter	
<b>1. INTRODUCTION.....</b>	<b>1</b>
1.1 Introduction.....	1
1.2 Reason for Research .....	2
1.3 Objectives .....	3
<b>2. BACKGROUND AND LITERATURE REVIEW .....</b>	<b>5</b>
2.1 Background.....	5
2.2 Existing SCL Products.....	6
2.2.1 Laminated Veneer Lumber (LVL).....	6
2.2.2 Parallel Strand Lumber (PSL).....	7
2.2.3 Laminated Strand Lumber (LSL).....	8
2.2.4 Scrimber.....	8
2.3 Mechanical Properties of SCL .....	10
2.4 SCL Furnish.....	12
2.4.1 Species Used in SCL Production .....	12
2.4.1.1 Current SCL Species Used in SCL Production.....	12
2.4.1.2 Potential Species for LSSCL Production.....	13
2.4.2 Strand Size .....	15
2.4.3 Strand Geometry .....	18
2.5 SCL Pressing .....	19
2.5.1 Electrical Resistance Heating .....	19
2.5.2 Radio Frequency Heating .....	21

<b>3. EXPERIMENTAL DESIGN AND RATIONALE .....</b>	<b>24</b>
3.1 Selection of Variables .....	24
3.1.1 Strand Geometry .....	25
3.1.2 Strand Size .....	27
3.1.3 Billet Lay-up .....	27
3.2 Hypotheses .....	30
3.3 Experimental Design .....	31
3.4 Size and Quantity of Specimens .....	33
3.4.1 Billet Size .....	33
3.4.2 Beam Size .....	33
3.4.3 Sample Size .....	33
3.5 Testing Protocol .....	34
3.5.1 Shear Strength Determination .....	35
3.5.2 Orientation of Testing Specimens .....	36
<b>4. MATERIALS AND METHODS .....</b>	<b>37</b>
4.1 Production .....	37
4.1.1 Log Harvesting and Bucking .....	37
4.1.2 Primary Log Breakdown .....	38
4.1.3 Grading .....	38
4.1.4 Strand Production .....	39
4.1.5 Relative Specific Gravity of Strands .....	40
4.1.6 Strand Drying and Conditioning .....	41
4.1.7 Resin Type and Application .....	42
4.1.8 Billet Lay-up .....	45
4.1.9 Pressing .....	50
4.1.9.1 Press Cycle .....	50
4.1.9.1.1 Press Close (Steps 1-3) .....	50

4.1.9.1.2	Press Hold/Cure (Step 4).....	51
4.1.9.1.3	Decompression (Steps 5-10) .....	51
4.1.9.2	Pressure .....	52
4.1.9.3	Radio Frequency .....	53
4.1.10	Dressing and Conditioning.....	54
4.1.11	Production Data Collection .....	56
4.2	Testing Methodology.....	57
4.2.1	Billet Breakdown and Test Specimen Preparation .....	57
4.2.2	Flexural Testing .....	58
4.2.3	Shear Testing .....	63
4.2.3.1	Shear Modulus.....	63
4.2.3.2	Shear Strength .....	64
4.2.3.2.1	Shear Blocks.....	64
4.2.3.2.2	Short-Span Shear Beams .....	65
4.2.4	Volumetric Shrinkage, Void Volume and Adhesive Joint Integrity .....	67
4.2.4.1	Volumetric Shrinkage.....	68
4.2.4.2	Void Volume .....	69
4.2.4.3	Adhesive Joint Integrity.....	70
4.2.5	Property Adjustments .....	70
4.2.5.1	Adjustments for Moisture Content .....	70
4.2.5.2	Adjustments for Density .....	71
4.2.6	Testing Data Collection .....	72
4.3.	Statistical Methodology.....	72
4.3.1	Main Factors and Levels.....	73
4.3.2	Hypothesis Testing .....	73
4.3.3	Analysis of Variance.....	74
4.3.4	Types of Error Due to Subsampling .....	75
4.3.5	Sample Statistical Analyses .....	76

4.3.6	Meeting the Assumptions of ANOVA.....	79
4.3.7	Weighted Least Squares Transformation.....	81
5.	<b>RESULTS AND DISCUSSION.....</b>	<b>84</b>
5.1	Preliminary Test Results .....	84
5.2	Statistical Analysis .....	85
5.3	Physical Properties .....	87
5.3.1	Density .....	87
5.3.1.1	Specific Gravity of Strands .....	87
5.3.1.2	Billet Density .....	89
5.3.1.3	Beam Density.....	91
5.3.1.4	Density Profile Among Beams Within Billets .....	93
5.3.2	Moisture Content.....	94
5.3.2.1	Strand Moisture Content .....	94
5.3.2.2	Billet Moisture Content.....	96
5.3.2.3	Beam Moisture Content .....	97
5.3.3	Void Volume.....	100
5.3.4	Volumetric Shrinkage .....	102
5.3.5	Adhesive Joint Integrity .....	104
5.4	Mechanical Properties .....	106
5.4.1	Modulus of Elasticity .....	106
5.4.1.1	Apparent Modulus of Elasticity ( $MOE_{app}$ ) .....	106
5.4.1.2	True Modulus of Elasticity ( $MOE_{true}$ ) .....	110
5.4.2	Shear Modulus (G).....	112
5.4.2.1	Mathematical Calculation of Shear Modulus .....	113
5.4.2.2	Empirical Determination of Shear Modulus .....	114
5.4.3	E/G Ratio .....	115
5.4.4	Modulus of Rupture .....	117

5.4.5	Maximum Shear Strength .....	121
5.4.5.1	Shear Blocks .....	121
5.4.5.2	Short-span Beams .....	124
5.4.6	Probability Results Summary for Factorial Analyses .....	127
5.5	Two-way Statistical Analyses - Analysis by Lap Type.....	128
5.5.1	Projected Design Values of the Non-lapped Treatments.....	129
5.5.2	Projected Design Values of the Lapped Treatments .....	129
<b>5.</b>	<b>CONCLUSIONS AND RECOMMENDATIONS.....</b>	<b>130</b>
6.1	Conclusions.....	130
6.1.1	Review of Hypotheses.....	130
6.1.2	Best Performing Treatment .....	131
6.1.2.1	Square vs. Triangular Strand Geometry .....	131
6.1.2.2	Large vs. Small Triangular Strand Size .....	132
6.2	Recommendations .....	132
6.2.1	Recommended Strand Size and Geometry .....	132
6.2.2	Recommendations for Future Research .....	136
6.3	Review of Objectives .....	138
	REFERENCES.....	139
	APPENDICES.....	143
	APPENDIX A Production and Testing Data.....	144
	APPENDIX B Coding Used to Conduct Statistical Analyses in SAS.....	153
	APPENDIX C Two-Way Analyses by Lap Type.....	155
	APPENDIX D Marketing concept for DeltaStrand Triangular Strand Lumber (TSL) .....	158
	BIOGRAPHY OF THE AUTHOR .....	159

## LIST OF TABLES

Table 2.1	A comparison of design values for various SCL and solid lumber products .....	10
Table 2.2	Selected properties of red maple.....	11
Table 2.3	Comparison of elastic properties of solid wood and SCL.....	11
Table 2.4	Standing volume and net annual change of Maine timber .....	13
Table 2.5	Average COV for selected properties of clear wood .....	16
Table 2.6	A comparison of important dielectric constants for curing of wood composites.....	22
Table 3.1	The 8 treatments of the experiment .....	32
Table 4.1	Percent of strands sampled for specific gravity by treatment .....	41
Table 4.2	Resin viscosity by treatment .....	43
Table 4.3	Open assembly time by treatment.....	44
Table 4.4	The press schedule used to produce the billets .....	50
Table 4.5	Maximum billet pressure by treatment .....	52
Table 4.6	A typical billet conditioning schedule .....	55
Table 4.7	Conditioning time constants .....	56
Table 4.8	Change of slope in the load-deflection curve and MOE with varying linear ranges .....	62
Table 4.9	Comparison of exponents used to adjust mechanical properties for specific gravity .....	72
Table 4.10	ANOVA for factorial treatment combination with subsamples.....	74
Table 4.11	Sample SAS statistical analysis for 2 x 2 x 2 full factorial .....	77
Table 4.12	Sample SAS one-way ANOVA table .....	78
Table 4.13	Sample SAS mean separation using Tukey's Test.....	79
Table 4.14	Meeting the assumptions of ANOVA.....	80
Table 4.15	Factorial analysis using weighted least squares .....	82
Table 4.16	Difference in significance between OLS and WLS .....	83
Table 5.1	Properties analyzed statistically including design and least square method used.....	85
Table 5.2	Summary data for strand specific gravity by treatment .....	87
Table 5.3	One-way analysis of variance results for strand specific gravity .....	88

Table 5.4	Mean separation for strand specific gravity by treatment.....	88
Table 5.5	Summary data for out-of-press billet density.....	89
Table 5.6	One-way analysis of variance results for billet density .....	90
Table 5.7	Mean separation for billet density by treatment.....	90
Table 5.8	Summary data for beam density .....	91
Table 5.9	Three-way analysis of variance results for beam density .....	92
Table 5.10	Mean separation for beam density by treatment .....	93
Table 5.11	Mean separation for beam density by beam number .....	93
Table 5.12	Summary data for moisture content of strands at time of lay-up .....	95
Table 5.13	One-way analysis of variance results for strand moisture content.....	95
Table 5.14	Summary data for out-of-press billet moisture content.....	96
Table 5.15	One-way analysis of variance results for billet moisture content .....	96
Table 5.16	Mean separation for billet moisture content .....	97
Table 5.17	Conditioning time and calculated moisture content of billets by treatment.....	97
Table 5.18	Summary data for beam moisture content .....	98
Table 5.19	Three-way analysis of variance results for beam moisture content .....	99
Table 5.20	Mean separation for beam moisture content by treatment .....	99
Table 5.21	Summary data for moisture content of shear samples .....	100
Table 5.22	Summary data for void volume .....	100
Table 5.23	One-way analysis of variance results for void volume .....	101
Table 5.24	Mean separation for void volume by treatment .....	101
Table 5.25	Summary data for volumetric shrinkage.....	102
Table 5.26	One-way analysis of variance for volumetric shrinkage.....	103
Table 5.27	Mean separation for volumetric shrinkage by treatment.....	103
Table 5.28	Summary data for $MOE_{app}$ of beams .....	107
Table 5.29	Three-way analysis of variance results for $MOE_{app}$ .....	108
Table 5.30	Mean separation for $MOE_{app}$ by treatment.....	108
Table 5.31	Summary data for $MOE_{true}$ of beams .....	111

Table 5.32	Three-way analysis of variance results for $MOE_{true}$ .....	111
Table 5.33	Mean separation for $MOE_{true}$ by treatment .....	112
Table 5.34	Mathematically determined shear modulus of beams .....	113
Table 5.35	Three-way analysis of variance results for shear modulus .....	114
Table 5.36	Empirically determined shear modulus of one beam.....	114
Table 5.37	Comparison of shear modulus depending on method .....	115
Table 5.38	Summary data for E/G ratio of beams .....	116
Table 5.39	Three-way analysis of variance results for E/G ratio.....	116
Table 5.40	Mean separation for E/G ratio .....	117
Table 5.41	Summary data for modulus of rupture of beams.....	118
Table 5.42	Three-way analysis of variance results for MOR .....	119
Table 5.43	Mean separation for MOR .....	119
Table 5.44	Projected allowable design bending stress by treatment.....	120
Table 5.45	Summary data for maximum shear strength of shear blocks .....	121
Table 5.46	Three-way analysis of variance for shear block maximum strength.....	123
Table 5.47	Mean separation for shear block maximum strength by treatment .....	123
Table 5.48	Summary data for maximum shear strength of short-span beams .....	125
Table 5.49	Three-way analysis of variance for short-span maximum shear strength.....	126
Table 5.50	Mean separation for short-span maximum shear strength .....	126
Table 5.51	Probability results summary for the three-way factorial analyses .....	127
Table 5.52	Projected design values by treatment for non-lapped beams .....	129
Table 5.53	Projected design values by treatment for lapped beams .....	129
Table 6.1	Comparison between desired minimum design values and treatment LT-L.....	132
Table 6.2	Expected design values at 43 lbs/ft <sup>3</sup> .....	135
Table A.1	Calculation of weight of strands used per layer .....	144
Table A.2	Production data collection sheet .....	145
Table A.3	Production data set.....	146
Table A.4	Testing data set .....	148

Table A.5	Preliminary test data summary .....	152
Table C.1	Factorial analysis for non-lapped $MOE_{app}$ .....	155
Table C.2	Mean separation for non-lapped $MOE_{app}$ .....	155
Table C.3	Factorial analysis for non-lapped MOR.....	155
Table C.4	Mean separation for non-lapped MOR .....	155
Table C.5	Factorial analysis for non-lapped shear blocks .....	156
Table C.6	Mean separation for non-lapped shear blocks.....	156
Table C.7	Factorial analysis for lapped $MOE_{app}$ .....	156
Table C.8	Mean separation for lapped $MOE_{app}$ .....	156
Table C.9	Factorial analysis for lapped MOR .....	157
Table C.10	Mean separation for lapped MOR.....	157
Table C.11	Factorial analysis for lapped shear blocks .....	157
Table C.12	Mean separation for lapped shear blocks.....	157

## LIST OF FIGURES

Figure 1.1	The product life cycle for engineered wood products.....	2
Figure 2.1	Running logs through the TVA log crusher.....	9
Figure 2.2	A crushed red maple log .....	10
Figure 2.3	Net annual change of standing timber in Maine .....	13
Figure 2.4	Residual stress in the bondline due to imperfect consolidation .....	14
Figure 2.5	Higher exclusion limits of SCL compared to solid lumber.....	16
Figure 2.6	Orthogonal randomization of LSSCL strands.....	16
Figure 2.7	Perpendicular earlywood/latewood orientation with respect to press force.....	18
Figure 2.8	Shear stress in the bondline when neither parallel or perpendicular to the press force.....	20
Figure 3.1	Conceptual model of factors which influence composite quality .....	24
Figure 3.2	Comparison of void volume between square and triangular strand beams.....	26
Figure 3.3	Diagram of initial lay-up of lapped beams.....	29
Figure 3.4	Diagram of final lay-up of lapped beams following cut and move.....	29
Figure 3.5	Conceptual view of the full factorial experimental design with subsampling .....	31
Figure 4.1	A typical truckload of red maple logs used in this experiment.....	37
Figure 4.2	Log breakdown on the portable band mill .....	38
Figure 4.3	Production of the square strands on the resaw .....	39
Figure 4.4	Specific gravity measurement of sample strands by water submersion.....	40
Figure 4.5	Application of resin to strands on the roller coater .....	43
Figure 4.6	The pre-weighed packs of strands for the lapped billet lay-up .....	45
Figure 4.7	Lay-up of the lapped billets .....	46
Figure 4.8	Strapping of the billet to prevent movement of strands during cutting.....	47
Figure 4.9	A billet being loaded into the press.....	47
Figure 4.10	Diagram of the press frame and beveled inserts .....	48
Figure 4.11	Diagram of the insulating/venting panels .....	49
Figure 4.12	Graph of a typical press cycle .....	52

Figure 4.13	Exponential conditioning behavior of the billets .....	54
Figure 4.14	Diagram of lapped billet breakdown into beams .....	57
Figure 4.15	Diagram of non-lapped billet breakdown into beams .....	58
Figure 4.16	Diagram of breakdown of beams into specimens for further testing .....	58
Figure 4.17	Third-point flexural testing setup.....	59
Figure 4.18	Bending moment and shear diagram for third-point loading .....	60
Figure 4.19	Typical full-range load vs. deflection curve for flexural test.....	62
Figure 4.20	A typical shear block .....	64
Figure 4.21	A shear block specimen loaded in the test fixture.....	65
Figure 4.22	Short-span shear test setup.....	67
Figure 4.23	The three types of variation present.....	75
Figure 5.1	Mean and standard error of strand specific gravity grouped by treatment.....	88
Figure 5.2	Mean and standard error of billet density grouped by treatment .....	90
Figure 5.3	Mean and standard error of beam density grouped by treatment .....	92
Figure 5.4	Mean and standard error of strand moisture content grouped by treatment.....	95
Figure 5.5	Mean and standard error of billet moisture content grouped by treatment .....	96
Figure 5.6	Mean and standard error of beam moisture content grouped by treatment.....	98
Figure 5.7	Mean and standard error of void volume grouped by treatment .....	101
Figure 5.8	Mean and standard error of volumetric shrinkage grouped by treatment .....	102
Figure 5.9	D1101 specimens showing typical distortion of the square strand treatments.....	104
Figure 5.10	D2559 specimens showing good bondline quality of the triangular treatments .....	105
Figure 5.11	Mean and standard error of $MOE_{app}$ grouped by treatment .....	107
Figure 5.12	Difference in slope of load-deflection curves recorded at load head and midspan.....	110
Figure 5.13	Mean and standard error of $MOE_{true}$ grouped by treatment .....	111
Figure 5.14	Mean and standard error of shear modulus grouped by treatment.....	113
Figure 5.15	Empirical determination of shear modulus .....	114
Figure 5.16	Mean and standard error of E/G ratio grouped by treatment .....	116
Figure 5.17	Mean and standard error of MOR grouped by treatment.....	118

Figure 5.18	Mean and standard error of shear block results grouped by treatment .....	122
Figure 5.19	Void spaces along the shear plane of shear block samples .....	124
Figure 5.20	Mean and standard error of short-span shear beam results grouped by treatment .....	125
Figure 6.1	Tip wedging and densification of the triangular strands .....	130
Figure 6.2	Density vs. MOE for LT-L .....	133
Figure 6.3	Density vs. MOR for LT-L .....	133
Figure 6.4	Density vs. maximum shear strength for LT-L .....	134
Figure 6.5	MOE vs. MOR for LT-L .....	134
Figure 6.6	Void space created by strand overlap .....	135
Figure 6.7	Comparison of yields for various SCL products .....	137
Figure 6.8	Comparison of resource and manufacturing costs of existing SCL products .....	138
Figure A.1	Marketing concept for DeltaStrand Triangular Strand Lumber (TSL) .....	158

## **Chapter 1**

### **INTRODUCTION**

#### **1.1. Introduction**

In its natural setting a tree is optimally designed to resist the forces of nature. Its composition is a compromise to the various vertical and horizontal forces subjected to it. When taken from the forest, sawn and used as a structural building material, however, its composition is no longer optimal. Knots and cross-grain are often found in the areas of greatest bending stress. Density gradients between earlywood and latewood can lead to zones susceptible to shear failures. Fungi and insects often use it for food or shelter.

In spite of these shortcomings, wood has still been the traditional structural building material of choice in North America. Its advantages are many, including high strength-to-weight ratios, workability, renewability, aesthetic value and cost. However, after a decades-long decline in the quality of solid-sawn lumber, wood is in danger of losing significant market share to non-wood products.

The response from the forest products industry was the invention of structural composite lumber (SCL). SCL is an attempt to re-engineer the tree to best resist forces subjected to it as a structural member. The tree is broken down into smaller components which are rearranged and reconstituted. The result is a product that possesses design values that are often significantly higher than even the top grades of solid-sawn lumber.

The enhanced properties and higher design values are obtained primarily through two techniques: defect randomization and densification of the wood fiber, both largely functions of the size, shape and composition (species) of the wood element. For reasons to be explained, certain geometries and species have traditionally been chosen. In terms of geometry, most SCL manufacturers use thin elements of rectangular cross section. Species chosen are either moderate density softwoods, or low-density, diffuse porous hardwoods. In the northeastern United States, moderate-to-high density, diffuse porous species are abundant. These species are not optimal as SCL furnish using existing strand sizes, geometries, and production techniques.

## 1.2. Reason for Research

The growth of SCL over the last two decades has been impressive, and continued growth is expected (APA, 2000). SCL prices have been maintained, and premiums justified based on steady demand for strong, stiff, dimensionally stable beams and columns. The forecasts for increasing demand and opportunities for new market entries have a variety of explanations including:

1. The SCL market, in spite of soaring production, has found a way to differentiate its products well enough to avoid becoming yet another commodity, such as oriented strand board (OSB). This has been accomplished through branding, proprietary design values, and training.
2. In terms of product life cycles, SCL products are poised to move into the rapid growth stage (Vloksey et al., 1994; Schuler et al., 2000) and will likely continue capturing market share from mature products such as glulam (Figure 1.1).

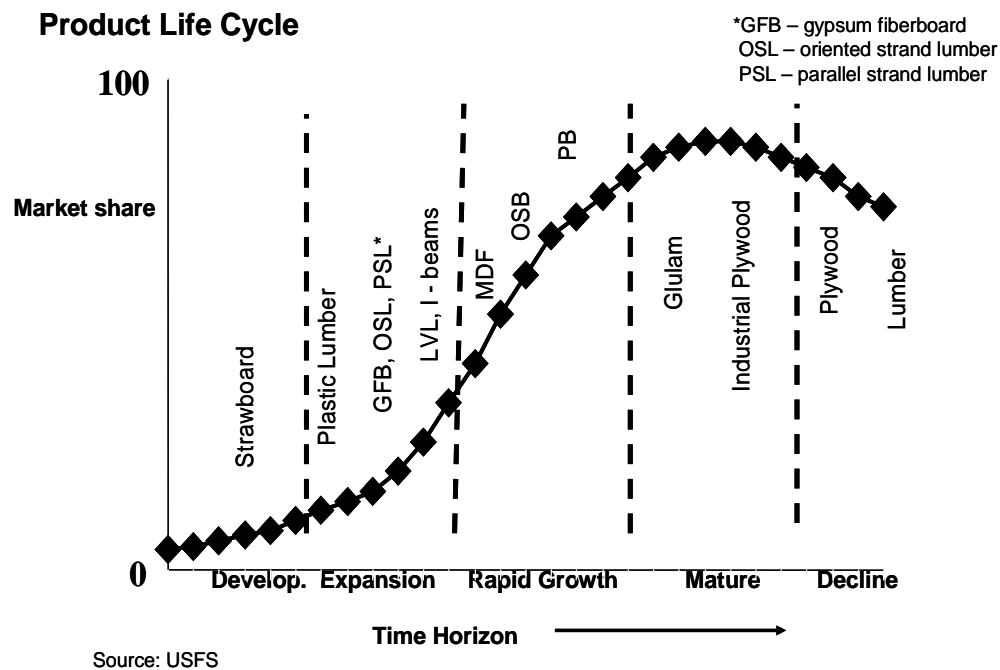


Figure 1.1 - The product life cycle for engineered wood products (from Schuler et al.)

3. The last new SCL product on the market, Laminated Strand Lumber (LSL), was introduced over a decade ago (1992).

4. Adoption of performance based codes allows builders and architects to take advantage of the performance enhancing properties of SCL. This allows for SCL to compete not only in the residential housing market, but also in the non-residential markets traditionally dominated by steel and concrete (Schuler and Adair, 1999).

In spite of exponential growth of the SCL industry in the United States, there is not a single manufacturing facility in the northeastern United States. This is perhaps most surprising in Maine, a state which is more than 90% forested and whose labor force craves the introduction of new market entries in the wake of recent closings and bankruptcies of long-standing forest product companies.

Two major issues will need to be addressed in order to establish a successful SCL manufacturing facility in the northeast (Fiutak et al., 2001). The first is developing a product which can use smaller, lower grade hardwood species allowing for a significant competitive advantage in terms of resource cost vs. SCL manufacturers who rely on veneer logs. The second is the development of new SCL technology whose unique process allows for the maximization of mechanical properties in spite of the higher density furnish from which it is made.

A product has been invented at the University of Maine which meets these criteria (Edgar et al, 2003). The product is referred to as Long-Strand Structural Composite Lumber (LSSCL). LSSCL is a PSL-type product made from four-foot long strands of symmetrical geometric cross-sections, whose least dimension is no smaller than 0.25", and with length-to-depth ratios ranging from 100 – 300. When referring specifically to the triangular strands, the product is referred to as Triangular Strand Lumber (TSL).

### **1.3. Objectives**

The objectives of this study were to:

1. Determine several strand sizes and geometries that allow for production of LSSCL using moderate-to-high density, diffuse porous, northeastern hardwoods. The strands should have a symmetrical cross section in order to attain transverse isotropic behavior in the LX and LY planes. The product should be such to allow for species interchangeability, allowing for substitution depending on availability and cost issues.

2. Develop laboratory-scale production and testing methods for LSSCL.
3. Quantify the change in selected mechanical properties due to varying strand geometry, size and lap type. As this is a new product concept with unpredictable mechanical performance, focus is on gathering as much data on as many properties as time and money permit.
4. Select a best performing treatment for possible production.
5. Determine whether the best performing LSSCL treatment possesses the following desired minimum design values, allowing for competition against existing SCL products:
  - a. Apparent modulus of elasticity ( $MOE_{app}$ ) – 1,800,000 psi
  - b. Allowable bending stress ( $F_b$ ) – 2900 psi
  - c. Allowable shear stress ( $F_v$ ) – 285 psi

If these minimum values are not met, make recommendations on product or process modifications that will allow these properties to be met.

## **Chapter 2**

### **BACKGROUND AND LITERATURE REVIEW**

This chapter serves as background to the various issues of greatest relevance in designing and conducting this experiment. The different types of SCL products in the marketplace are first reviewed. Selected mechanical and elastic properties of SCL products are then tabulated, allowing for comparisons against results obtained for LSSCL given in Chapter 5. Issues related to the selection of SCL furnish are then discussed, focusing on species, strand size and strand geometry. Finally, a discussion on heated platen vs. radio frequency curing (the two curing methods available) is given.

#### **2.1. Background**

Throughout the forest products industry it is heard that the days of relying on an unlimited resource of large, clear trees to produce high-grade, structural lumber are over. These trees have either been predominantly harvested or are protected under federal and state law. Equally problematic is the genetically deficient crop of harvestable trees inherited as a result of decades of high grading, the process of removing the largest, straightest and healthiest trees, leaving behind the worst trees as the genetic stock of the future (Hoadley, 1980). All of this dictates the need for wood products that can be made from smaller, lower-grade logs of a variety of species.

Engineered Wood Products (EWP) were developed with these challenges in mind and represent the future of the forest products industry. The manufacturing process involves taking roundwood and breaking it down into veneers, strands or flakes which are then dried, coated with resin and cured into a billet under pressure and heat (Smulksy, 1997). The relatively small wood elements *potentially* allow for use of smaller, lower grade logs which are abundant in most regions of the United States (size alone may dictate the lower grade classification - many EWP still require higher quality in terms of sweep and presence of decay). Use of smaller or lower grade logs gives a potential competitive advantage to EWP manufacturers in terms of resource costs.

Structural Composite Lumber (SCL) forms a group of EWP that possess strength and stiffness properties that in most cases exceed those of the highest grades of lumber, allowing for use in structural applications. SCL is generally available in larger sizes than solid wood, as dimensions are limited only by manufacturing constraints (e.g. size of the press). The increased properties and reduced variability allow for higher design values and, in conjunction with size availability, price premiums to be charged. In spite of higher prices, SCL compares well against other structural products such as steel, concrete and non-wood composites on a performance vs. cost basis.

SCL comes in a variety of forms, including Laminated Veneer Lumber (LVL), Parallel Strand Lumber (PSL), and Laminated Strand Lumber (LSL). In contrast to engineered wood panel products which often use cross-alignment of layers to balance properties in both longitudinal and transverse directions, the primary end use of SCL as beams and columns dictate the general orientation of the wood fiber along the long axis of the member, thereby optimizing axial properties.

## **2.2. Existing SCL Products**

Examination of existing SCL products is informative in the development of a competing product. The following sections provide a general overview of the four products currently recognized as SCL under the International Code Council's Acceptance Criteria 47 - Criteria for Structural Composite Lumber (ICC, 2003). Although glue laminated timber (glulam) is also a potential competitor, it is not included as it is not recognized as a SCL product. The information provided is based primarily on a SCL overview given by Nelson in Smulsky's book on engineered wood products (Smulsky, 1997). Production related issues are first addressed, followed by a comparison of design values.

### **2.2.1. Laminated Veneer Lumber (LVL)**

LVL was the first SCL product produced in the United States, originally introduced to the market in the early 1960's by Weyerhaeuser, followed by TrusJoist in 1968. Currently, many manufacturers throughout the world produce LVL.

Production involves the peeling of veneer-grade logs. The veneers are sorted by grade, with the higher quality veneers strategically placed in the outer plies to optimize mechanical performance. The need for veneer grade logs means several things:

1. The resource cost is relatively high as these logs command a premium.
2. Feasible economies of scale restrict production to regions of North America that produce veneer logs of the desired species. Historically, this gave a competitive advantage to the western and southern states/provinces.
3. Little flexibility exists in production. As the resource is restricted to relatively few species that are typically in high demand, the industry is exposed to excessive risk of resource price fluctuations (Schuler and Adair, 2000).

#### **2.2.2. Parallel Strand Lumber (PSL)**

PSL was introduced in 1984 by MacMillan Bloedel Ltd, and currently produced only by TrusJoist/Weyerhaeuser under the trade name Parallam®. PSL is made from peeled and graded veneers which are then clipped into rectangular strands approximately 1/8" thick and 3/4" wide. Lengths vary, which allows for use of roundup, fishtail and other pieces of less-than-full width veneer (Nelson, 1997). PSL possesses the highest allowable bending strength values of all engineered wood products, due in part to uniform densification during microwave pressing as well as the primary use of clear sapwood which is higher-than-average in strength compared to the rest of the wood fiber in the log (Nelson, 1997). The use of microwave curing also allows for production of large cross section members. These large sizes can only be achieved by other SCL products through the use of built-up beams. There are three disadvantages of PSL as well. First, as with LVL, peeling produces lathe checks, which are known to have an adverse effect on strength properties. Second, although much material is recovered as scrap from primary veneer producers such as plywood and LVL, the process still relies on expensive, veneer grade logs of few species. Finally, high density makes the product quite heavy, which can complicate traditional field installations by contractors already reluctant to try new products.

### **2.2.3. Laminated Strand Lumber (LSL)**

LSL was introduced to the market in 1992 by TrusJoist MacMillan. Currently LSL is produced under the trade name Timberstrand® at plants in Deerwood, MN, Hazard, KY and Kenora, Ontario. LSL is one of the most efficient SCL products on the market today (Knudson, 1992). It purports to use 76% of the wood fiber in the log, which gives a competitive advantage over PSL (64%), LVL (52%) and sawn lumber (40%) (Nelson, 1997). LSL does not rely on peelable veneer logs, but rather produces strands by sending logs through a strander, a rotating disc with a series of knives attached that cuts into the side grain of a log. This permits use of smaller and/or scraggily logs. Strands produced are approximately 0.03” thick, 2-4” wide and 12” long, giving a length-to-depth ratio of 400. LSL relies on lower density species, with a current preference for aspen (*Populus spp.*), yellow-poplar (*Liriodendron tulipifera*) and cucumber tree (*Magnolia acuminata*). The appreciable enhancements of LSL’s mechanical properties vs. its low density parent species is due in great part to densification values close to 100% achieved during steam injection pressing (Specific gravity for *Populus tremuloides* = 0.36; SG of Aspen LSL = 0.66). LVL and PSL, by comparison, have specific gravity values that deviate far less from the parent species (Janowiak et al., 2001). However, LSL currently has design values for bending strength and stiffness that are lower than both LVL and PSL, making inroads to the SCL market more challenging.

### **2.2.4. Scrimber**

Scrimber, although never put into mass production, is another SCL product worth mentioning. Scrimber is a unique SCL product that involves whole-log reduction, allowing for yields in excess of 90%. Debarked logs are crushed as they are passed through a series of rolls, and then ‘scrimmed’, a process of separating the crushed log into a loose mat of interconnected strands (Hutchings & Leicester, 1988; Sheriff, 1998). These strands are then dried, coated with adhesives and laid up into mats for pressing. As with LSL, the Scrimber process can use small, crooked logs, often in the 4 – 8” diameter classification. This allows for use of small diameter, pre-commercial thinnings from plantation forests, an inexpensive resource which gives Scrimber a competitive advantage over most other SCL products. The process was developed in Australia in 1975, and a pilot plant was put into operation during the early 1990’s. The plant was shut down a few years later due to manufacturing problems. Georgia Pacific bought the rights to the process soon thereafter, only to abort the project a year later. Currently, the rights belong to a small North

American company that is attempting to revive the product using southern yellow pine thinnings (Timtek, 2001). On the plus side, the product has been shown to possess strength and stiffness values that allow for competition with other SCL products, with significantly lower manufacturing costs. However, several problems exist including:

1. Difficulty in crushing many species. The only species shown to crush well are those with anatomical planes of weakness, preferably in 2 dimensions. For softwoods, this requires uneven grained species such as the southern yellow pines. For hardwoods, ring porous species with large ray cells are ideal. Marra et al. (1975) and Day (1974) conducted studies on the crushing qualities of a variety of northeastern species with a log crusher built by the Tennessee Valley Authority and found red oak to be the only species that could feasibly produce quality strands for composite production. As part of the present research red maple, beech, birch and northern white cedar were crushed with the same log crusher producing strands of exceptionally low quality (Figures 2.1, 2.2).
2. Difficulty in controlling radio frequency curing, due in part to density and moisture content variation throughout the mat.
3. Significant damage done to the wood fiber during the crushing process.



*Figure 2.1 – Running logs through the TVA log crusher*



Figure 2.2 – A crushed red maple log

### 2.3. Mechanical Properties of SCL

For comparative purposes, a listing of selected design values of SCL and solid lumber is shown (Table 2.1). The values listed are taken from the manufacturer's literature, and are of the top performing product in a given category. For example, TrusJoist produces two versions of LSL, 1.3E and 1.7E. As the 1.7E product possesses higher design values, these are presented.

Table 2.1 – A comparison of design values for various SCL and solid lumber products

Product	Density (lbs/ft <sup>3</sup> )	MOE x 10 <sup>6</sup> (psi)	F <sub>b</sub> (psi)	F <sub>v</sub> (psi)
Microlam® (LVL)	42 <sup>a</sup>	1.9	2,600	285
Parallam® (PSL)	45 <sup>a</sup>	2.0	2,900	290
Timberstrand® (LSL)	46 <sup>a</sup>	1.7	2,600	400
Scrimber® <sup>d</sup>	44	2.3	2,400	-
DF-L Select Structural <sup>c</sup>	31 <sup>b</sup>	1.9	1,500	180
Red Maple Select Structural <sup>c</sup>	34 <sup>b</sup>	1.7	1,300	210

<sup>a</sup> From TrusJoist design tables. Based on reported plf. MC not specified

<sup>b</sup> Based on specific gravity reported in Wood Handbook at 12% MC x 62.4

<sup>c</sup> MOE, F<sub>b</sub> and F<sub>v</sub> from 2001 NDS Supplement, Table 4A

<sup>d</sup> Values reported by Jarck and Sanderson (2000). The values are the high end of a reported range. As a density range was not presented, the values are suspect at the given density

Note the significantly higher strength values of SCL products vs. the top grade of solid lumber. Also note that PSL has design values that exceed all other SCL products, the one exception being the considerably higher allowable longitudinal shear strength of LSL. Explanations by Janowiak et al. (2001) include the possible negative influence of lathe checks and macropores in PSL and LVL, and the positive effects of intense composite manufacture (high heat/pressure) on LSL.

As red maple was the sole species used in this experiment, a listing of selected properties of solid, clear wood is presented for subsequent reference (Table 2.2). Note that these are average values from a large sampling, while those in Table 2.1 are design values, based on near-minimum properties and further reduced by a safety factor.

*Table 2.2 – Selected properties of red maple*

MC	SG <sup>a</sup>	MOE * 10 <sup>6</sup> (psi)	MOR (psi)	Shear Parallel to Grain (psi)
Green	0.49	1.39	7,700	1,150
12%	0.54	1.64	13,400	1,850

<sup>a</sup> Oven dry weight, volume at specified MC  
Source: Wood Handbook (USDA, 1999)

Since SCL design values are proprietary, any new product must eventually develop a complete set of its own design values. Although determination of all design values was beyond the scope of this project, several properties of LSSCL were measured (including MOE, MOR, and shear strength). Of increasing importance in 3-D wood design is a deeper knowledge of lesser-known/published elastic properties such as MOE in the transverse direction and shear modulus. Studies by Janowiak et al. (2001) have shown that these values vary considerably among SCL products as well as in comparison to solid wood (Table 2.3).

*Table 2.3 - Comparison of elastic properties of solid wood and SCL*

	Longitudinal : Transverse MOE (E <sub>1</sub> :E <sub>2</sub> )	MOE <sub>true</sub> : Shear Modulus (E:G)
<b>Solid wood</b>	24:1	15:1
<b>LVL</b>	34:1	42:1
<b>PSL</b>	35:1	44:1
<b>LSL</b>	9:1	27:1

LSL possesses less pronounced orthogonal behavior than both PSL and LVL. Again, this may be due to the negative effect of lathe checks on PSL and LVL. Also note the significantly higher E/G ratios for SCL products vs. solid wood.

## **2.4. SCL Furnish**

### **2.4.1. Species Used in SCL Production**

#### **2.4.1.1. Current Species Used in SCL Production**

LVL and PSL were invented as byproducts of the plywood industry and therefore the original species were predetermined. As plywood veneers are peeled preference traditionally was given to the large softwoods of the south and northwest, which were historically available in large diameters, high volumes and at satisfactory prices. Douglas-fir (*Pseudotsuga menziesii*) and southern yellow pine (*Pinus spp.*) were the principal species chosen, both of which possess favorable strength-to-weight ratios. The primary softwood species in the northeast - white pine (*Pinus strobus*), balsam fir (*Abies balsamea*), eastern spruce (*Picea spp.*), eastern hemlock (*Tsuga canadensis*) and northern white cedar (*Thuja occidentalis*) – do not compare favorably in terms of density, size, growth rate, or volume. Location of these desired species, along with proximity to primary breakdown facilities, explains the traditional regional trend of SCL production. More recently, yellow-poplar (*Liriodendron tulipifera*) has been used in LVL and PSL production, a somewhat unique hardwood species that produces large, clear, straight boles ideal for peeling. This resource is located along the mid-Atlantic region allowing for entry of SCL production facilities on the eastern seaboard.

LSL's properties are based primarily on densification, and therefore the choice of low density, fast growing and abundant species such as aspen (*Populus spp.*) and yellow-poplar (*Liriodendron tulipifera*) is both practical and economical. Aspen is a northern species, with production facilities in Minnesota and Ontario. Yellow-poplar is abundant in the mid-Atlantic states, with a facility in Kentucky. As described, SCL production facilities currently exist in the north, south, east and west, but none in the northeast.

#### 2.4.1.2. Potential Species for LSSCL Production

In the northeastern United States, moderate-to-high density hardwoods are abundant. According to the 1995 Forest Inventory and Analysis (USDA, U.S. Forest Service, Northeastern Research Station), the four species in Maine with the highest net annual growth are red maple (*Acer rubrum*), sugar maple (*Acer saccharum*), American beech (*Fagus grandifolia*) and yellow birch (*Betula alleghaniensis*) (Figure 2.3).

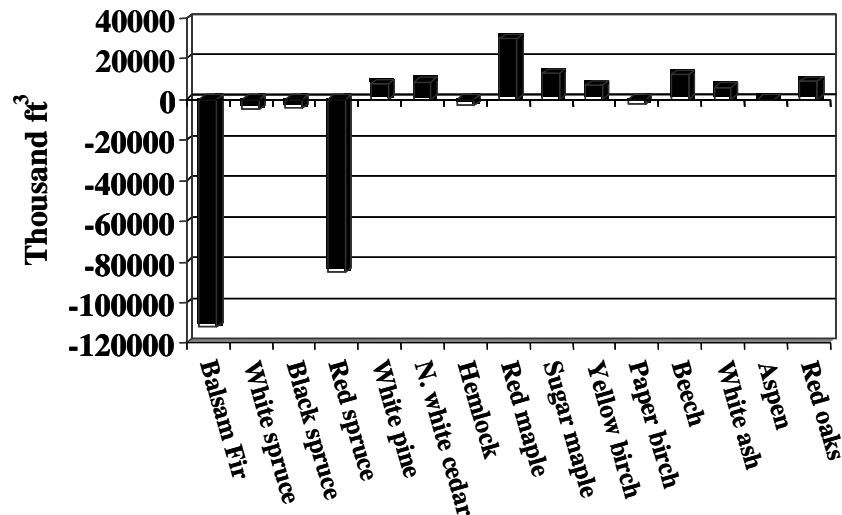


Figure 2.3 - Net annual change of standing timber in Maine (USDA)

In 1995, standing volume of these species in Maine was 6.2 billion cubic feet with a net annual growth of 66.9 million cubic feet (Table 2.4). Growth of these species exceeds removal 2 to 1, meaning excess supply should keep resource costs low into the foreseeable future. The figures suggest looking at these four species for LSSCL production.

Table 2.4 – Standing volume and net annual change of Maine timber (millions of cubic feet)

Species	Standing Volume	Net growth	Removals	Net change
Red maple	2,676.7	66.92	-34.73	32.19
Sugar maple	3,516.0 <sup>a</sup>	29.74	-14.50	15.24
Beech	<sup>a</sup>	26.00	-11.79	14.21
Yellow birch	<sup>a</sup>	17.94	-12.69	5.25
<b>TOTAL</b>	<b>6,192.7</b>	<b>140.60</b>	<b>73.70</b>	<b>66.90</b>

<sup>a</sup> Total standing volume for sugar maple, beech and yellow birch reported as a group

Source: USDA, 1995

Note that red maple alone accounts for nearly half of this net annual growth. Throughout the northeast, red maple is the poster child for the undesirable, overabundant and underutilized species. The Maine Forest Service, in its 1999 State of the Forest report to the 119<sup>th</sup> Legislature on Agriculture, Conservation and Forestry states “The increased presence of red maple implies that it is gradually replacing other native species of higher value and broader economic importance. Forest management techniques that discriminate against red maple by harvesting it and leaving more valuable species to grow can certainly reverse this trend”. This attitude from the state may make removal of significant quantities of red maple less political and more economical.

The northeastern hardwood species mentioned have traditionally been thought of as too dense for SCL production. Higher pressures are thought necessary to consolidate the furnish, with the following negative consequences:

1. Anatomical damage to the wood fiber during pressing. Geimer et al. (1985) documented the processing-induced damage on the strength of wood composites. Studies by Shaler (1986) confirmed that excessive densification can lead to a decrease in flexural properties. Aspen OSB was manufactured to three target densities, roughly corresponding to specific gravities of .56, .67 and .83. Although MOE and MOR values are known to be positively correlated with density, values were found to be significantly lower at the .83 level, likely an indication of damage to the strands during pressing.
2. Residual stress on the bondline. The higher density strands, especially if large, have greater stiffness (EI) meaning higher pressures are required to bend them, force intimate contact with adjacent strands, reduce void spaces and ensure proper wetting of the adhesive. It is postulated that this will leave a bondline under considerable residual stress (Figure 2.4).

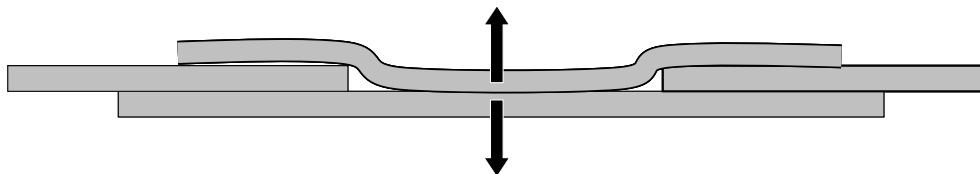


*Figure 2.4 – Residual stress in the bondline due to imperfect consolidation*

3. Excessive composite density, making the product too heavy and unreceptive to common fasteners.
4. Greater dimensional instability due to springback.

The solution to using high density species may, then, lie in finding a strand geometry that promotes intimate strand contact either at lower pressures or compaction (densification) ratios.

#### **2.4.2. Strand Size**

Marra (1992) gives a comprehensive explanation of the effects of wood element size on a variety of properties. A summary of his findings is relevant to all aspects of this experiment, and are therefore dealt with in some detail. Using clear, straight grained lumber as a reference point, he mentions that each subsequent division comes with associated benefits as well as undesirable side effects in terms of both product properties as well as economics. He lists trends which he terms the laws of diminishing dimensions. Several of these are listed (*in italics*), along with discussion on their relevance to the experiment at hand where appropriate:

1. *The strength of reconstituted products tends to decrease with decreasing wood element dimensions when compared at the same density. However, the strength lost:*
  - a. *Can be recouped by increasing density.* The target density (12% MC basis) for this experiment is 40 lbs/ft<sup>3</sup>, compared to a published value of 33.7 lbs/ft<sup>3</sup> for solid red maple.
  - b. *Can be partially recouped by increasing resin content.*
  - c. *Can be mostly recouped by aligning wood elements.* Strand alignment of LSSCL should be relatively high compared to products such as LSL.
  - d. *Is often offset by greater uniformity, leading to higher exclusion limits, and therefore higher design values.* As seen in Figure 2.5, the composite product could have a lower mean strength, but due to decreased variation, have higher design values.

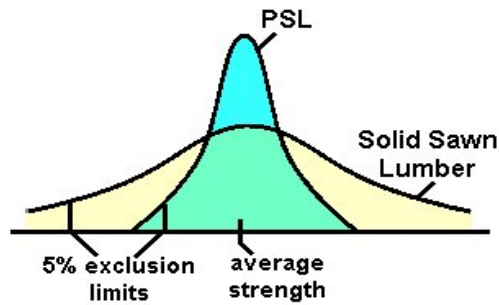


Figure 2.5 – Higher exclusion limits of SCL compared to solid lumber (from Boyer)

It was anticipated that LSSCL would have significantly lower coefficients of variation (COV) than those of solid wood as shown in Table 2.5 (USDA, 1999).

Table 2.5 – Average COV for selected properties of clear wood

	SG	MOE	MOR	Shear
COV (%)	10	22	16	14

2. Shape and size stability of reconstituted panels improve with decreasing dimensions.
3. The subdivision of wood into smaller and smaller dimensions allows manipulation of the tropic properties of the composite.

Due to layup method, most SCL products maintain an orthogonal configuration, resulting in anisotropic behavior. LSSCL has orthogonal randomization of the strands (Figure 2.6), meaning that the composite should exhibit transverse isotropy (having equal properties whether tested in the LX or LY plane) assuming that other gradients due to hot-pressing are not present.

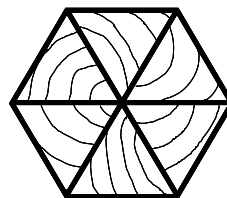


Figure 2.6 – Orthogonal randomization of LSSCL strands

4. *As dimensions are reduced, the surface area per pound of wood increases dramatically.* If resin is based on a percent of the furnish weight, such as with LSL, the amount of glue per unit surface area decreases. If based upon a constant spread rate, as with LVL and LSSCL, the amount of resin required increases. Larger strands are then desirable as resin represents a large percentage of material cost in SCL production.
5. *The smaller the element, the more energy required in breakdown as well as reconstitution.*
6. *As wood is subdivided into smaller dimensions, species differences become less crucial.* As one of the goals of the research is to allow for species mixing, this becomes important.
7. *As wood is subdivided, processes become more capital intensive and less labor intensive.*
8. *Wood should not be subdivided any more than necessary to obtain a desired result.* This suggests that the largest strand that meets minimum mechanical performance be chosen.

These rules of thumb do not clearly indicate an optimal strand size, but rather show that the decision must be based upon maximization of the various mechanical and economic trade-offs that exists in choosing larger vs. smaller strand size. A smaller strand maximizes defect randomization, yet increases energy and resin consumption. A larger strand may increase yields and maintain wood's natural axial strength, yet may lead to poor consolidation of the composite.

Another important issue regarding strand size is the length to depth (l/d) ratio, also known as the slenderness ratio. Barnes (2001, 2002), who holds the patents on both PSL and LSL, has written extensively on how varying slenderness ratios, strand angles and processing parameters effect the flexural properties of these products. He found that increasing l/d ratios result in improved properties of the composite. Stofko (1960) sought to quantify the effect of the slenderness ratio on various mechanical properties of waferboard. He concluded that for bending strength, the greatest increase was found in the ratio range of 35-120. Strength continued to increase at a slower pace between 120-300, with the maximum in the 250-300 range. Above 300, no increase was found.

### 2.4.3. Strand Geometry

There has been a slow evolution over the last several decades towards the use of composite geometries which may enhance mechanical performance, save on material costs or both. Engineered wood I-joists are a classic example. However, when it comes to the furnish of these composites, all SCL products on the market today use rectangular cross sections. The literature on SCL, therefore, has little discussion on the topic of shapes other than rectangles.

The principal reason for the exclusive use of rectangular furnish may be due to the fact that standard equipment historically has been manufactured to cut, slice, strand or clip in the vertical and horizontal planes. This makes for machinery that is likely cheaper to build and easier to control, operate and maintain. Even rotary style breakdown such as that used in veneer peeling and LSL stranding produces material of rectangular cross section.

For LVL and PSL, the original use of uneven-grained softwoods led to the rectangular shape being optimal in terms of maximum densification at a given pressure. As with plywood, the furnish is laid up with the tangential surfaces parallel to the press platens, with the lower density earlywood perpendicular to the force of the press (Figure 2.7). This orientation allows for significant densification during hot pressing as the earlywood is easily compressed.



*Figure 2.7 – Perpendicular earlywood/latewood orientation with respect to press force (photo by author)*

With the more homogenous structure of diffuse porous woods, the orientation of the strand with respect to the force of the press no longer has importance in terms of densification, and the rectangular shape provides a less specific advantage. It is the author's contention, then, that the use of diffuse porous woods *potentially* allows for use of shapes other than rectangles, as the furnish can be uniformly densified from any direction.

## **2.5. SCL Pressing**

The choice and control of the heat source used in the hot-pressing of SCL is critical to understanding and/or controlling the physical and mechanical properties of the product. Several different types of heating mechanisms are used in SCL production, including hot oil (LVL), steam injection (LSL), radio frequency (LVL) and microwave (PSL).

The 4 x 8 press available for this experiment could use either electrical resistance or RF heating. RF was chosen due to speed of cure and uniformity of heating throughout the billet. A description of each curing method is discussed, as several options will exist in production, each having its advantages and drawbacks.

### **2.5.1. Electrical Resistance Heating**

The principal problem with conventional heating involves the severe thermal gradient which is established during pressing. The gradient is present throughout the press cycle, meaning the core sees significantly different conditions than the face layers. The process of heat and vapor transfer during hot pressing has been well documented (Kamke and Casey, 1988; Zombori et al., 2002). A brief summary is informative when outlining the advantages of RF heating.

When a billet comes in contact with heated platens, heat is transported towards the core by means of conduction. As wood is a good insulator, this heat transfer is relatively slow and the surface quickly rises above the boiling temperature of water. The moisture present at these surface layers is vaporized creating a gradient in both temperature and vapor pressure. The differential vapor pressure drives the moisture towards the core, where the dew point may be exceeded and the water condensed. Thus, in the first stages of the press cycle, the surface layers see higher temperatures and lower moisture contents than the core.

The higher temperatures increase plasticization, which in turn, allows for increased (yet non-uniform) densification. However, the lower moisture content raises the glass transition temperature ( $T_g$ ) of both the lignin and the hemicellulose considerably, often above the local temperatures seen even at the surface (Wolcott et al., 1990). This combination of high temperature, still below the  $T_g$  of the amorphous polymers, and high pressure makes the wood susceptible to considerable damage during this early stage. During the later stages of the cycle, the core achieves temperatures above 212 °F where the moisture is vaporized. The vaporization process requires energy (latent heat) which reduces the speed at which the core catches up with the surface temperature. In short, these complex temperatures and pressure gradients produce conditions that are both difficult to monitor and control, leading to challenging quality control issues.

Differential temperatures also mean that the bond lines are forming at different times. This may not be problematic in products whose bond lines are mostly in the same planes. In LVL, for example, the surface bond lines will begin curing prior to those in the core. However, the principle force is normal to the bond line, meaning that it is solely in compression. LSSCL, unlike other SCL products, has strands of symmetrical cross section, creating the potential for bond lines in an infinite number of planes. This means that the downward force acts not only normal and parallel to the bond line, but any position in between (Figure 2.8). Consequently, many of the bond lines may be subjected to shear forces which the author contends are detrimental to a bond line which has not fully cured.

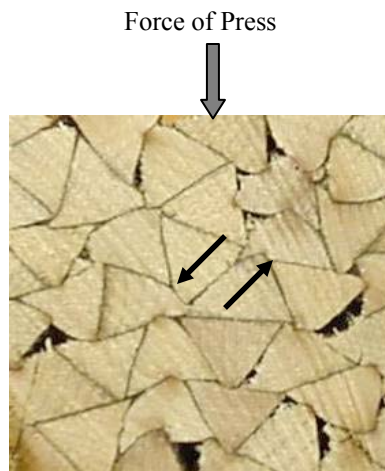


*Figure 2.8 – Shear stress in the bondline when neither parallel or perpendicular to the press force.*

Curing of SCL using heated platens also leads to a vertical density gradient (VDG) within the board. This can be advantageous in some applications, such as when LVL is used as scaffolding. The increased density on the top and bottom surfaces produces an I-beam effect, increasing strength and stiffness properties. However, in most cases it is ideal to have uniform properties throughout the cross section of a member.

### **2.5.2. Radio Frequency Heating**

Although rife with its own complexities, RF has two key advantages: speed of cure and uniform heating throughout the billet. Exactly that property of wood (a good insulating material) which makes heating by conduction difficult also makes heating with RF quite simple. If insulating materials (also known as non-conductors or dielectrics) are placed between two conducting materials (such as the platens of a press) and a voltage differential induced, an electric field is generated (Anon., 1975). This electric field can be controlled so that the platens alternate charge from positive to negative. Polar molecules within the insulator, such as the water present in wood, will align themselves according to the field, creating a back and forth motion. This movement creates friction, and consequently significant amounts of heat. The electric field permeates the insulating material completely, meaning that heat is generated uniformly throughout the billet. With uniform heating, plasticization and densification of the wood is constant throughout, giving more stable and predictable properties.

The amount of RF energy absorbed and stored in the material depends in great part on the dielectric constant of the wood and resin (Bogdan, 1996). The dielectric constant is the ratio of the capacitance of a capacitor using the material as the dielectric to the capacitance of the same capacitor using air as the dielectric (the dielectric constant for air is therefore one). The dielectric constant varies with changes in physical parameters such as temperature, moisture content, density and grain direction. It also varies in extremely complex fashion with changes in frequency (Lin, 1967). Table 2.6 gives a relative comparison of the various constants of principal concern in the curing of wood composites.

*Table 2.6 – A comparison of important dielectric constants for curing of wood composites*

<b>Material</b>	<b>Temperature °F</b>	<b>Dielectric Constant (@ 1 MHz)</b>
Air	-	1
Wood, dry <sup>a</sup>	Not reported	3
Phenol-Formaldehyde resin <sup>b</sup>	135	4.9
Water <sup>b</sup>	77	78.2
Wood, wet <sup>a</sup>	Not reported	100

<sup>a</sup> Wood Handbook (USDA, 1999)

<sup>b</sup> Mark, et al. (1986)

With the dielectric constant being so dependent on moisture content, it is clear that it can change quite dramatically during a press load. The idea of uniform heating must then be qualified for inhomogeneities of the dielectric properties of the wood during a press load. This means that differences in moisture content and density, for example, will produce potentially drastic differences in both heating and curing rates. As a consequence, it is critical that the wood furnish used in production (a) is dried to a uniform moisture content and (b) if species are to be mixed, they should have similar densities.

It is especially challenging to control RF during the press close step(s). With conventionally heated platens, the press can be closed slowly while the furnish is being heated, thereby ensuring sufficient plasticization of the wood fiber prior to the use of high pressures, avoiding anatomical damage. With RF, however, it is desirable to maintain the platens in a stationary position while the RF is on. This is due to the fact that the capacitance of the load is partly a function of the distance between the electrodes. As the platens approach one another, the capacitance increases, and an excess of charge can build up on the electrodes. This situation often leads to an arc, where the excess charge passes through an area of higher conductivity (least resistance), carbonizing the fiber through which it passes. As carbon is an excellent conductor of electricity, restarting the RF will only lead to further arcing, meaning that once an arc occurs the press cycle cannot be continued and the billet must be discarded. As this results in significant losses of time and material, it is desirable to keep the platens stationary while the RF is on.

The amount of time the RF needs to be on to achieve cure temperature can be roughly estimated using the following three step process (Pitcher, 1998):

1. Calculate the BTUs required to heat the billet to the desired temperature

$$\text{BTU} = (\text{Weight of wood \& adhesive})(\text{Specific heat of wood})(\Delta T) \quad (3.8)$$

2. Convert BTU's to kilowatt minutes

$$\text{KW min} = \text{BTU}/56 \quad (3.9)$$

3. Convert kilowatt minutes to time by dividing by the KW rating of the generator

$$\text{Min} = \text{KW min}/\text{KW of generator} \quad (3.10)$$

This estimate does not account for several variables which significantly affect curing time including MC, spread rate and amperage to name a few. These calculations are therefore only recommended as a starting point.

## Chapter 3

### EXPERIMENTAL DESIGN AND RATIONALE

The objective of this chapter is to provide detailed explanation and rationale behind the design of the experiment. The rationale behind choosing the control variables is first discussed. The hypotheses are then stated, followed by the experimental design chosen to test these. Finally, an explanation regarding the choice of the testing protocol is given.

#### 3.1. Selection of Variables

There exist many factors which affect billet quality/strength (Figure 3.1).

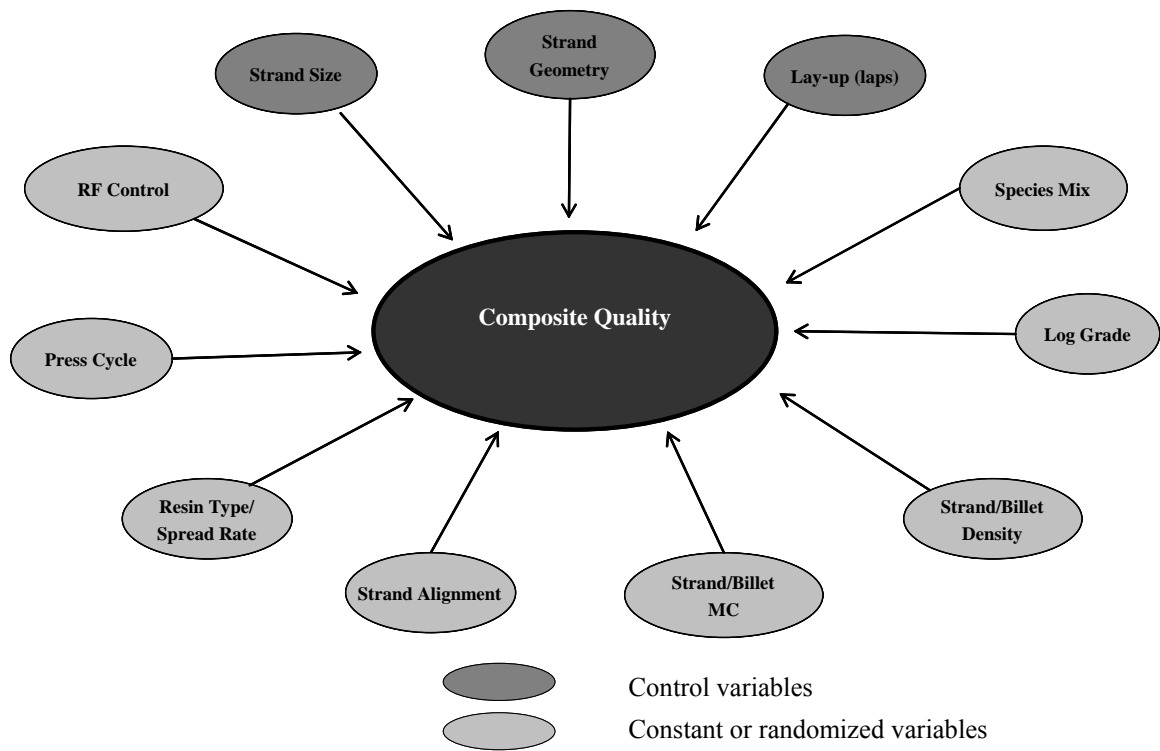


Figure 3.1 – Conceptual model of factors which influence composite quality (by author)

Of these many factors, it was reasoned that the most critical were strand size, strand geometry and lap method. Manipulation of these three variables allows for a best-performing furnish to be determined (a logical first step in designing a new SCL product) using a method of lay-up that simulates that likely to be

used in production. Each of these is discussed below in detail. The remaining variables were either set as constants, randomized or not manipulated (only recorded), and will be discussed in the following chapter.

### **3.1.1. Strand Geometry**

Traditionally, SCL manufacturers have used thin, rectangular elements produced from either moderate density softwoods or low density hardwoods. Higher density hardwood species have been avoided, as they require higher pressures to adequately densify and consolidate the wood furnish. These higher pressures can lead to increased manufacturing costs, damage to the wood fiber and/or a product that is too dense, making it heavy and unreceptive to common mechanical fastening techniques.

It is postulated that one way to allow for use of a high density furnish is to select a strand geometry that allows for adequate consolidation of the wood elements without significant densification of the wood fiber. The resulting product would have approximately the same density as other SCL products, but achieve this by means of the inherent density of the species, rather than through densification. The author conceived of an isosceles, triangular strand geometry as optimal to meet these goals.

Choice of this geometry was primarily based on the following desired properties:

1. Ability to consolidate in the composite, thereby minimizing void space as well as residual stresses on the bondline.
2. Tendency to align along the longitudinal axis of the member, thereby maximizing axial properties. This is critical as SCL is most often used as a bending member or column, where maximum axial strength is desired.
3. Symmetrical strand cross section, allowing for the composite to possess isotropic behavior in the transverse directions. This property could potentially be used as a marketing tool when competing against the more orthogonal behavior of existing SCL products.
4. Patentability. A unique product was sought which would allow for competition against existing products not only in terms of mechanical performance, but also in terms of marketability.

For comparative purposes, a second geometry was selected. A square was the only other symmetrical geometry which could feasibly be produced in the laboratory. Preliminary testing had indicated that square strand billets, while possessing inferior properties to triangular, may achieve design values that would allow for competition with existing SCL products. However, as design values are based on near minimum properties, concern was raised that square strand beams would *occasionally* fail at significantly lower loads than the triangles. This is due to the unavoidable, periodic large void space in an area of high stress. Figure 3.2 shows the cross section of some of the preliminary beams, showing the significantly higher void space volume of the square strand beams.

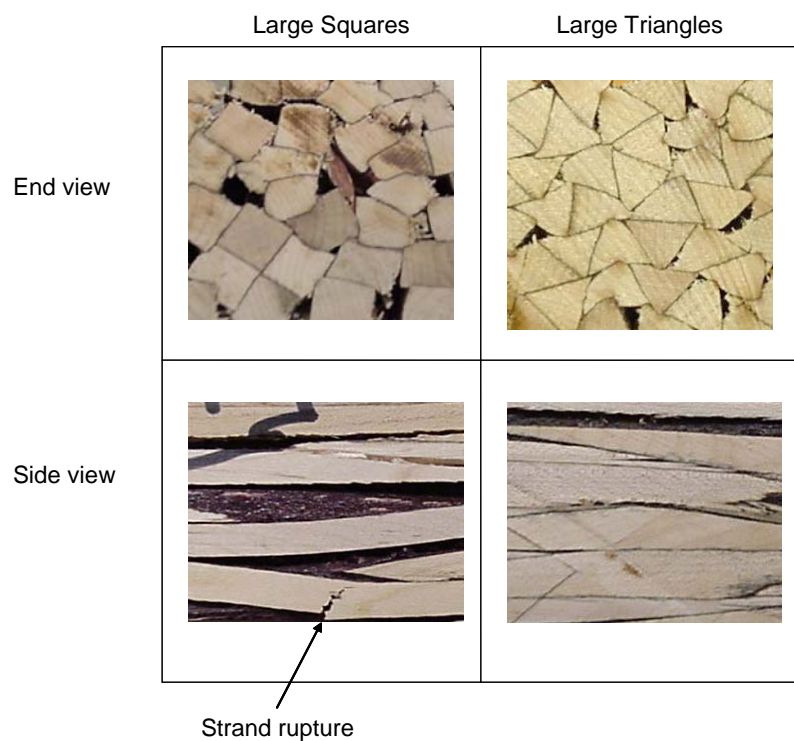


*Figure 3.2 – Comparison of void volume between square and triangular strand beams*

Even if the triangles were to produce billets superior to squares, the squares still could still be chosen for manufacturing assuming they possess mechanical properties that allow for direct competition with existing SCL products and do not have excessive coefficients of variation. This might occur, for example, if it is determined that producing square strands is significantly cheaper than triangles, as machinery would likely be either stock or easily modified.

### **3.1.2. Strand Size**

Following inspection of a typical sort of 5-12" diameter red maple logs, a strand length of 48" was chosen as a four foot bolt was the longest deemed regularly obtainable without significant sweep. In terms of thickness, two sizes were desired for comparison using the maximum range deemed feasible. These sizes were selected for both mechanical (slenderness ratios desired in the 100-200 range) and practical reasons (ability to cut the strands safely with existing equipment). With a 48" length, the desired l/d ratios give a range of 0.24 - 0.48 inches.

For the smaller size, it was determined that cutting strands less than 1/4" in cross section could not be done safely and without a vast majority snapping during sawing. The smaller strand, which allows for maximum defect randomization and the largest feasible slenderness ratio (192), was chosen at 0.25". For the large size, it was theorized that strands any larger than 7/16", where not lined up perfectly, would make intimate contact with adjacent strands difficult and leave bondlines under residual stress. Void spaces at the lap joint would also be large, assuming that the higher density furnish would not fully compress. The larger strand, allowing for higher yields during primary (saw) breakdown, was then chosen at 0.4375" giving a slenderness ratio of 110 (Note that dimensions given are for the length of the strand side. For triangular strands, the strand height is slightly smaller, 0.2165" for small triangles; 0.3789" for large triangles).

### **3.1.3. Billet Lay-up**

A method of billet lay-up was sought which would simulate continuous press production currently used in the SCL industry. Using an existing method would allow for either stock or used equipment in production, likely reducing capital expenditures during a mill start-up. Two methods are discussed below, listing their advantages and disadvantages.

The first method, used in OSL production, uses a random lay-up where strands are oriented in the longitudinal direction and fall randomly from a conveyor onto a forming mat. An advantage of this approach with LSSCL is that strands of varying lengths could be used. This means that strands broken upon secondary breakdown need not be culled, increasing yields significantly. The drawback to this lay-up

using the large LSSCL strands is difficulty in controlling strand alignment as well as the uniformity of billet density. In continuous production, it is feared that the long strands will occasionally get caught either on themselves, or in the aligning discs, causing a backup of strands which when released will fall to the forming mat in bunches rather than evenly. An uneven density profile not only could cause variable mechanical properties, but also problems with controlling RF energy during curing.

The second method is a staggered lay-up, such as that used in LVL. Sheets of veneers are laid one on top of the other in staggered fashion, allowing for a continuous lay-up. Density is easily controlled, void spaces are in predictable locations at the lap joint and strand deviations from the longitudinal axis are minimized. A PSL-type product could use this method by pre-weighing a group of parallel aligned strands of equal length to form a sheet, similar to veneer. The staggered method was chosen as it was reasoned, after consultation with industry professionals, that an LVL-type lay-up would provide for the best strand alignment and uniformity of billet density.

There are limitless lap configurations which could be used in a staggered lay-up. The lay-up decided upon staggered eighteen “sheets” of strands (nine layers) measuring 14” x 48” every 6 inches, with a two inch lap at the joints. A side view of the layup is presented in Figures 3.3 and 3.4.

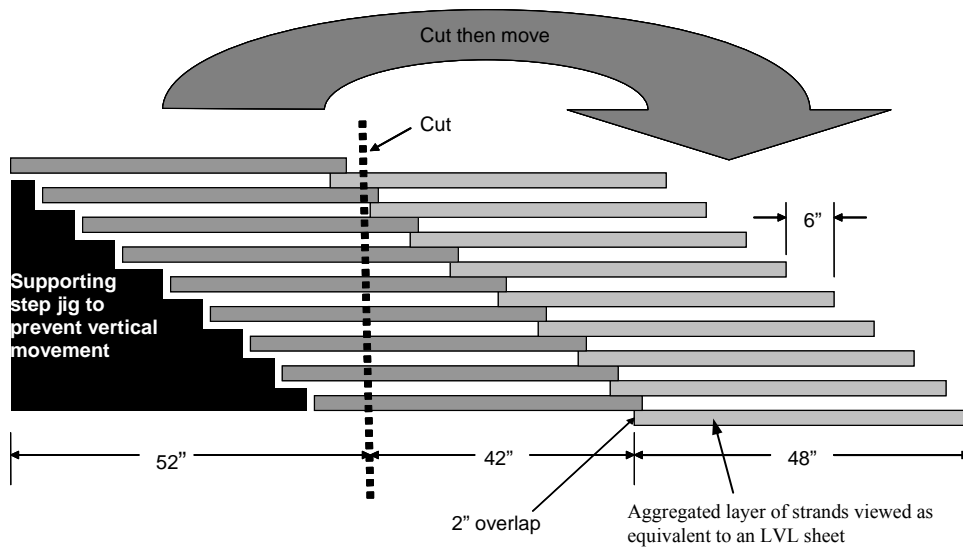


Figure 3.3 – Diagram of initial lay-up of lapped beams (sideview)

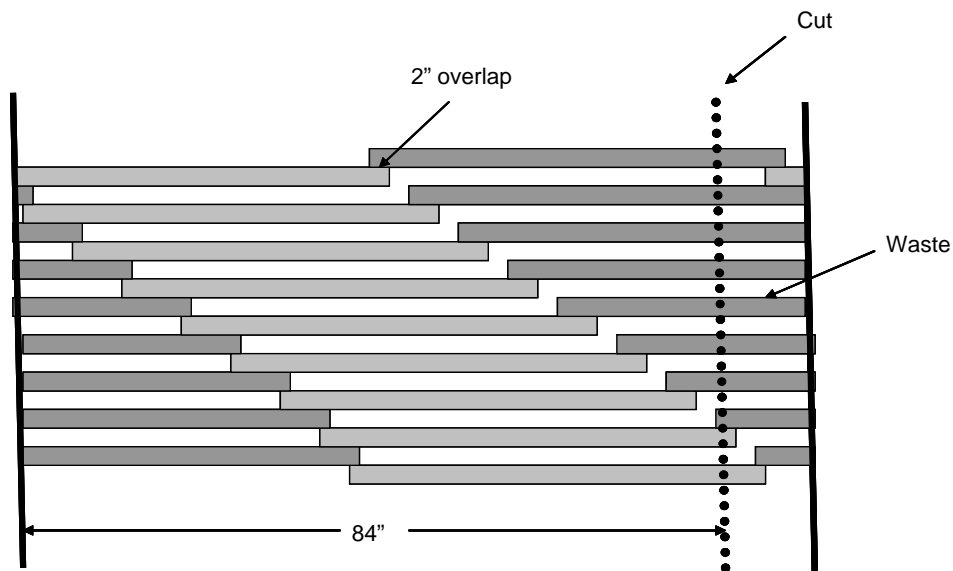


Figure 3.4 – Diagram of final lay-up of lapped beams following cut and move (side view)

The choice of the overlap lengths of 6" and 2" was made after consultation with industry professionals who indicated that these simulate the lengths used in current LVL production. With these overlap lengths, nine layers of strand sheets were chosen, as this evenly distributes the lap joints along the length of the billet.

As such, a line drawn through any point along the billet (Figure 3.4) will always cut through either 9 or 10 layers (10 at the 2" overlap). Note that in LVL production, the staggered fan that is produced at the beginning of the lay-up is cut and discarded. The reason the cut-and-move method was used here was to conserve strands.

Non-lapped billets were chosen as a control. The non-lapped lay-up produces billets which allow a clean interpretation of the interaction between strand size and geometry without the complex confounding that lap joints add. They also provide a comparative group that allows for determination of the effect of lap joints and potential calculation of a "knock-down factor" for said laps. This would be especially useful when comparing different lap types vs. a control, such as butt joints, different overlap lengths or use of scarfed strands at the lap. However, the non-lapped billets do not give values which are particularly useful in terms of production recommendations, as lap joints are inevitable in a continuous press production operation.

### **3.2. Hypotheses**

The following hypotheses were tested:

1. *The triangular strand beams will have significantly less void space than square strand beams.* The triangular shape allows for improved consolidation (nestling/alignment) of the strands using any feasible production lay-up (Figure 3.2).
2. *The triangular strands will produce stronger and stiffer beams than those made from square strands.* This hypothesis is formed as a result of hypothesis number one. Additionally, it is assumed that the square strand beams will occasionally have a large void space in an area of critical stress. Due to this, the strength effect will likely be seen more in allowable bending stress (based on near-minimum strength) than average modulus of rupture.
3. *The large triangular strands will produce stronger and stiffer beams than the small triangular strands.* Larger triangular strands possess sufficient weight that upon being dropped into a forming mat, the strands will stay essentially aligned in the longitudinal direction of the billet, which will avoid the negative impact of grain angle deviations on mechanical properties. Additionally, although smaller

strands mean greater defect randomization, the small knots common in red maple have a greater negative impact on a small strand than on a larger one.

4. *Non-lapped beams will be both stronger and stiffer than lapped beams.* The presence of the lap joint will have a negative impact on all mechanical properties.

### 3.3. Experimental Design

This section provides an overview of the experimental design, including description of all treatments as well as rationale for sample size selection. Specific statistical methods are presented in Chapter 4.

As two levels were chosen for each of three factors, a 2 x 2 x 2 full-factorial, completely random design (CRD) with subsampling was chosen to test the hypotheses (Figure 3.5).

The three factors were:

Factor A: Strand size

$a_1$  = Large (7/16")

$a_2$  = Small (1/4")

Factor B: Strand geometry

$b_1$  = Square

$b_2$  = Triangle

Factor C: Billet lay-up

$c_1$  = Laps

$c_2$  = No laps

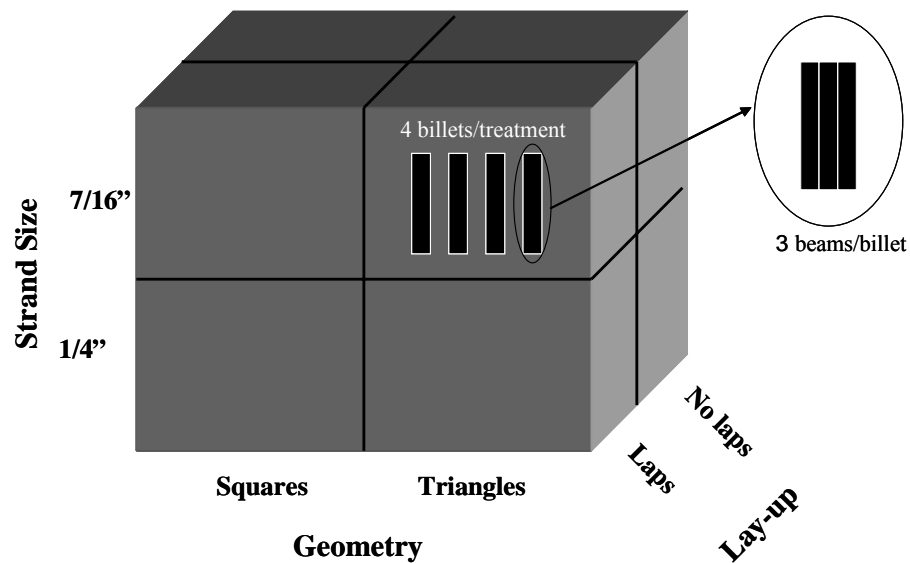


Figure 3.5 – Conceptual view of the full factorial experimental design with subsampling

The 2 x 2 x 2 design yields the following 8 treatments (Table 3.1):

Table 3.1 – The 8 treatments of the experiment

Treatments	Abbreviation*	Factors	Strand Size (A)		Strand Geometry (B)		Lay-up Type (C)		# Billets	# Beams
		Levels	7/16" (a <sub>1</sub> )	1/4" (a <sub>2</sub> )	Square (b <sub>1</sub> )	Triangle (b <sub>2</sub> )	Lap (c <sub>1</sub> )	No Lap (c <sub>2</sub> )		
1	LS-L		■		■		■		4	12
2	LS-NL		■		■			■	4	12
3	LT-L		▲			▲	▲		4	12
4	LT-NL		▲			▲		▲	4	12
5	SS-L			■	■		■		4	12
6	SS-NL			■	■			■	4	12
7	ST-L			▲		▲	▲		4	12
8	ST-NL			▲		▲		▲	4	12
	TOTALS								32	96

\* First letter=Large/Small; Second letter=Square/Triangle; Third & Fourth Letter=Lap/NoLap

The full-factorial design allows for testing of each main effect, as well as interactions between these effects (Steel et al., 1997). The fact that the three factors each have only two levels, allowed for the following seven single-degree-of-freedom F-Tests:

1. Factor A: Do large strands perform equally to small?
2. Factor B: Do square strands perform equally to triangles?
3. Factor C: Do billets with laps perform equally to non-lapped?
4. Factor A x B: Is response to strand size equal at the different levels of geometry?
5. Factor A x C: Is response to strand size equal at different levels of lay-up?
6. Factor B x C: Is response to strand geometry equal at different levels of lay-up?
7. Factor A x B x C: Is response to strand size equal at the different levels of geometry and lay-up?

### **3.4. Size and Quantity of Specimens**

#### **3.4.1. Billet Size**

Lapped billets were made to the largest length possible. The top platen of the 4' x 8' press, which was also the insulated electrode for the RF system, was 94" long. As excess charge can build up on the edges of this electrode, the manufacturer recommended keeping the billet a few inches away from each edge to avoid arcing. A length of 84" was chosen. As many SCL products have an approximate width of two inches, thickness was chosen at 2.1", allowing for a final dressed dimension of 2.00". The 14" width was chosen primarily due to machining concerns, as billets any larger would be difficult to handle. Size of the non-lapped billets were the same, with the exception of length which was dictated by the 48" long strands. Ripping an inch from each side, and two from each end gave final billet dimensions of 2" x 12" x 80" (lapped) and 2" x 12" x 44" (non-lapped).

#### **3.4.2. Beam Size**

The width (depth when turned on edge) of the beams ripped from the billets was dictated by the chosen l/d ratio of 21. ASTM D5456 (ASTM, 2001) requires an l/d ratio between 17 and 21. The higher l/d ratio was chosen to minimize deflections caused by shear, and more closely approximate pure bending stress. This ratio dictated beam sizes of 2" x 3.75" x 80" (lapped) and 2" x 2" x 44" (non-lapped). Three beams could be obtained from the lapped billets, five from the non-lapped.

#### **3.4.3. Sample Size**

The number of billets and beams produced was based primarily on practical considerations. In terms of time and money, the maximum deemed feasible was 4 billets per treatment, for a total of 32. Once ripped into beams, the result was 12 (lapped) and 20 (lapped) beams per treatment. In order to keep sample sizes equal for lapped and non-lapped beams, only 12 of the 20 non-lapped beams were used. The remaining 8/treatment were set aside for future testing. The total number of beams was then 12 per treatment, 96 in total.

Note that the use of subsamples (beams cut from the billets) means that there are two types of variation present: among the four billets of each treatment (among experimental units) and among the 3 beams within each billet (within experimental units). This must be taken into consideration when building the statistical model statement to be used in hypothesis testing within the analysis of variance. The default error term must be overridden and specified so that total error is used. This will be explained in detail in Chapter 5.

### **3.5. Testing Protocol**

The objective of the testing program was to evaluate selected physical and mechanical properties of LSSCL so that comparisons could be made both among treatments and against existing SCL products. Mechanical testing was done in accordance with ASTM D5456 – Standard Specification for Evaluation of Structural Composite Lumber Products (ASTM, 2001). This standard was chosen since ICC code approval of this product would fall under AC47 – Criteria for Structural Composite Lumber, which requires compliance with D5456. What follows is a listing of the properties chosen for testing as well as rationale behind these choices. Chapter 4 details how these tests were conducted.

D5456 requires testing of six principal properties: Modulus of elasticity, modulus of rupture, tension parallel to grain, compression parallel to grain, longitudinal shear and connector withdrawal. Time did not permit the testing of all the properties listed. For that reason, the three most commonly referenced properties for SCL were first chosen, namely 1) modulus of elasticity (to determine design bending modulus -  $MOE_{app}$ ), 2) modulus of rupture (to determine allowable bending stress -  $F_b$ ) and 3) longitudinal shear (to determine allowable shear stress -  $F_v$ ). As discussed in section 2.3, the E/G ratios for SCL products are considerably higher than that of solid wood. For that reason, G and E/G ratios, both derived from the flexural results, were also determined.

It was hypothesized that varying strand sizes and geometries would produce differential distribution and size of void spaces. This could potentially lead to differential volumetric shrinkage values, depending on treatment. Void volume and volumetric shrinkage were therefore selected for determination.

Finally, as the quality of a composite is in very large measure a function of the adhesive bond strength, the adhesive joint integrity was investigated.

### **3.5.1. Shear Strength Determination**

Special mention is given to the topic of shear strength. ASTM D5456 (ASTM, 2001) requires that shear blocks be used for determination of allowable longitudinal shear strength, tested according to ASTM D143 (ASTM, 2000). Although shear blocks were tested, they may not be the most appropriate method to evaluate the maximum shear strength of this product concept. The actual shear area of these blocks varies depending on the size and location of the void spaces. In some cases, there may exist large voids along the shear plane, meaning the actual shear area is smaller than the nominal value calculated via exterior dimensions. For this reason, it was decided to also test short-span shear beams as a comparative tool.

The reason short-span beams are not permitted for use in shear strength determination, and why a specific standard for their testing does not exist for wood, is likely due to the complex nature of the various stresses which are developed when testing short beams in flexure. ASTM D2344 (ASTM, 2000), the standard for testing short-beam strength of polymer matrix composite materials discusses this complexity, noting that classical beam theory is inadequate to determine shear stresses of these beams (it only predicts shear stress on planes midway between the loading head and reactions). This is due to the fact that the assumed parabolic shear stress distribution is not constant across the length of the beam and is heavily influenced by the complex stress combinations (shear and compression) found at the load head and reactions. The standard concludes that “unless mid-plane interlaminar failure has been clearly observed, the short-beam strength determined from this test method cannot be attributed to a shear property”. Making matters worse, the nature of the stress distribution changes as the span/depth ratio is changed (The recommended span to depth ratio in this standard is 6:1). In spite of these reservations, the data from short-span beam testing was determined as an adjunct to the shear block data.

### **3.5.2. Orientation of Testing Specimens**

ASTM D5456 (ASTM, 2001) requires testing of certain properties in both the LX and LY planes. For solid wood, this is performed in order to determine the differential properties along both the radial and tangential planes. For wood composites, the method of manufacture often causes differential properties in both planes. Production of LVL with conventional platens is a good example, where a through-the-thickness density gradient is produced. Although nominal LX and LY axes can be determined for LSSCL, growth ring orientation was assumed to be completely randomized (see Section 2.4.2), and therefore testing along both axes has reduced significance. Therefore, testing was only performed in one plane (edgewise for bending and short-span shear beams, randomly for shear blocks).

## Chapter 4

### MATERIALS AND METHODS

The objective of this chapter is to detail the materials and methods used to carry out the experiment. First, the production method is presented in a step-wise sequence. Testing methods follow, including calculations used to determine properties. Finally, a complete explanation of the statistical methodology used to analyze the data is presented, including examples of each step.

#### 4.1. Production

##### 4.1.1. Log Harvesting and Bucking

Although a mix of several medium-to-high density northeastern hardwoods are envisioned as potential furnish for LSSCL, red maple (*Acer rubrum*) was the only species used in this experiment. The use of a single species prevented the potential confounding of differing species mixes among billets.

All trees were harvested within a 30 mile range of Orono, Maine, mostly from the town of Lagrange. Three truckloads were delivered to a landing area (one in August, October and January) each consisting of approximately 8 cords of 16-22 foot long, 5-12 inch diameter logs (Figure 4.1). The logs were bucked with a chainsaw to either eight or five feet, depending on the sweep present in the log.



*Figure 4.1 – A typical truckload of red maple logs used in this experiment*

#### 4.1.2. Primary Log Breakdown

Within two months of harvesting, logs were sawn into boards on a 24 horsepower Timber Harvester portable band mill using 1 ¼" wide blades. The logs were first canted, and the slabs discarded. A flitch of boards either 5/16" or ½" thick (for eventual dressing to ¼" or 7/16" strands, respectively) was then cut from each log (Figure 4.2). If any wane was present, boards were run through a Wood Mizer edger.



*Figure 4.2 – Log breakdown on the portable band mill*

As an attempt to achieve randomization, boards were taken from the top of the flitch and randomly assigned to storage racks representing the two geometries. As boards were cut to either ¼+" or 7/16+", this randomization could not be performed for the size factor.

#### 4.1.3. Grading

An estimated 40% of the logs exhibited some degree of heart rot. Although no traditional visual or mechanical attempts at grading were made, only boards primarily clear of rot were kept. The reason for this culling is that a product made from this process will likely specify a pulp grade sort with no heart rot. Note that color is not a good indicator of rot in red maple. All logs exhibited a darkened center, known as pathological heartwood which is due to a responsive phenolic deposition rather than fungal action (Zabel and Morrell, 1992; Shigo and Larson, 1969; Shigo and Hillis, 1973). If this colored wood was solid, it was

kept. The areas infected by heart rot were easily detected as the darkened wood had streaks of yellow discoloration and was softened.

#### **4.1.4. Strand Production**

Boards were cut to four feet in length and planed down to either  $\frac{1}{4}$ " or  $\frac{7}{16}$ ". Any noticeable defects revealed by planing, such as decay and large knots, were removed on the table saw. This was done to expedite the stranding process so as not to waste time cutting strands that would break due to knots or rot. The boards were then stranded to one of the four sizes. The triangular strands were cut on a Delta table saw, with a  $\frac{1}{8}$ " thick blade tilted to  $30^\circ$ . The first strand (with a square edge) was discarded. The isosceles strands were then produced by repeated sawing and flipping of the board. The square strands were cut on a Tri-State Re-Rip Saw (model # TRR 46) rigged with seven  $\frac{1}{8}$ " circular blades separated by spacers allowing for either  $\frac{1}{4}$ " or  $\frac{7}{16}$ " strands to be cut (Figure 4.3). In a further attempt to avoid decay, strands were slightly bent by hand as they came off the saw. If brittle failure occurred (indicating decay), the strand was discarded.



*Figure 4.3 – Production of the square strands on the resaw*

Strands were bundled into packs representing approximately one billet (~75 lbs) and stored in an unheated shed.

#### 4.1.5. Relative Specific Gravity of Strands

It was expected that considerable variation existed in physical and mechanical properties between trees as well as within trees (Haygreen and Boyer, 1996). With red maple, this includes variation in density, heart rot, incipient decay, and percent sapwood. In spite of this variation, a completely random design was chosen as attempts were made to ensure that furnish in each billet was representative of the full variation of the population.

Realizing the potential inadequacies of the randomization techniques described above, specific gravity measurements were taken on 15 randomly chosen strands from each billet. Four inch sections were cut from each strand and specific gravity measured per ASTM D2395 (ASTM, 2002) - water submersion method (Figure 4.4).

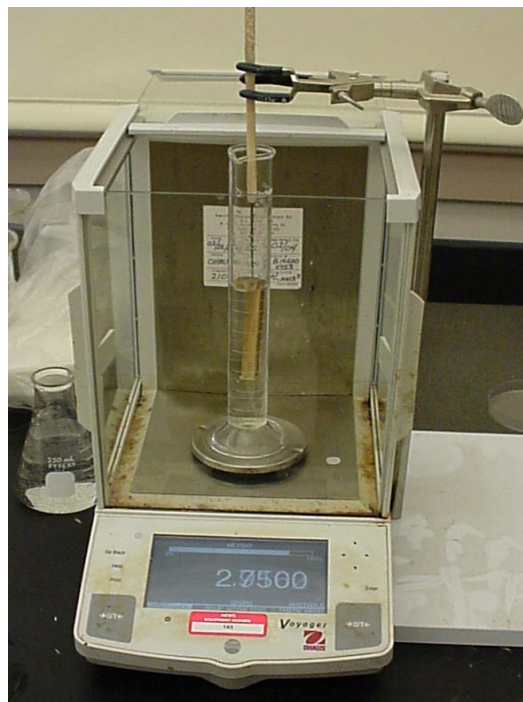


*Figure 4.4 – Specific gravity measurement of sample strands by water submersion*

As the average number of strands per billet varied depending on size and geometry, the percentage of strands sampled per billet varied (Table 4.1).

*Table 4.1 - Percent of strands sampled for specific gravity by treatment*

TRT#	TRT Type	TRT Abbreviation	Average # of strands/billet <sup>a</sup>	% of strands sampled
1	Large-Square-Lapped	LS-L	303	5.0
2	Large-Square-Non lapped	LS-NL	167	9.0
3	Large-Triangle-Lapped	LT-L	610	2.5
4	Large-Triangle-Non lapped	LT-NL	411	3.7
5	Small-Square-Lapped	SS-L	960	1.6
6	Small-Square-Non lapped	SS-NL	582	2.6
7	Small-Triangle-Lapped	ST-L	1621	0.9
8	Small-Triangle-Non lapped	ST-NL	945	1.6

<sup>a</sup> Calculated as the total weight of strands per billet/average weight of 6 individual strands

Although variation was not controlled, this sampling allowed for quantification of the relative variation of strand density from billet to billet.

#### **4.1.6. Strand Drying and Conditioning**

All strands were dried in a 5,000 board foot Nyle dehumidification dry kiln equipped with a 5 horsepower compressor. A drying rack was built consisting of 10 screened shelves, approximately 4' x 4' and spaced 4" apart. Strands were placed on the screens to a depth of ~3", leaving a ~1" space for air flow. Although drying stresses were not of concern, warping was and relatively mild conditions of 100 F° and 76% RH were used. The moisture content (MC) of the strands going into the kiln varied depending on how long the boards/strands were in the storage racks following primary processing. Random samples showed initial moisture contents ranging from 21-45%. Drying time varied depending on the strand geometry, ranging from 17 hours (ST) to 22 hours (LS). The drying cycle was terminated when sample strands averaged 6% MC. Once dried, the strands were bundled in approximately 75 lb packs and placed in a conditioning chamber set to 86 F° and 30% RH. The strands remained in the chamber between 30-60 days, depending

on when the billet was made. It was imperative to have uniform moisture content of the strands at the time of pressing to avoid uneven heating/curing during RF pressing.

#### **4.1.7. Resin Type and Application**

A phenol-formaldehyde liquid resin from Borden Chemical (Cascophen TJ1-5058B) was used. The adhesive was similar to that used in Parallam production. The adhesive was formulated with a 50% solids content plus a 1% wax emulsion, added to reduce moisture adsorption and enhance durability. Since the resin had only a two-week shelf life, it was shipped in 5 gallon containers and frozen upon arrival at -5° C. The resin was in the freezer no more than 45 days and thawed approximately 24 hours prior to use. The time from thaw until use averaged 3.2 days, and in no case exceeded 14 days. The effects of freezing the resin are not known, but the manufacturer states that any deleterious effects should be minor at most.

Viscosity was checked prior to each billet lay-up with a Brookfield viscometer using a #3 spindle at 12 rpm to check against the recommended viscosity range of 350-550 cps @ 22 C°. The average viscosity was 1297 cps at 19 C°, with a range from 780 – 1860 (Table 4.2). Some of the higher viscosities may have been due to lower adhesive temperatures. Viscosity adjustments for temperature were not known and therefore it was not clear if the viscosity was within the recommended range. This led to some concern that the viscosity was too high and a lack of flow may have existed. However, bond line quality appeared to be high, as evidenced by a very low percentage of adhesive failures during subsequent flexural and shear testing.

Resin was applied to the strands using a 22" Black Bros. roller coater (Figure 4.5). The target spread rate was 38 lbs/MDGL (per one thousand square feet of double glue line, 19 lbs on each strand side). Verifying the spread rate using strands was attempted, but deemed ineffective. This was due to the low weight and surface area of the strands which led to high error and poor repeatability. To get a more accurate determination of spread rate, 1/4" (or 7/16") x 8" x 10" boards were used.

Table 4.2 – Resin viscosity by treatment

TRT#	TRT Type	n	Mean Viscosity (cps)	Std Dev	COV (%)	Mean Temp (°C)	Std Dev	COV (%)
1	LS-L	24 <sup>a</sup>	1495	237	15.8	21.0	0.0	0.0
2	LS-NL	24	1320	0	0.0	20.0	0.0	0.0
	LS	48	1407	181	12.9	20.5	0.5	2.6
3	LT-L	24	1403	605	43.1	18.3	2.4	12.9
4	LT-NL	24	1860	242	13.0	19.0	1.2	6.1
	LT	48	1631	492	30.2	18.6	1.8	9.5
5	SS-L	24	1260	321	25.5	19.5	0.6	3.0
6	SS-NL	24	780	0	0.0	19.0	0.0	0.0
	SS	48	1020	332	32.5	19.3	0.5	2.4
7	ST-L	24	1273	298	23.4	17.0	4.8	28.0
8	ST-NL	24	983	92	9.3	18.0	2.2	12.0
	ST	48	1128	256	22.7	17.5	3.5	19.8
TOTALS		192	1297	401.1	30.9	19.0	2.18	11.5

<sup>a</sup> 6 strands from each of 4 billets



Figure 4.5 – Application of resin to strands on the roller coater

It is important to note that the spread rate was difficult to control for the triangular strands. Each strand was run through the roller coater three times (as opposed to twice for the square strands). Strands were rotated so that resin was applied by the bottom roller. The tip of the triangle, however, picked up some resin from the top roller which dripped down the adjacent sides. It was clear that the triangular strands, especially the small triangles, had a spread rate well in excess of that measured by the sample boards. This could be a significant confounding variable and concern was raised for potential effects on the results of mechanical testing. One likely impact was to increase the density of the small triangle billets. Although density is known to increase mechanical properties of solid wood, the contribution of the resin to density may in fact lead to a decrease in properties of composite products.

The recommended open assembly time for this resin was 90 minutes. Due to the method of resin application (manual feeding through a roller coater – 2 times for each square strand, 3 times for each triangle strand), it was impossible to meet this recommendation. As seen in Table 4.3, the open assembly time ranged from 21 minutes (LS-NL) to 5 hours and 50 minutes (ST-L).

*Table 4.3 – Open assembly time by treatment*

<b>TRT#</b>	<b>TRT Type</b>	<b>n</b>	<b>Average (hr:min)</b>	<b>Std Dev (hr:min)</b>	<b>COV (%)</b>
<b>1</b>	<b>LS-L</b>	4	0:55	0:05	10.5
<b>2</b>	<b>LS-NL</b>	4	0:21	0:02	11.8
<b>3</b>	<b>LT-L</b>	4	2:37	0:31	20.2
<b>4</b>	<b>LT-NL</b>	4	1:15	0:10	14.4
<b>5</b>	<b>SS-L</b>	4	1:55	0:07	6.1
<b>6</b>	<b>SS-NL</b>	4	0:47	0:10	21.9
<b>7</b>	<b>ST-L</b>	4	5:50	0:21	6.3
<b>8</b>	<b>ST-NL</b>	4	2:41	0:09	5.9

An assumption was made that the elongated layup time would not significantly affect the quality of the bondlines. This assumption was made based upon the results of preliminary testing where the resin was applied to strands and allowed to dry overnight (19 hours on average) prior to layup. Those test billets

performed equally to specimens tested in this experiment in terms of both MOE and MOR, leading to the conclusion that open assembly time was not a major confounding variable.

#### **4.1.8. Billet Lay-up**

Billets were laid up with a target density of 40 lbs/ft<sup>3</sup> (weight @ 12% MC/volume @ MC out of press). At the time of layup a weight of strands corresponding to the desired billet density was removed from the conditioning chamber. For lapped billets, the strands were divided into 18 packs which formed the 9 layers of the layup (Figure 4.6). The calculation of the weight of strands used per layer is shown in Appendix A (Table A.1).



*Figure 4.6 – The pre-weighed packs of strands for the lapped billet lay-up*

Billets were laid up by hand on a forming table, aligning all strands as best possible along the longitudinal axis of the billet. This technique was used to assure uniform strand alignment from billet to billet to avoid confounding of this critical variable.

A sheet of ¼" pegboard, slightly longer and wider than the billet, was first placed on top of the table. As the pegboard remained beneath the billet during pressing (described below), it prevented strand movement

of the mat during press loading. The peg board was notched on the sides, allowing for placement of ratchet straps, used to further prevent strand movement during press loading. A permeable nylon peel ply was then laid across the table which served to contain the strands during pressing, prevent adhesion to the insulating panels and allow moisture to escape during pressing.

The billets without laps had the four foot strands stacked directly on top of one another. The lapped billets used a staggered layup as previously described in Section 3.1.3. When the first of 18 packs was coated in resin, the layer was placed at one end of the table (Figure 4.7).

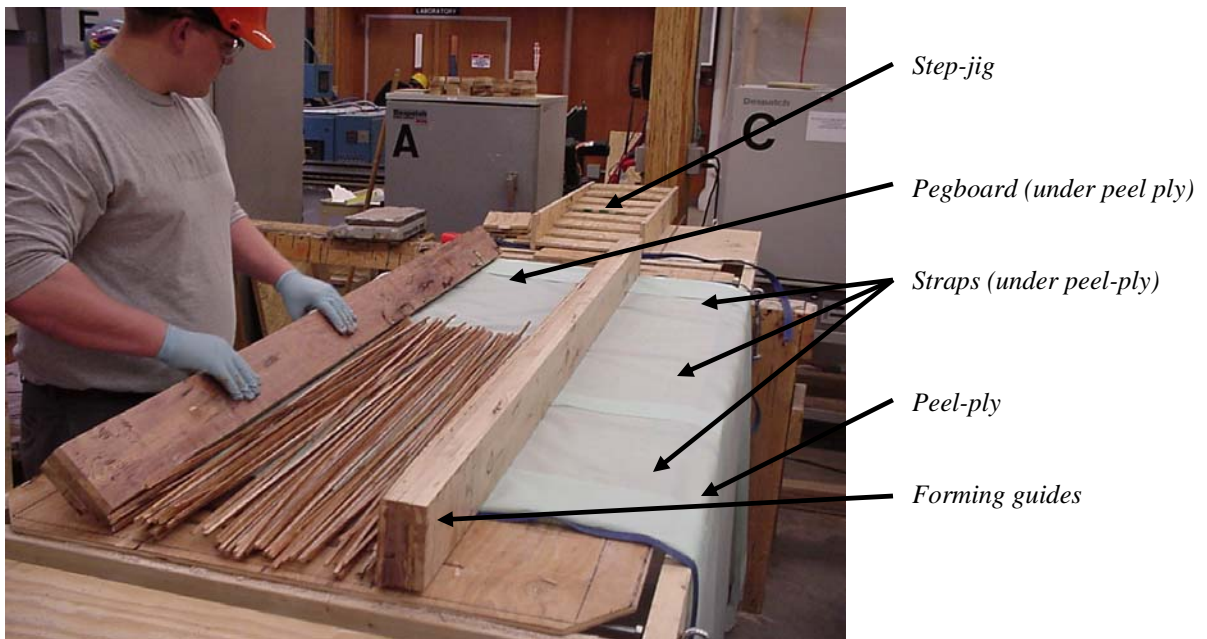


*Figure 4.7 – Lay-up of the lapped billets*

The next layer was laid up at the other end, overlapping the previous layer by two inches. The far end of this second layer sat on the first step of the step-jig, used to prevent vertical movement of the strands during layup. This process was continued until all 18 layers were placed.

The next step involved cutting the mat approximately in half. To prevent strand movement during cutting, the mat of strands was strapped tight between two pieces of plywood (Figure 4.8).



*Figure 4.8 – Strapping of the billet to prevent movement of strands during cutting*

Once the mat was cut, the far end (secured by the plywood and strap) was transferred and laid atop the near staggered fan. The near end was then strapped as previously described and the mat cut to the final length of 84". The mat was then wrapped in the peel ply, straps tightened and loaded into the press (Figure 4.9).



*Figure 4.9 – A billet being loaded into the press*

Initial billets showed that density could not be controlled due to lateral movement of the strands during consolidation. To prevent this movement, a press frame was devised and fabricated from a unidirectional

fiberglass-epoxy composite (Figure 4.10). The composite had a bending modulus of 5,400,000 psi, stiff enough to prevent bowing of the frame during pressing.

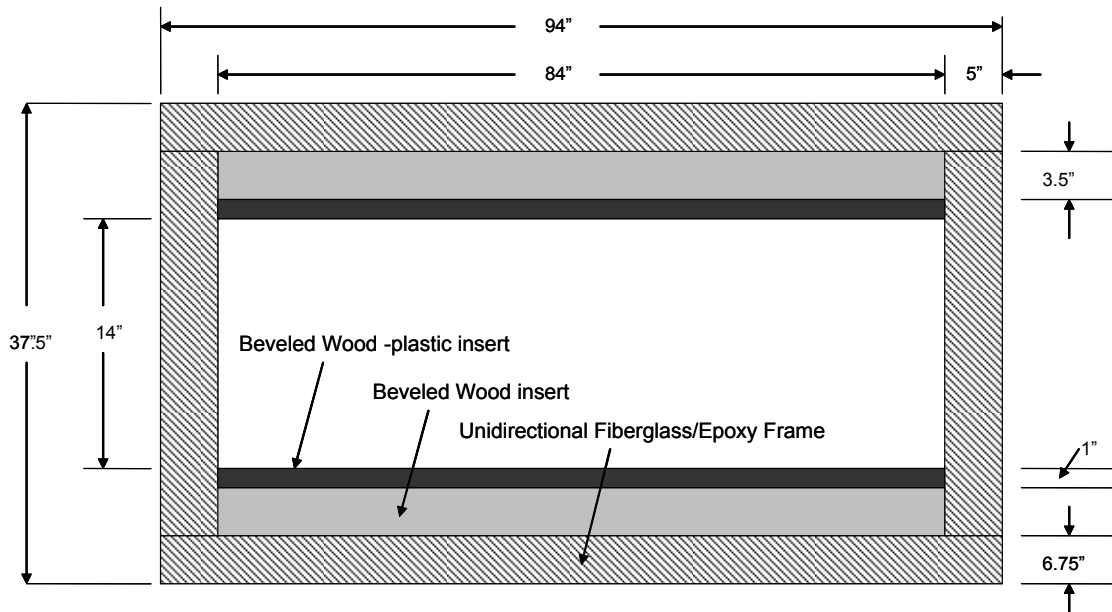
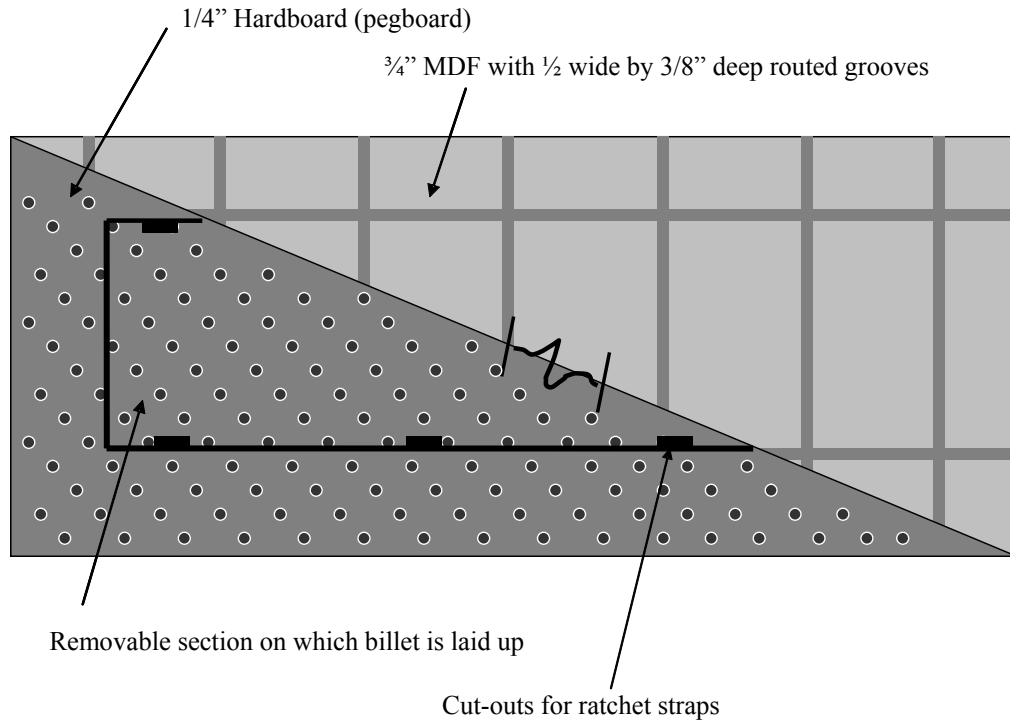


Figure 4.10 – Diagram of the press frame and beveled inserts

Though reduced, lateral movement of strands during pressing resulted in considerable friction between the pressed billet and the frame such that removal after the press cycle was problematic. To solve this, beveled ( $6^\circ$ ) inserts were made which were placed along the long leg of the frame. The larger insert was made from wood and the smaller one from a polyethylene-sawdust composite. The wood plastic composite was used for two reasons: 1) It possessed a lower coefficient of friction so removal was facilitated, 2) It was cheap and easy to replace, so was considered sacrificial. This was important as the method of removing the billet from the frame involved pounding on the wood-plastic insert with a hammer and steel dowel.

In order to avoid heat conduction to, and condensation at the cold RF electrodes/platens, a combination insulating/venting panel was fabricated and placed on both on top and bottom of the billet/press frame assembly during pressing (Figure 4.11).



*Figure 4.11 – Diagram of the insulating/venting panels*

The panels consisted of 1/4'' pegboard (hardboard) glued to a 3/4'' MDF panel containing routed grooves. The panel provided significant insulation and also allowed steam to pass through the holes/grooves and out of the press (facilitated by fans mounted to the RF shielding).

The billet was then placed into the press within the press frame which sat atop the bottom insulating/venting panel. The wood and wood-plastic spacers were laid along side the billet. The straps containing the billet were then removed and the peel ply tucked underneath the spacers and tugged tight. This ensured that during pressing, the strands remained within the borders of the press frame. Finally, the top insulating/venting panel was placed on top of the billet.

While ideally the order of billet manufacture would be randomized to avoid any systematic bias, this was not possible for the ongoing experiment. The principal reason for this involved student labor issues, as some treatments took significantly longer to layup than others. Production of the 32 billets lasted 35 days, and were fabricated in the following order: SS-L, ST-L, SS-NL, ST-NL, LT-L, LT-NL, LS-NL, LS-L.

#### 4.1.9. Pressing

All billets were pressed in an Erie Mill & Press 4' x 8', 1800 ton hydraulic press controlled by an Allen-Bradley PLC and Citect software. The press was fitted with a Thermex-Thermatron 10 KV, 5 MHz radio frequency generator. Pressure (both ram and billet), position (controllable to +/- 0.0003"), RF anode current amperes and delivered energy (KWsec) were recorded at one-second intervals for each press load.

##### 4.1.9.1. Press Cycle

Selection of the press cycle is critical to the quality of the billets produced. Some detailed explanation is therefore warranted regarding development the main steps of the chosen press cycle (Table 4.4).

*Table 4.4 – The press schedule used to produce the billets*

Step #	Ramp time (min:sec)	Dwell time (min:sec)	Position (inches)	RF	
1	1:30	0:30	3.150	Off	Close
2	0:01	0:30	3.150	On	
3	1:30	0:30	2.150	Off	
4	0:01	12:00 <sup>a</sup>	2.150	On	Hold/Cure
5	0:01	1:00	2.150	Off	
6	0:30	0:30	2.200	Off	Decompress
7	0:30	0:30	2.250	Off	
8	0:30	0:30	2.350	Off	
9	0:30	0:30	2.500	Off	
10	0:15	0:15	28.000	Off	

<sup>a</sup> 8:30 for non-lapped billets

##### 4.1.9.1.1. Press Close (Steps 1-3)

As the RF could not be turned on while the platens were moving, step one was set to slowly bring the press to 3.150", a full inch from the final close position. The average pressure at the end of step one was 15 psi, thus avoiding high pressure while the furnish was at ambient temperature.

The RF was turned on for step two, holding the position from the previous step. As the metallic thermocouples on hand could not be used in the RF field, a temperature vs. time curve could not be established. Ideally, this preheating step would continue until temperatures close to the curing temperature of the resin (212 °F) were reached, allowing for some plasticization of the wood fiber, without initializing the curing reaction of the resin. Thirty seconds were chosen as a conservative value, to ensure that the curing temperature was not reached.

Step three took two minutes to bring the platens to their final position of 2.150". This distance was chosen to ensure that the billet saw the full force of the press (i.e. so that the 2.10" thick press frame did not take any of the applied load). Although not quantified, it was hoped that this relatively slow closing would allow the strands (especially the triangles) to consolidate better than if the press were quickly closed, minimizing both void space as well as damage to the strands.

#### **4.1.9.1.2. Press Hold/Cure (Step 4)**

Once at the final position, the RF was turned on for full curing of the billet. The current was set at 2.3 amperes, chosen as test billets indicated this was the highest amperage possible without any arcing. The times (8:30 minutes for non-lapped, 12 minutes for lapped) were selected to ensure the billets reached the desired curing temperature of 220°F. Temperatures were determined using a digital thermocouple (precision to 0.1°F) with type K wire. Readings were taken once the billet was removed from the press by inserting the wire in a hole drilled 1" deep, 1" from the edge in the center of the billet.

#### **4.1.9.1.3. Decompression (Steps 5-10)**

Several decompression steps were used in order to avoid heat (steam) blows caused by vapor pressures in excess of the adhesive bond strength at the time of press opening. It was assumed that higher steam pressures are built up in the billets with lower void volumes, increasing the risk of heat blows. This meant that decompression was especially critical for the small, triangular strands which (as seen in 5.3.3) had the lowest percent void volume. A typical graph of the press cycle is shown in Figure 4.12.

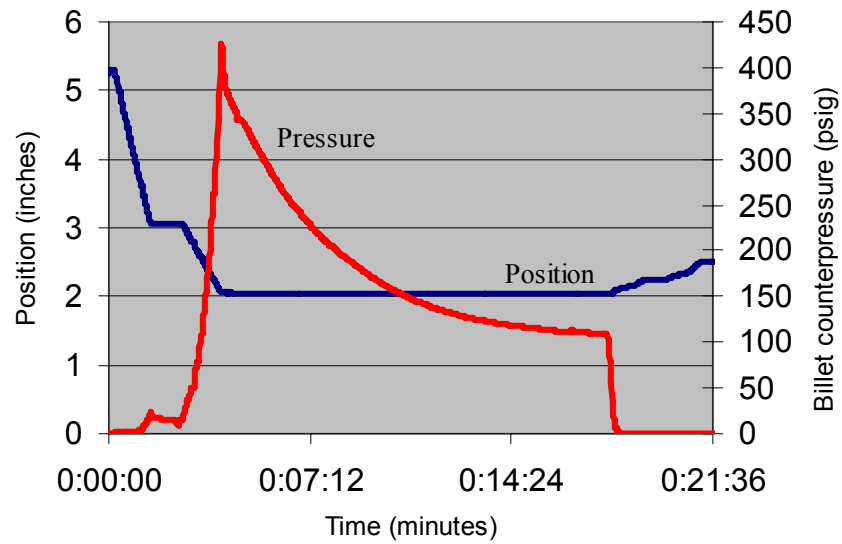


Figure 4.12 – Graph of a typical press cycle

#### 4.1.9.2. Pressure

The press was set in position control, to ensure that the desired dimensions (and therefore density) were reached. Note that in position control, there is no control over pressure. This caused pressures to vary from billet to billet. Maximum pressure by treatment is shown in Table 4.5.

Table 4.5 – Maximum billet pressure by treatment

TRT#	TRT Type	n	Mean (psi)	Std Dev (psi)	COV (%)
1	LS-L	4	901	135	14.9
2	LS-NL	4	536	21	3.9
3	LT-L	4	524	122	23.2
4	LT-NL	4	433	69	16.0
5	SS-L	4	520	21	4.1
6	SS-NL	4	706	56	7.9
7	ST-L	4	645	97	15.1
8	ST-NL	4	449	78	17.3

#### 4.1.9.3. Radio Frequency

Measurement of the energy supplied to the load was somewhat difficult without sophisticated measuring devices, such as a calorimeter. To estimate the calculation of delivered energy, a few assumptions were made, all of which were based upon information provided by the manufacturer:

1. The RF voltage was a constant 10 kilovolts. In reality, the actual voltage changes during the cycle, depending on the DC current or large amperage draws. However, this variation was likely no more than ~200 volts (< 2%).
2. The frequency was a constant 5 MHz. In reality, the frequency also changes, likely between 5-7 MHz depending on the capacitance of the load at any given point in time.
3. The efficiency of the RF generator was 65%.
4. The idle current (idle loss), a measure of the current lost in the circuitry of the system before it reaches the electrodes, was 0.5 amperes at any given point in time.

The manufacturer provided the following equation to calculate the delivered energy (E) to the load as:

$$E = \sum_{t=1}^n [(I_t - k) * V * E_f] \quad (4.1)$$

Where:

- E = Delivered Energy (Kilowatt seconds = Joules)  
t<sub>1</sub> = Time at which RF is enabled (seconds)  
n = Time at which RF is disabled (seconds)  
I<sub>t</sub> = Anode current (amperes) at time t  
k = Idle current (a constant 0.5 amps)  
V = Volts (a constant 10,000 volts)  
E<sub>f</sub> = Efficiency of system (a constant 0.65)

By summing the delivered power at each second, total delivered energy can be calculated. The average total delivered energy per billet was 7204 and 10124 kilowatt seconds for non-lapped (8:30 minutes) and lapped billets (12:00 minutes), respectively.

#### 4.1.10. Dressing and Conditioning

Upon removal from the press, the billet was weighed and dressed. One inch was ripped from each side, and two inches removed from each end. Approximately 1/16" was planed off each face, giving a final thickness of 2.00 inches. Moisture content samples were taken from the middle 6" of the 1" wide side trim and moisture content determined (oven dry method).

The billets were then stacked (using ½" stickers) in an environmental conditioning chamber set to conditions of 70 °F and 65% relative humidity, giving an approximate equilibrium moisture content (EMC) of 12% (USDA, 1999). This EMC, however, is calculated based on desorption. ASTM D4933 (ASTM 1999) states that for adsorption, only ~85% of the EMC will be obtained. The final expected EMC at these conditions for adsorption was therefore  $12\% \times 0.85 = 10.2\%$ .

ASTM D4933 details a procedure to estimate the time required to reach equilibrium. The calculations are based upon knowledge that wood gains/loses moisture in an exponential fashion, with rapid moisture changes early on followed by a tapering off as equilibrium is approached. One beam from each of the eight treatments was weighed every couple of days early on, then approximately once a week thereafter. Examination of change in weight vs. time for the SS-L beams shows this exponential behavior (Figure 4.13).

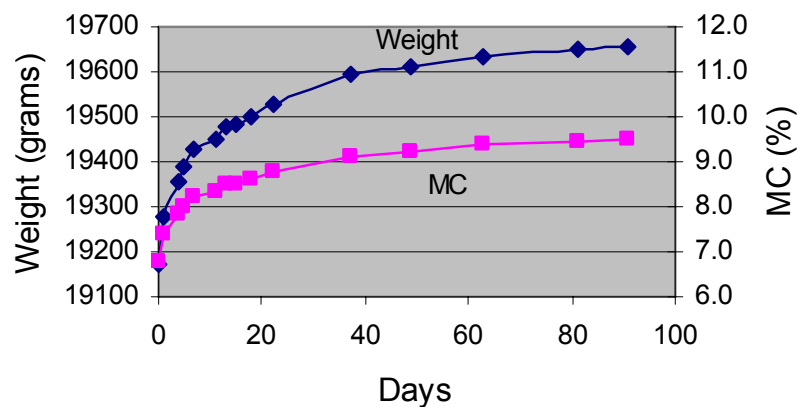


Figure 4.13 – Exponential conditioning behavior of the billets

The time required to obtain a 63.2% change from initial to final MC is referred to as one time constant.

The calculation of MC at one time constant is calculated as:

$$MC_{tc1} = MC_i + 0.632 (MC_f - MC_i) \quad (4.2)$$

where:

$MC_{tc1}$  = Moisture content at one time constant

$MC_i$  = Initial moisture content

$MC_f$  = Final Moisture content

Using the average MC of billets out of the press of 7.1 % (see Section 5.3.2.2) as the initial value, and a final EMC of 10.2% as calculated above, the estimated MC at one time constant was calculated as:  $7.01 + 0.632 (10.2 - 7.1) = 9.06\%$ . The next step was to calculate how many days equates to one time constant. Table 4.6 shows the conditioning schedule for the SS-L billets, which were the first billets made and therefore conditioned for the longest period of time. The time constant is the number of days required to go from 7.1 to 9.1 %, approximately 36 days.

*Table 4.6 – A typical billet conditioning schedule*

<b>Date</b>	<b># Days</b>	<b>Weight (g)</b>	<b>MC (%)</b>
4/10/2003	0	19174	6.8
4/11/2003	1	19277	7.4
4/14/2003	4	19358	7.8
4/15/2003	5	19390	8.0
4/17/2003	7	19429	8.2
4/21/2003	11	19452	8.3
4/23/2003	13	19479	8.5
4/25/2003	15	19483	8.5
4/28/2003	18	19502	8.6
5/2/2003	22	19529	8.8
5/17/2003	37	19592	<b>9.1</b>
5/29/2003	49	19613	9.2
6/12/2003	63	19634	9.4
6/30/2003	81	19649	9.4
7/10/2003	91	19656	9.5

A chart was then produced to estimate the amount of time required to attain the final EMC, or any MC in between (Table 4.7). It was decided that being within one percent of the final EMC was sufficient, giving an estimated minimum conditioning time of approximately 45 days. Because there was a 35 day period from production of billet #1 to #32, the billets were conditioned for different amounts of time. All billets were conditioned for the minimum 45 day period calculated above.

*Table 4.7 – Conditioning time constants*

# Time Constants	Expected MC (%)	% of change	Expected # Days
1	9.06	63.2	36
2	9.77	86	72
3	10.05	95	108
4	10.14	98	144
5	10.17	99	180

Once all billets were considered sufficiently equilibrated, they were dressed to final dimensions of 2” x 12” x 44” (non-lapped) or 80” (lapped), ripped into beams (see Section 4.2.1), labeled and returned to the conditioning chamber. Seven days later, testing began and beams were removed one by one in a random fashion during the two week testing period. This additional period allowed the beams to equilibrate even further. At the time of testing, all beams were within 1% of the estimated EMC of 10.2%.

Once the beams were tested in flexure, and specimens for further tests cut, they were returned to the conditioning chamber. Note that although the shear block samples were in the conditioning chamber 3-4 weeks longer than the flexural samples, the average moisture content (9.88%) was exactly the same, indicating that the flexural beams were likely equilibrated at the time of testing.

#### **4.1.11. Production Data Collection**

Production data was collected on all appropriate variables. The data collection sheet used (Table A.2) as well as the full data set (Table A.3) are included in Appendix A.

## 4.2. Testing Methodology

### 4.2.1. Billet Breakdown and Test Specimen Preparation

Each billet was ripped into either three (lapped billets) or five (non-lapped billets) beams as shown in Figures 4.14 and 4.15. For the non-lapped billets, beams 2 and 4 were saved for future testing.

Typical beam breakdown into specimens is shown in Figure 4.16. The beams were first tested for flexural stiffness and strength. After failure, the section of the billet in the center with bending failures was removed (3). A moisture content section (2) was taken from this center piece. This left two smaller beams. The larger piece was marked and set aside for testing in short-span shear (1), while the smaller remnant was used for shear block testing (4) as well as volumetric shrinkage (5).

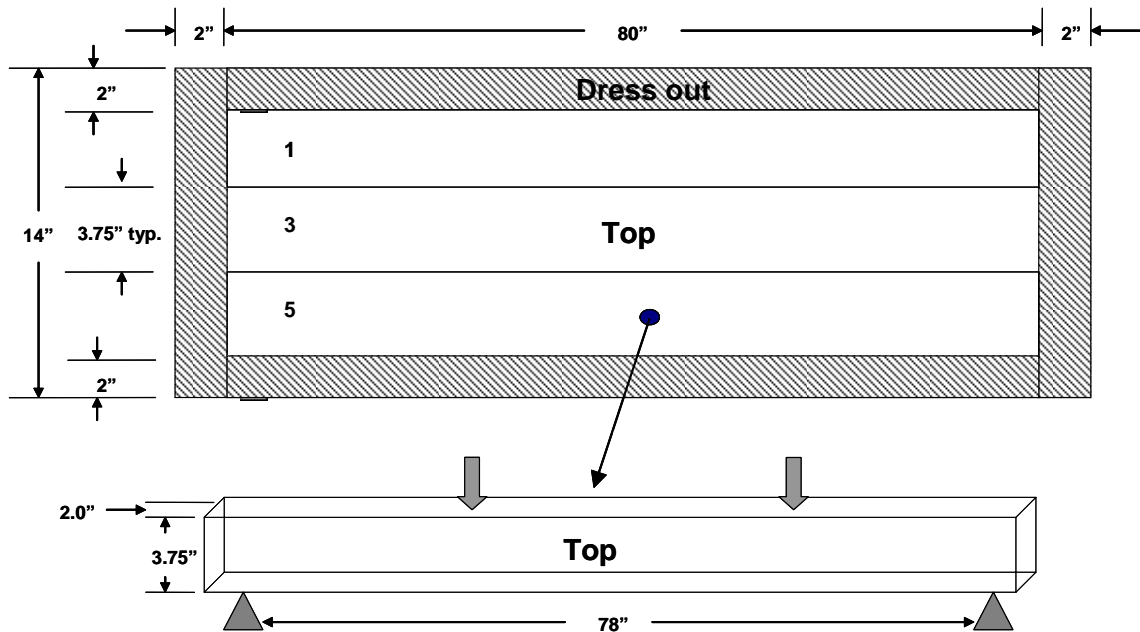


Figure 4.14 – Diagram of lapped billet breakdown into beams

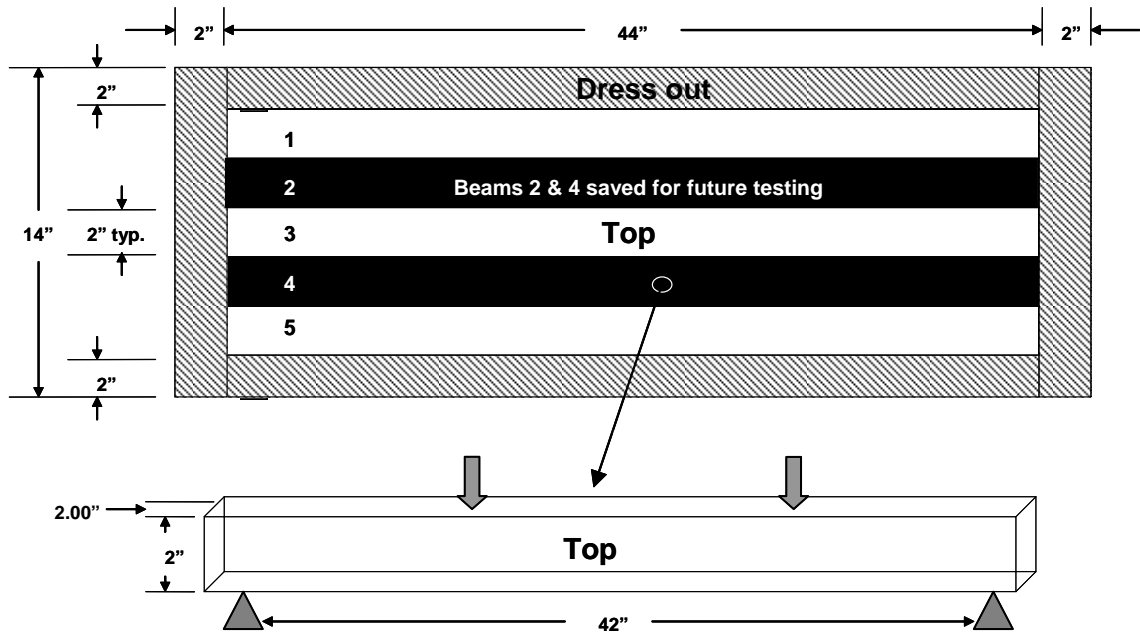


Figure 4.15 – Diagram of non-lapped billet breakdown into beams

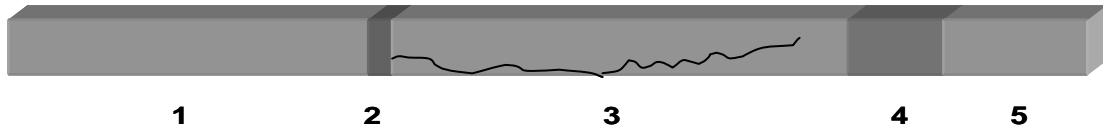
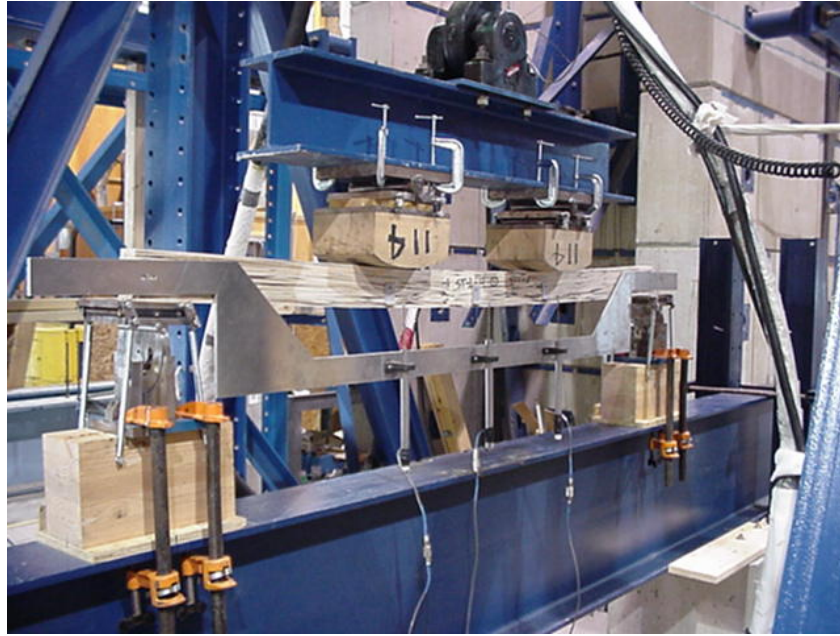


Figure 4.16 – Diagram of breakdown of beams into specimens for further testing

#### 4.2.2. Flexural Testing

Flexural testing under third-point loading was carried out on all beams in accordance with ASTM D198 (ASTM, 1999). Lapped beams were tested first, followed by non-lapped. A random number table was used to choose the order in which beams were tested. Loads were applied with a Shore Western 3,000 psi hydraulic actuator mounted to a steel H-frame, rigged with a Lebow Inc. 55 kip load cell (Figure 4.17).



*Figure 4.17 – Third-point flexural testing setup*

The hard maple load heads had a radius of curvature of 13.2" and 6.1" for the lapped and non-lapped beams, respectively. These load heads were fabricated to conform to the standard that requires the radius of curvature to be between 2 and 4 times the width of the beam. The steel reaction plates ( $\frac{1}{2}$ " x 4" x 6") were rigged with rollers to create a simply supported beam condition.

The crosshead rate was 0.20" (lapped) or 0.15" (non-lapped) per minute. Average time to failure was 9:59 (lapped) and 9:44 (non-lapped) with all beams failing within the prescribed 6 - 20 minute range. Deflection was measured with three  $\pm 2$ ",  $\pm 10$  volt DC, Schaevitz linear variable displacement transducers (LVDTs). The LVDTs were calibrated according to ASTM D6027 (ASTM, 2003). The LVDTs had an allowable percent error of 0.25 ( $0.01$ " accuracy required by ASTM D198 divided by the 4" calibrated range of LVDT \* 100). The LVDTs were mounted on a  $\frac{1}{4}$ " thick aluminum yoke at midspan and under both load heads. The voltages from both the load cell and LVDT's were collected through a 15 channel multiplexing unit and a 12 bit data acquisition card at a rate of 1 point per second. This voltage information was controlled and collected by National Instruments Labview software.

Recording deflection at both midspan and under the load heads allowed for calculation of both apparent ( $MOE_{app}$ ) and true ( $MOE_{true}$ ) modulus of elasticity. This is due to the fact that under third point loading, the area between the load heads is subject to a constant bending moment, meaning no shear stresses exist (Figure 4.18).

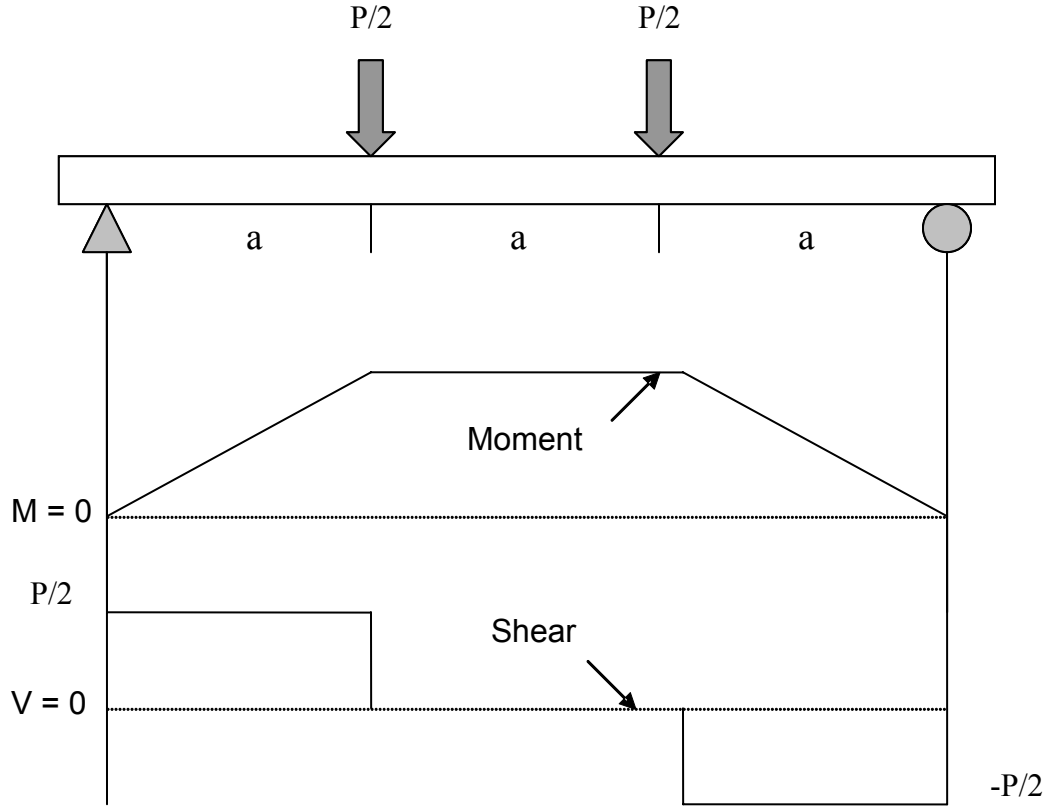


Figure 4.18 - Bending moment and shear diagram for third-point loading

Flexural properties were calculated according to ASTM D198 (ASTM, 1999) as follows:

$$MOE_{app} = \left( \frac{P}{\Delta_{midspan}} \right) \left( \frac{L^3}{4.7bh^3} \right) \quad (4.3)$$

$$MOE_{true} = \left( \frac{P}{\Delta_{loadhead}} \right) \left( \frac{L * \left( \frac{L^2}{3} \right)}{4bh^3} \right) \quad (4.4)$$

$$MOR = \frac{M_{max} C}{I} = \frac{\left( \frac{P_{max} * L}{6} \right) \left( \frac{h}{2} \right)}{\frac{bh^3}{12}} \quad (4.5)$$

Where:

P = Load (lbs)

$\Delta_{loadhead}$  = Average deflection at the loadheads (in.)

$\Delta_{midspan}$  = Deflection at midspan (in.)

P/ $\Delta$  = Slope of the load vs. deflection curve in the range of 200-1000 lbs.

L = Span (78" for lapped beams, 42" for non-lapped)

b = Width (in.)

h = Depth (in.)

$M_{max}$  = Maximum bending moment (in. lbs)

C = Distance from neutral axis to point of maximum bending stress (in.)

I = Moment of inertia (in<sup>4</sup>)

The raw voltage data collected was then transformed to either load or position by first subtracting the reference voltage and then multiplying by the calibration constant (K) of the measuring device. This allowed for calculation of load and deflection at each of the three LVDTs as well as the average deflection at the load heads. Two methods were used to select the linear range used in the MOE calculations. First, a deflection vs. load plot was created for beam #2 from each of the eight treatments. This allowed for a visual approximation of the linear range, which in all cases terminated at 1000 lbs, +/- 100. Figure 4.19 shows a typical graph.

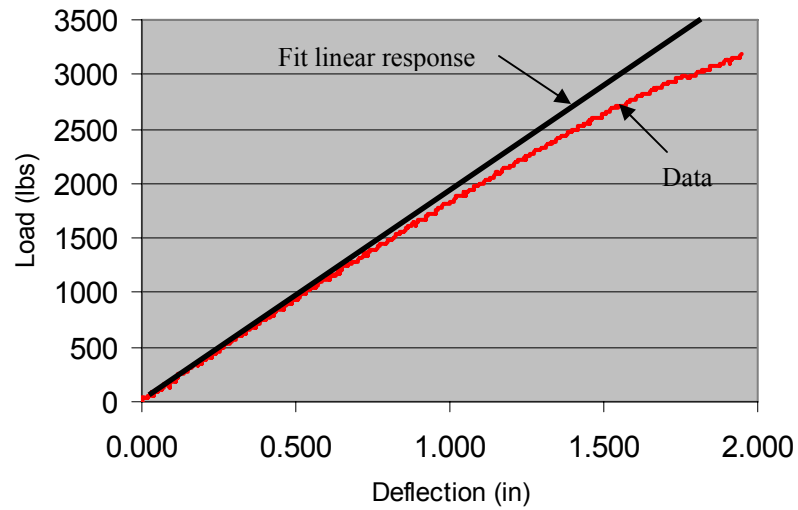


Figure 4.19 – Typical full-range load vs. deflection curve for flexural test

A second method was employed which calculated the slope of the load (P) vs. deflection ( $\Delta$ ) curve, the apparent and true MOE as well as the E/G ratio for a variety of ranges. This was done again on beam #2 from each of the eight treatments. An example from one beam is shown in Table 4.8.

Table 4.8 –Change of slope in the load-deflection curve and MOE with varying linear ranges

Lb range	P/ $\Delta$ slope - LH	P/ $\Delta$ slope - MS	MOE app	MOE true	E/G
200-3000	12562	1695	1.67	1.62	-15
$r^2$	0.9929	0.9974			
200-2500	13396	1769	1.74	1.72	-5
$r^2$	0.9939	0.9991			
200-2000	14376	1812	1.79	1.85	16
$r^2$	0.9944	0.9993			
200-1500	15521	1846	1.82	2.00	45
$r^2$	0.9953	0.999			
200-1000	16834	1878	1.85	2.17	79
$r^2$	0.9942	0.9979			
200-500	15056	1827	1.80	1.94	35
$r^2$	0.9591	0.9878			

Although only the cases with the lower load range limit of 200 lbs are presented here, similar tables were created with lower range values of 100 and 300 lbs. as well. Note that the first two ranges in the table have negative E/G ratios, which are not possible and indicate being clearly beyond the linear range. The 200 –

1000 lb range gave the highest slope and therefore largest MOE value. When results from these two methods were taken together, it was decided that the most appropriate and consistent linear range was 200 – 1000 lbs.

#### 4.2.3. Shear Testing

##### 4.2.3.1. Shear Modulus

Shear modulus, also known as modulus of rigidity (G) was calculated for all beams. As  $MOE_{true}$  was already determined, G could be back-calculated by rearranging Eq. 4.6 to solve for G (Eq. 4.7):

$$MOE_{true} = \frac{\left( \frac{P}{\Delta_{midspan}} \right) * L^3}{4.7bh^3 \left( 1 - \frac{\frac{P}{\Delta_{midspan}} * L}{5bhG} \right)} \quad (4.6)$$

$$G = \frac{\left( \frac{P}{\Delta_{midspan}} \right) * L}{5bh \left( 1 - \frac{\frac{P}{\Delta_{midspan}} * L^3}{4.7bh^3 * MOE_{True}} \right)} \quad (4.7)$$

Where:

P = Load (lbs)

$\Delta_{midspan}$  = Deflection at midspan (in.)

P/ $\Delta$  = Slope of the load vs. deflection curve in the range of 200-1000 lbs.

L = Span (78” for lapped beams, 42” for non-lapped)

b = Width (in.)

h = Depth (in.)

For comparative purposes, G was also determined using the test methods described in ASTM D198 (ASTM, 1999). Four beams were tested, one from each of the lapped beam combinations (LS-L, SS-L, LT-L, ST-L) prior to being tested in flexure to failure as described above. The test was conducted by center-point flexural loading of the beams over four different spans. As prescribed, the four spans were chosen to give equal increments of  $(h/L)^2$  between them, within the range of 0.0025 – 0.035. With  $h=3.75$ ”

for the lapped beams, the following four  $(h/L)^2$  points were calculated: 0.0025, 0.0133, 0.0242, 0.035. From these, the four spans (and l/d ratios) were calculated as 75" (20), 32.5" (8.7), 24.1" (6.4), 20" (5.3).  $MOE_{app}$  was calculated for each span, with deflection measured to within 0.001" using a dial indicator. The shear modulus is proportional to the best-fit line of the plot of  $(h/L)^2$  vs.  $1/MOE_{app}$ . Shear modulus was then calculated as  $1.20/\text{slope of the } (h/L)^2 \text{ vs. } 1/MOE_{app}$ .

#### **4.2.3.2. Shear Strength**

Maximum shear strength was determined in two ways: Shear blocks and short-span beams forced into shear failure. Both tests were conducted on a 22 kip Instron Universal Testing Machine.

##### **4.2.3.2.1. Shear Blocks**

Shear blocks (Figure 4.20) were made and tested according to ASTM D143 (ASTM, 2000).

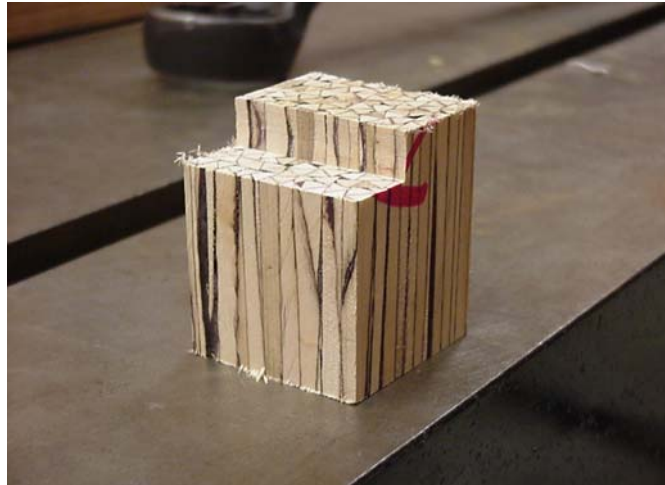


*Figure 4.20 – A typical shear block*

The blocks were tested in a shear fixture attached to the Instron testing machine (Figure 4.21). Specimens were tested at a crosshead rate of 0.020" per minute. Although D143 requires testing in both the LX and LY planes, this was not done due to presumed transverse isotropy (see Sections 2.4.2 and 3.5.2).

Maximum shear strength was calculated as:

$$\tau_{\max} = \frac{P}{A} \quad (4.8)$$

Where:

$\tau_{\max}$  = Maximum shear strength (psi)

P = Load at time of shear failure (lbs)

A = Shear area (in<sup>2</sup>)



*Figure 4.21 – A shear block specimen loaded in the test fixture*

#### **4.2.3.2.2. Short-Span Shear Beams**

Although a specific standard to determine maximum shear strength using short-span beams does not exist for wood, ASTM D198 (ASTM, 1999) does address testing beams in flexure to evaluate shear properties (Section 8.5.1), noting that span/depth ratios less than 10 provide a high percentage of shear failures.

The critical span required to ensure shear failure of a short beam tested in flexure can be estimated if approximate values of MOR ( $\sigma_{\max}$ ) and maximum shear strength ( $\tau_{\max}$ ) are known. Average  $\sigma_{\max}$  was known from flexural testing, with averages of 8,760 and 10,533 psi for lapped and non-lapped beams respectively. Maximum shear strength values for this material were not known. The Wood Handbook gives an average maximum shear value parallel to grain of 1,850 psi (12% MC) for red maple. However,

this is for small, clear, solid wood specimens. The shear strength design value for PSL (the most similar SCL product to LSSCL) is 290 psi. Multiplying by the safety factor of 3.15 (specified in D5456) gives 914 psi. As this represents the lower fifth percentile value, using 1,000 psi should give a conservative average value.

The testing of short-span shear beams is performed using center-point loading. Therefore:

$$M_{\max} = \text{Maximum bending moment} = PL/4 \quad (4.9)$$

$$\sigma_{\max} = (M_{\max}(c))/I = (3PL)/(2bh^2) \quad (4.10)$$

$$\tau_{\max} = (3P)/(4A) \quad (4.11)$$

P, the force required to break the beam in shear, can then be calculated:

$$\begin{array}{l} \text{Lapped} \\ \tau_{\max} = (3P)/(4A) \end{array}$$

$$1000 \text{ psi} = (3P)/30$$

$$P = 10,000 \text{ lbs}$$

$$\begin{array}{l} \text{Non-lapped} \\ \tau_{\max} = (3P)/(4A) \end{array}$$

$$1000 \text{ psi} = (3P)/16$$

$$P = 5,333 \text{ lbs}$$

Using the flexure formula (4.10) and solving for L (4.12), the span at which the beam is equally likely to fail in bending or shear is calculated.

$$L = (\sigma_{\max} 2bh^2)/(3P) \quad (4.12)$$

Lapped

$$L = (8,760 * 2 * 2 * 3.75^2) / (3 * 10,000) = 16.43''$$

Non-lapped

$$L = (10,533 * 2 * 2 * 2^2) / (3 * 5,333) = 10.53''$$

ASTM D198 (ASTM, 1999) offers a simplified approach by solving equations 4.11 and 4.12 simultaneously, yielding the following relationship:

$$\frac{a}{h} = \frac{MOR}{4\tau} \quad (4.13)$$

Where:

a = span/2 (in.)

h = depth of beam (in.)

$\tau$  = maximum shear strength (psi)

This allows for a prediction that beams with span/depth ratios less than 16” (lapped) or 10” (non-lapped) will provide a high percentage of shear failures. Spans chosen were 14” and 7.5” for lapped and non-lapped beams respectively, giving an l/d ratio in both cases of 3.75.

All beams were tested in center-point loading (Figure 4.22) at a crosshead rate of 0.15” (lapped) or 0.10” (non-lapped) per minute.



*Figure 4.22 – Short-span shear test setup*

Maximum shear strength was calculated as:

$$\tau_{\max} = \frac{3V}{2A} = \left( \frac{3P}{4A} \right) \quad (4.14)$$

#### **4.2.4. Volumetric Shrinkage, Void Volume and Adhesive Joint Integrity**

Volumetric shrinkage, void volume and adhesive joint integrity were evaluated simultaneously using modified ASTM test methods D143 (ASTM, 2000) and D1101 (ASTM, 1997). This simultaneous procedure was carried out as it allowed for maximum data acquisition given time and money constraints.

#### 4.2.4.1. Volumetric Shrinkage

Volumetric shrinkage tests were carried out on the lapped beams only, as remnants of sufficient size did not exist for the non-lapped beams (Figure 4.16, #5). One specimen was tested from each lapped beam, for a total of 48. The specimen dimension of 2" x 2" x 6" required by ASTM D143 could not be obtained consistently, therefore the test beams had dimensions of only 2" x 2" x 4". Weights (to 0.0001g) and dimensions (to 0.0005") were determined using an Ohaus electronic balance and Starrett digital calipers, respectively. The testing was conducted as follows:

1. Weight and volume (external dimensions) were taken on the conditioned specimens (at approximately 10% MC).
2. Specimens were submerged under water in a pressure vessel, separated by stickers and weighted down. A vacuum of 25 mm Hg was drawn and held for 30 minutes.
3. The vacuum was released and air pressure of 75 psi applied for 2 hours.
4. Specimens were drip dried and weighed.
5. Green volume was determined with both calipers and water submersion according to ASTM D2395 (ASTM, 2002).
6. Specimens were oven dried at 219° F for 24 hours in a forced hot air oven.
7. Weights and volume (with calipers) were measured.
8. Volumetric shrinkage was calculated as:

$$VS = \left( \frac{V_{gx} - V_{od}}{V_{gx}} \right) * 100 \quad (4.15)$$

where:

VS = Volumetric shrinkage (%)

$V_{gx}$  = Green volume based on exterior dimensions ( $\text{in}^3$ )

$V_{od}$  = Oven dry volume ( $\text{in}^3$ )

#### 4.2.4.2. Void Volume

Since green volume was determined with both calipers and water submersion, an approximate void space volume could be calculated:

$$VV = V_{gx} - V_{sub} \quad (4.16)$$

where:

$VV$  = Void volume (in<sup>3</sup>)

$V_{gx}$  = Green volume based on exterior dimensions (in<sup>3</sup>)

$V_{sub}$  = Green volume based on water submersion method (in<sup>3</sup>)

Void volume was then calculated as a percent of green volume:

$$\%VV = \left( \frac{VV}{V_{gx}} \right) * 100 \quad (4.17)$$

where:

$\%VV$  = Percent void volume (%)

$VV$  = Void volume (in<sup>3</sup>)

$V_{gx}$  = Green volume based on exterior dimensions (in<sup>3</sup>)

The accuracy of the two volume measurement methods was of some concern. The water submersion method was considered the most accurate, as specimens were fully saturated (so that no water adsorption occurred during weighing) and surface irregularities were not at issue. However, specimens were submerged only until air bubbles ceased to form (approximately 10 seconds). It is possible that there were void spaces in the interior of the specimens that were completely encapsulated, and remained free of water during submersion. This would lead to an underestimation of the void volume using this method.

Measuring the volume based on exterior dimensions was also problematic. First, void spaces on the surface, especially prevalent with the large square specimens, were not accounted for. This, again, leads to underestimation of the void volume. Also, as will be seen in the following section, some specimens distorted considerably during cycling and therefore taking measurements at only one point along the specimen calls into question the accuracy of the readings. However, while the precision of the nominal

measurements of volumetric shrinkage and void volume are in question, the relative comparison was of primary concern and is likely still valid.

#### **4.2.4.3. Adhesive Joint Integrity**

Both ASTM D1101 (ASTM, 1997) and ASTM D2559 (ASTM, 2003) require calculation of a percentage of adhesive failure at the bondline. This was not feasible with LSSCL, for a couple of reasons. First, the bondlines were too numerous and small to precisely quantify delamination. Second, as void spaces are inherent to the product, it is difficult to differentiate between void space and delamination. Because of this, only a qualitative evaluation of bondline quality could be made.

Following the calculation of volumetric shrinkage and void volume, the same 48 specimens were qualitatively evaluated for bondline quality. The specimens were visually examined to look for any clear signs of delamination. An attempt was then made to break the specimens apart by hand.

ASTM D2559 is considered a more rigorous test of adhesive quality than that of D1101. In addition to the vacuum/pressure soaking, specimens are subjected to steaming, and the cycle is repeated three times. To further evaluate the quality of the adhesive bond, two samples of each lapped geometry (total of 8 specimens) were cut (2" x 3.75" x 4") and tested under D2559. Evaluation of the bondline was performed as described above.

#### **4.2.5. Property Adjustments**

##### **4.2.5.1. Adjustments for Moisture Content**

As moisture content (MC) is known to have a significant effect on mechanical properties, all test values obtained were adjusted to the average MC of that property according to Eq. 4.18 (ASTM D2915, 1998).

$$P_2 = P_1[(\alpha - \beta M_2)/(\alpha - \beta M_1)] \quad (4.18)$$

Where:

$M_1$  = MC of test specimen (%)

$M_2$  = Average MC of all test specimens of that property (must be  $\leq 22\%$ ) (%)

$P_1$  = Property at test MC

$P_2$  = Property adjusted to average MC of that property

$\alpha$  = Moisture content constant (MOE = 1.44; MOR = 1.75; Shear = 1.33)

$\beta$  = Moisture content constant (MOE = 0.0200; MOR = 0.0333; Shear = 0.0167)

#### 4.2.5.2. Adjustments for Density

An adjustment for the difference in density was required in order to allow for proper treatment comparisons without the significant confounding of density differences. Since slight moisture content variation existed from beam to beam, adjustments were made based on specific gravity (Oven-dry weight, volume at test MC basis) rather than density. Density was converted to specific gravity using equation 4.19.

$$SG = \frac{\left( \frac{Density \frac{lbs}{ft^3}}{1 + \left( \frac{MC}{100} \right)} \right)}{62.4 \frac{lbs}{ft^3}} \quad (4.19)$$

Although clear positive correlations exist between specific gravity and mechanical properties, there is differing opinion as to the exact mathematical nature of this relationship. Bodig & Jayne (1982) found that an exponential relationship best described the variation of the mechanical property over the entire range of densities used in their experiment. Equation 4.20 presents the reduced equation they used to adjust values for changes in specific gravity.

$$Y_1 = Y(D_1/D)^b \quad (4.20)$$

Where:

$Y_1$  = value at new specific gravity

$Y$  = Initial value

$D_1$  = New specific gravity

$D$  = Initial specific gravity

$b$  = exponent for strength property

The Wood Handbook (USDA, 1999) also reports an exponential relationship, though it uses different exponents. A comparison of the exponents used by both the Wood Handbook and Bodig & Jayne for the mechanical properties to be determined in this experiment is presented in Table 4.9.

*Table 4.9 – Comparison of exponents used to adjust mechanical properties for specific gravity*

<b>Property</b>	<b>Bodig &amp; Jayne<sup>a</sup></b>	<b>Wood Handbook<sup>a</sup></b>
MOE	1.00	0.70
MOR	1.25	1.13
Shear parallel	-	1.13

<sup>a</sup> Values based on wood at 12% moisture content

It is important to note that these exponential expressions were derived from experiments on clear, solid wood. It cannot be determined at this point whether these equations accurately predict changes in mechanical properties of the LSSCL wood composite being manufactured and tested in this experiment. Experiments by Barnes (Barnes 2000), however, verified use of these exponential equations for numerous wood composites.

MOE, MOR and maximum shear strength were adjusted to the average specific gravity of all beams tested using the equations from the Wood Handbook. These were chosen over those in Bodig & Jayne for three reasons: (1) A value for shear parallel to grain was included, (2) Values were given for hardwoods and softwoods and, (3) The data is likely more up to date.

#### **4.2.6. Testing Data Collection**

Testing data was collected on all appropriate variables. The full data set is included as Table A.4 in Appendix A.

#### **4.3. Statistical Methodology**

This section provides specific details of how the statistical analysis was conducted. Most of the information was taken from Steel et al (1997). All analyses were done with the SAS statistical software package, Version 8.1.

#### 4.3.1. Main Factors and Levels

The three main factors, along with the 2 levels of each factor, are restated.

Factor A: Strand size

Factor B: Strand geometry

Factor C: Billet lay up

$a_1$  = Large (7/16")

$b_1$  = Square

$c_1$  = Laps

$a_2$  = Small (1/4")

$b_2$  = Triangle

$c_2$  = No laps

#### 4.3.2. Hypothesis Testing

The factorial design allows for testing of both main as well as simple effects (interactions between these effects) (Steel et al., 1997). Since the three main factors each have only two levels, seven single-degree-of-freedom hypotheses (F-tests) may be tested. The null hypothesis ( $H_0$ ) in each case is that no significant difference exists. Each of the seven hypotheses is presented, and an example of the specific hypothesis test is provided for the first test in each category.

##### Main effects

1. Factor A ( $a_1$  vs.  $a_2$ ): Do large strands perform equally to small?

$$H_0: a_1b_1c_1 + a_1b_1c_2 + a_1b_2c_1 + a_1b_2c_2 - a_2b_1c_1 - a_2b_1c_2 - a_2b_2c_1 - a_2b_2c_2 = 0$$

2. Factor B ( $b_1$  vs.  $b_2$ ): Do square strands perform equally to triangles?
3. Factor C ( $c_1$  vs.  $c_2$ ): Do billets with laps perform equally to non-lapped?

##### Simple effects (Two-way Interaction)

4. Factor A x B (A vs. B): Is response to strand size equal at the different levels of geometry?

$$H_0: a_1b_1c_1 + a_1b_1c_2 - a_2b_1c_1 - a_2b_1c_2 = a_1b_2c_1 + a_1b_2c_2 - a_2b_2c_1 - a_2b_2c_2$$

5. Factor A x C (A vs. C): Is response to strand size equal at different levels of lay-up?
6. Factor B x C (B vs. C): Is response to strand geometry equal at different levels of lay-up?

##### Simple effects (Three-way Interaction)

7. Factor A x B x C (A vs. B vs. C): Is response to strand size equal at the different levels of geometry and lay-up?

$$H_0: a_1b_1c_1 + a_1b_1c_2 - a_2b_1c_1 - a_2b_1c_2 - a_1b_2c_1 - a_1b_2c_2 + a_2b_2c_1 + a_2b_2c_2 = 0$$

#### 4.3.3. Analysis of Variance

In order to confirm or refute the seven hypotheses for each dependent variable, an analysis of variance (ANOVA) procedure was performed. The PROC GLM (General Linear Model) command was used. The linear model is shown in Equation 4.21. Table 4.10 presents the analysis of variance table.

$$Y_{ijk} = \mu + \alpha_i + \beta_j + \gamma_k + (\alpha\beta_{ij}) + (\alpha\gamma_{ik}) + (\beta\gamma_{jk}) + (\alpha\beta\gamma_{ijk}) + \varepsilon_{ijk} \quad (4.21)$$

Where:

$Y_{ijk}$	= Result (data point)
$\mu$	= Treatment mean
$\alpha_i$	= Component of deviation from mean due to Factor A
$\beta_j$	= Component of deviation from mean due to Factor B
$\gamma_k$	= Component of deviation from mean due to Factor C
$\alpha\beta_{ij}$	= Component of deviation from mean due to the interaction of Factor A and B
$\alpha\gamma_{ik}$	= Component of deviation from mean due to the interaction of Factor A and C
$\beta\gamma_{jk}$	= Component of deviation from mean due to the interaction of Factor B and C
$\alpha\beta\gamma_{ijk}$	= Component of deviation from mean due to the interaction of Factor A, B and C
$\varepsilon_{ijk}$	= Component of deviation from mean not due to any of the factors (error, residual)

The specific model statement used in SAS was:

*MODEL DEPENDENTVARIABLE = Size, Geometry, Laptype, Size\*Geometry, Size\*Laptype, Geometry\*Laptype, Size\*Laptype\*Geometry;*

Table 4.10 –ANOVA table for factorial treatment combination with subsamples

Source	d.f.	Type III SS	Mean Square	F <sub>calc</sub>	Pr > F
<b>Treatment (model)</b>	<b>31</b>				
Strand Size	1				
Geometry	1				
Lap type	1				
Strand Size*Geometry	1				
Strand Size*Lap type	1				
Geometry*Lap type	1				
Strand Size*Geometry*Lap type	1				
<b>Total Experimental Error</b>	<b>24</b>		<sup>a</sup> Best estimate of $(\sigma^2 + s \sigma_E^2)/\sigma^2$		
(within + among exp. units)			$\sigma^2 + s \sigma_E^2$		
<b>Sampling Error</b>	<b>64</b>		Best estimate of $\sigma^2$		
(within exp. units)			$\sigma^2$		
<b>TOTAL</b>	<b>95</b>				

<sup>a</sup> See section 4.3.4 for explanation of symbols

#### 4.3.4. Types of Error Due to Subsampling

The error term of the model statement is composed of the following components (Figure 4.23):

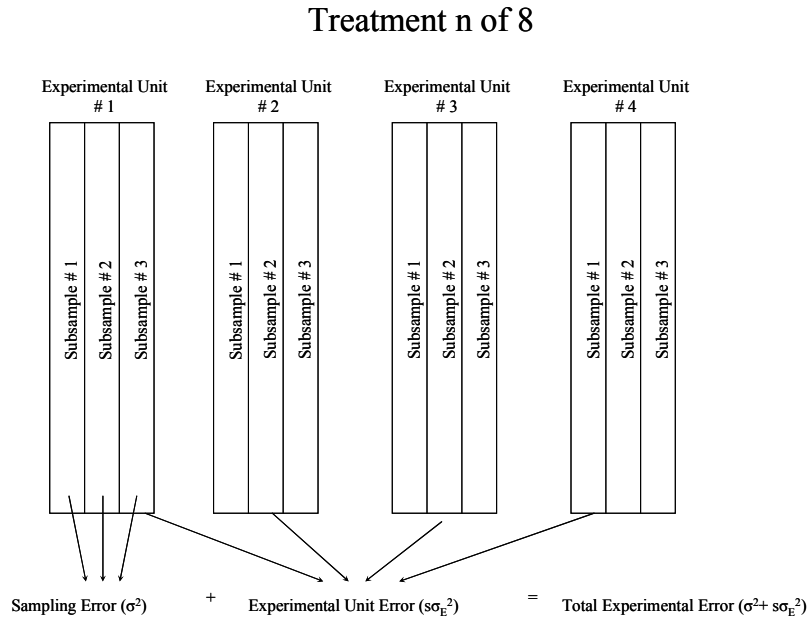


Figure 4.23 – The three types of variation present

1. Sampling Error ( $\sigma^2$ ). The within-experimental-unit error due to subsampling. This is the variation among beams not explained by the model. The sampling error is the best estimate of the population variance.
2. Total Experimental Error ( $\sigma^2 + s\sigma_E^2$ ). The within-experimental-unit error + the among-experimental-unit error. This is the variation among beams plus the variation among billets not explained by the model. This is the term that must be used in hypothesis testing. Since SAS uses Sampling Error as the default, this must be overridden by specifying the Total Experimental Error as the error term in hypothesis testing. The command used was:

```
Test h = Size, Geometry, Laptype, Size*Geometry, Size*Laptype, Geometry*Laptype,
Size*Laptype*Geometry, e = Billetnumber*Size*Geometry*Laptype;
```

Note that this error term is also required when conducting mean separation.

3. Experimental Unit Error ( $\sigma^2_E$ ). The among-experimental-unit-error. Note that this is not explicitly calculated in the analysis. Since Total Experimental Error and Sampling error are known, Experimental Unit Error can be back calculated:

$$\sigma^2_E = ((\sigma^2 + s \sigma^2_E) - \sigma^2) / s \quad (4.22)$$

Most experiments will show that variation among experimental units is greater than variation within experimental units (Steel et al, 1997). This can be determined by looking at the F-test for the experimental error term. The F-Value =  $(\sigma^2 + s \sigma^2_E) / \sigma^2 = 1 + s \sigma^2_E / \sigma^2$  is the ratio of variation among experimental units to variation within experimental units. If the F-test is significant, the variation among experimental units is greater than variation within experimental units.

#### 4.3.5. Sample Statistical Analyses

To explain how the statistical analyses were conducted in this experiment, an actual SAS printout followed by interpretation is presented (Table 4.11). The example that follows uses apparent modulus of elasticity (MOEAPP) as the dependent variable. The lightened text in the table indicates tests which are invalid, either due to use of Type I sums of squares (only valid for equal sample sizes) or use of the incorrect SAS default error term (sampling error) in the denominator of the F value calculation. Probability of > F values in bold text are significant at the chosen alpha level of 0.05.

Some key results of the analysis include:

1. The sampling error,  $\sigma^2$ , is 2,877,336,783, the best estimate of the population variance.
2. The total experimental error,  $\sigma^2 + s \sigma^2_E$ , is 7,938,419,942, the mean square of the Experimental Error term.
3. The experimental unit error can be calculated as  $\sigma^2_E = (\text{Total Experimental Error} - \sigma^2) / \# \text{ subsamples} = (7,938,419,942 - 2,877,336,783) / 3 = 1,687,027,720$ .
4. The F-Test of the experimental error term,  $(\sigma^2 + s \sigma^2_E) / \sigma^2 = 1 + s \sigma^2_E / \sigma^2$  (comparing among-experimental-unit and within-experimental-unit variation), is 0.0007 which is significant, meaning that the variation among billets is greater than within billets. This is a good sign, and shows that the differences in density between beams in a billet likely did not affect the outcome.

Table 4.11 – Sample SAS statistical analysis for 2 x 2 x 2 full factorial

Dependent Variable: MOEAPP					
Source	DF	Sums of Squares	Mean Square	F Value	Pr > F
Model	31	811336011574	26172129406	9.1	<.0001
Error	61	175517543762	2877336783		
Corrected Total	92	986853555336			
	R-Square	COV	Root MSE	MOEAPP Mean	
	0.822144	3.08	53640.81	1739251	
Source	DF	Type I SS	Mean Square	F Value	Pr > F
STRSIZE <sup>a</sup>	1	412815874492	412815874492	143.47	<.0001
GEOMETRY	1	44380670197	44380670197	15.42	0.0002
LAPTYPE	1	123446012130	123446012130	42.90	<.0001
STRSIZE*GEOMETRY	1	24170156714	24170156714	8.40	0.0052
STRSIZE*LAPTYPE	1	5712280756	5712280756	1.99	0.1639
GEOMETRY*LAPTYPE	1	222664012	222664012	0.08	0.7818
STRSIZE*GEOMETRY*LAPTYPE	1	10066274677	10066274677	3.50	0.0662
STRSIZE*GEOM*LAPT*BILLET#	24	190522078595	7938419942	2.76	0.0007
Source	DF	Type III SS	Mean Square	F Value	Pr > F
STRSIZE	1	419764288754	419764288754	145.89	<.0001
GEOMETRY	1	45107472776	45107472776	15.68	0.0002
LAPTYPE	1	117962661602	117962661602	41.00	<.0001
STRSIZE*GEOMETRY	1	24034117883	24034117883	8.35	0.0053
STRSIZE*LAPTYPE	1	5403860030	5403860030	1.88	0.1756
GEOMETRY*LAPTYPE	1	161066850	161066850	0.06	0.8138
STRSIZE*GEOMETRY*LAPTYPE	1	9583912971	9583912971	3.33	0.0729
STRSIZE*GEOM*LAPT*BILLET#	24	190522078595	7938419942	2.76	<b>0.0007<sup>b</sup></b>
Tests of Hypotheses Using the Type III MS for STRS*GEOM*LAPT*BILLE as an Error Term					
Source	DF	Type III SS	Mean Square	F Value	Pr > F
STRSIZE	1	419764288754	419764288754	52.88	<b>&lt;.0001</b>
GEOMETRY	1	45107472776	45107472776	5.68	<b>0.0254</b>
LAPTYPE	1	117962661602	117962661602	14.86	<b>0.0008</b>
STRSIZE*GEOMETRY	1	24034117883	24034117883	3.03	0.0947
STRSIZE*LAPTYPE	1	5403860030	5403860030	0.68	0.4175
GEOMETRY*LAPTYPE	1	161066850	161066850	0.02	0.8879
STRSIZE*GEOMETRY*LAPTYPE	1	9583912971	9583912971	1.21	0.2828

<sup>a</sup> Lightened text represent invalid tests

<sup>b</sup> Bolded Pr>F values indicate a significant difference exists

5. As the probability of a larger F value ( $Pr > F$ ) is less than our chosen alpha level of 0.05 for STRANDSIZE, GEOMETRY and LAPTYPE, we reject the null hypothesis and conclude that apparent modulus of elasticity ( $MOE_{app}$ ) is significantly different for these three variables.
6. No significant differences exist in the remaining tests, meaning there are no significant interactions.
7. The COV of 3.08 % reported is the Within-Experimental Unit COV. That is,  $COV(s) = \sqrt{\sigma^2/\text{mean}}$ . The Among-Experimental Unit COV could also be calculated as  $COV(\text{exp}) = \sqrt{\sigma^2_E/\text{mean}} = 2.36\%$ . Note that these two COV's cannot be compared one to the other, but rather, allow for comparison with future experiments.

Due to the fact that one of the goals of this experiment was to recommend a best-performing treatment for possible production, it was decided that in addition to the factorial analysis, a one-way analysis would also be conducted on the eight treatment groups, followed by mean separation. This approach allowed for ranking of the treatments in order of performance. A sample ANOVA (Table 4.12) as well as mean separation (Table 4.13) are presented. Note that the same  $MOE_{app}$  data used in the factorial analysis is also presented here.

Table 4.12 – Sample SAS one-way ANOVA table

<b>Dependent Variable: MOEAPP</b>					
<b>Source</b>	<b>DF</b>	<b>Sums of Squares</b>	<b>Mean Square</b>	<b>F<sub>calc</sub></b>	<b>Pr &gt; F</b>
Model	31	811336011574	26172129406	9.1	<.0001
Error	61	175517543762	2877336783		
Corrected Total	92	986853555336			
	<b>R-Square</b>	<b>CV</b>	<b>Root MSE</b>	<b>MOEAPP Mean</b>	
	0.822144	3.084134	53640.81	1739251	
<b>Source</b>	<b>DF</b>	<b>Type I SS</b>	<b>Mean Square</b>	<b>F Value</b>	<b>Pr &gt; F</b>
STRANDLAP	7	620813932978	88687704711	30.82	<.0001
STRANDLAP*BILLETNO	24	190522078595	7938419941.5	2.76	0.0007
<b>Source</b>	<b>DF</b>	<b>Type III SS</b>	<b>Mean Square</b>	<b>F Value</b>	<b>Pr &gt; F</b>
STRANDLAP	7	612162206162	87451743737	30.39	<.0001
STRANDLAP*BILLETNO	24	190522078595	7938419941.5	2.76	<b>0.0007</b>
Tests of Hypotheses Using the Type III MS for STRANDLAP*BILLETNO as an Error Term					
<b>Source</b>	<b>DF</b>	<b>Type III SS</b>	<b>Mean Square</b>	<b>F Value</b>	<b>Pr &gt; F</b>
STRANDLAP	7	612162206162	87451743737	11.02	<b>&lt;0.0001</b>

Table 4.13 – Sample SAS mean separation using Tukey's Test

Tukey's Studentized Range (HSD) Test for MOEAPP				
NOTE: This test controls the Type I experimentwise error rate, but it generally has a higher Type II error				
Alpha		0.05		
Error Degrees of Freedom		24		
Error Mean Square		7.93844E9		
Critical Value of Studentized Range		4.68376		
Minimum Significant Difference		122638		
Harmonic Mean of Cell Sizes		11.57895		
NOTE: Cell sizes are not equal.				
Means with the same letter are not significantly different.				
	<b>Tukey Grouping <sup>a</sup></b>	<b>Mean</b>	<b>N</b>	<b>STRANDLAP</b>
B	A	1854912	12	LTNL
	A			
	A	1848641	10	LSNL
	A			
	A	1779806	12	LSLAP
	A			
	A	1751253	12	SSNL
	A			
	A	1750031	12	LTLAP
	A			
B	D	1671777	12	SSLAP
	D			
	D	1650263	11	STNL
	D			
	D	1618138	12	STLAP
	D			

<sup>a</sup> Groupings connected by the same letter belong to the same population

The Tukey test is a conservative mean separation technique, maintaining the risk of a Type I error at 5% for the entire experiment, but increasing the risk of Type II errors (Steel et al, 1997). The Tukey's test was chosen for its analytical rigor. Since gross differences were sought, a mean separation technique that only controls comparisonwise error rates at 5% (such as Fisher's Protected LSD) could also be used with success and would likely find more significant differences than the Tukey's test.

#### 4.3.6. Meeting the Assumptions of ANOVA

Tests were conducted to ensure that the assumptions of the analysis of variance were met (a statistical consultant recommended that this be done on the one-way analysis rather than the factorial). The following two assumptions were tested:

1. Normality - The test of normality was carried out on the residuals. Determination of normality was based on the Shapiro-Wilk W-Statistic. If the probability of  $> W$  was not significant ( $> 0.05$ ), the data was deemed normally distributed.
2. Equality of Variance – A Levene's Test was used to test equality of variance among the eight treatment groups. The Levene's test conducts an analysis of variance on the absolute value of the residuals. If the F-test for the Total Experimental Error term was not significant, variance was deemed equal.

Table 4.14 shows that there were variables (in bold) that did not meet these two assumptions. Note that most of the data was normally distributed, but several had unequal variance. The unequal variance was expected before hand. For example, it was known that the large squares would have significantly larger and more sporadic void spaces and therefore likely have larger variation. Square root and logarithmic transformations were attempted without success.

*Table 4.14 – Meeting the assumptions of ANOVA*

Dependent Variable	ANOVA Assumptions	
	Normality	$\sigma^2$ Equality
	<i>Prob &gt; W</i>	<i>Prob &gt; F</i>
STRAND DENSITY (SG)	0.1189	0.8305
BILLET DENSITY	0.0689	0.1304
BEAM DENSITY	<b>0.0005</b>	0.0889
STRAND MC	0.4495	0.1242
BILLET MC	0.1241	0.0919
BEAM MC	<b>0.0095</b>	<b>0.0154</b>
MOE <sub>APP</sub>	0.3159	<b>0.0378</b>
MOE <sub>TRUE</sub>	0.5021	<b>0.0007</b>
SHEAR MODULUS	<b>&lt;0.0001</b>	<b>0.0019</b>
E/G	0.6463	0.1631
MOR	0.3381	<b>0.0013</b>
SHORT-SPAN SHEAR	0.0654	0.7358
SHEAR BLOCKS	0.5455	<b>0.0365</b>
VOID VOLUME	0.7308	0.2807
VOLUMETRIC SHRINKAGE	0.2079	0.0247

#### 4.3.7. Weighted Least Squares Transformation

It was decided to transform the data for variables that did not meet the normality and equality of variance assumptions using Weighted Least Squares (WLS). The weight was calculated by taking the reciprocal of the variance for each experimental unit (billet). This means that values for beams from billets with higher variance were given less weight, while those from beams with lower variance were given more weight. Equations 4.23 and 4.24 present examples of these weighted calculations:

$$SSE_{Error} = \sum \left( \frac{1}{Variance} \right) (residual)^2 = \sum \left( \frac{1}{Variance} \right) (Y_i - \bar{Y}_{..})^2 \quad (4.23)$$

$$SST_{Total} = \sum \left( \frac{1}{Variance} \right) (Y_i - \bar{Y}_{..})^2 \quad (4.24)$$

Where:

$Y_i$  = Observation value

$\bar{Y}_{..}$  = Mean of beams from that billet

$\bar{Y}_{..}$  = Overall mean of all beams

An example of the SAS printout using WLS is given in Table 4.15. Note that the mean square of the sampling error term is 1.00, indicating that the weighting was done correctly. Also note that the overall mean changes. For this reason, the probabilities from the WLS were be used, but not the means nor COVs.

In terms of mean separation, the SAS help feature (SAS Version 8.1) points out that mean separation of data transformed by WLS is not well understood. For this reason, the mean separation from the ordinary least square (OLS) analysis was used. In comparing the OLS with the WLS printouts for the ongoing example, note that all conclusions regarding significance remain the same with the exception of the Geometry factor which in WLS is now no longer significant.

A table was generated (Table 4.16) to compare the results based on both OLS and WLS. If a difference in the significance of the tests existed, the WLS analysis was used. If there was no difference in significance, the OLS results were used as the multiple comparisons are more clearly matched with the F-test results.

Table 4.15 – Factorial analysis using weighted least squares

Dependent Variable: MOEAPP					
Source	DF	Sums of Squares	Mean Square	F Value	Pr > F
Model	31	980.4	31.63	31.63	<.0001
Error	61	61	1.00		
Corrected Total	92	1041.4			
	R-Square	CV	Root MSE	MOEAPP Mean	
	0.941426	0.000057	1.00	1739428	
Source	DF	Type I SS	Mean Square	F Value	Pr > F
STRSIZE	1	446.8	446.8	446.8	<.0001
GEOMETRY	1	184.2	184.2	184.2	<.0001
LAPTYPE	1	146.9	146.9	146.9	<.0001
STRSIZE*GEOMETRY	1	14.3	14.3	14.3	0.0004
STRSIZE*LAPTYPE	1	5.8	5.8	5.8	0.0188
GEOMETRY*LAPTYPE	1	14.0	14.0	14.0	0.0004
STRSIZ*GEOMET*LAPTYP	1	22.4	22.4	22.4	<.0001
STRS*GEOM*LAPT*BILLE	24	145.7	6.0	6.0	<.0001
Source	DF	Type III SS	Mean Square	F Value	Pr > F
STRSIZE	1	150.4	150.4	150.4	<.0001
GEOMETRY	1	16.1	16.1	16.1	0.0002
LAPTYPE	1	42.2	42.2	42.2	<.0001
STRSIZE*GEOMETRY	1	8.6	8.6	8.6	0.0047
STRSIZE*LAPTYPE	1	1.9	1.9	1.9	0.1690
GEOMETRY*LAPTYPE	1	0.05	0.05	0.05	0.8109
STRSIZ*GEOMET*LAPTYP	1	3.4	3.4	3.4	0.0686
STRS*GEOM*LAPT*BILL	24	145.7	6.0	6.0	<.0001
Tests of Hypotheses Using the Type III MS for STRS*GEOM*LAPT*BILLE as an Error Term					
Source	DF	Type III SS	Mean Square	F Value	Pr > F
STRSIZE	1	150.4	150.4	150.4	<.0001
GEOMETRY	1	16.1	16.1	16.1	0.1158
LAPTYPE	1	42.2	42.2	42.2	0.0144
STRSIZE*GEOMETRY	1	8.6	8.6	8.6	0.2452
STRSIZE*LAPTYPE	1	1.9	1.9	1.9	0.5774
GEOMETRY*LAPTYPE	1	0.05	0.05	0.05	0.9231
STRSIZ*GEOMET*LAPTYP	1	3.4	3.4	3.4	0.4592

Table 4.16 - Difference in significance between OLS and WLS

Dependent Variable	Significant Differences (PROB > F)						
	STRSIZE		GEOMETRY		LAPTYPE		
	STRSIZE	GEOMETRY	LAPTYPE	STRSIZE *	GEOMETRY *	LAPTYPE *	STRSIZE * GEOMETRY
BEAM MC	<b>&lt;0.0001</b>	<b>0.0003</b>	<b>0.0226</b>	0.2497	0.1661	<b>0.0191</b>	0.2492
BEAM MC	<b>0.0001</b>	<b>0.0020</b>	0.0588	0.3465	0.2564	0.0518	0.3460
MOE <sub>APP</sub>	<b>&lt;0.0001</b>	<b>0.0254</b>	<b>0.0008</b>	0.0947	0.4175	0.8879	0.2828
MOE <sub>APP</sub>	<b>&lt;0.0001</b>	0.1158	<b>0.0144</b>	0.2452	0.5774	0.9231	0.4592
MOE <sub>TRUE</sub>	<b>&lt;0.0001</b>	<b>0.0219</b>	<b>0.0005</b>	<b>0.0099</b>	0.1337	0.6132	<b>0.0115</b>
MOE <sub>TRUE</sub>	<b>0.0004</b>	0.1820	<b>0.0337</b>	0.1294	0.3930	0.7765	0.1383
SHEAR MODULUS	0.5057	0.1955	0.2066	0.4153	0.3224	0.3260	<b>0.0162</b>
SHEAR MODULUS	0.7266	0.4925	0.5033	0.6682	0.6018	0.6045	0.1885
MOR	<b>0.0398</b>	0.0516	<b>&lt;0.0001</b>	0.5130	0.6225	0.7825	0.6693
MOR	0.1552	0.1795	<b>&lt;0.0001</b>	0.6580	0.7393	0.8521	0.7729
SHEAR BLOCKS	0.2642	<b>0.0021</b>	0.0989	<b>0.0017</b>	0.9260	0.2424	0.1498
SHEAR BLOCKS	0.4388	<b>0.0260</b>	0.2488	<b>0.0228</b>	0.9490	0.4174	0.3158

☐ Ordinary least squares  
☒ Weighted least squares  
**Bold** Significant Pr < 0.05

<b>0.0000</b>
0.0000

 Border around two cells signifies a difference between significance of OLS and WLS

## **Chapter 5**

### **RESULTS AND DISCUSSION**

The objective of this chapter is to present and discuss the results of the experiment. As LSSCL is a new product concept, focus is given to providing data on as many variables as possible. The chapter begins with discussion of preliminary testing which preceded (and gave reason for) the current experiment. Statistical analysis is then presented on both physical and mechanical variables, first in a three-way factorial structure which looks at the effects of strand size, geometry and lap type. This is followed by a section in which lapped and non-lapped beams are investigated separately using a two-way factorial (size and geometry). Finally, projected design values are presented.

#### **5.1. Preliminary Test Results**

Prior to designing the experiment presented in this thesis, preliminary testing was conducted (a summary of results is presented as Table A.5 in Appendix A). Discussion of the preliminary testing is limited to this section. Beginning in Section 5.2, all discussion pertains to the experiment as described heretofore.

There were three reasons for the preliminary testing:

1. To determine if LSSCL possessed values of MOE and MOR that would allow it to compete in the SCL market. The results, albeit with small sample sizes and values unadjusted for moisture content or density, showed promise. The mean  $MOE_{app}$  was  $1.75 \times 10^6$  psi, and an  $F_b$  (based on the volume adjusted minimum for the treatment) of 3,792 psi. The project, as explained in this thesis, was undertaken based on the promise of these initial results.
2. To determine if liquid or powdered PF resins would be used. An analysis of variance showed that liquid resin gave significantly higher MOE and MOR values and was thus selected.
3. To provide a rough estimate of the variance, which was useful in the selection of appropriate sample size.

## 5.2. Statistical Analysis

Statistical analyses were conducted on the fifteen physical and mechanical properties listed in Table 5.1. (coding used in the analyses is presented in Appendix B). The table specifies the statistical design(s) as well as least square method used in the analysis of variance. The statistical design chosen depended on the information desired for the given variable. In some cases one method was sufficient, while in others three separate methods were deemed necessary.

*Table 5.1 – Properties analyzed statistically including design and least square method used*

Dependent Variable		Statistical design method			Least square method
		One- way	Three-way Factorial	Two-way Factorial	
Physical properties					
1	Strand specific gravity	●			Ordinary
2	Billet density	●			Ordinary
3	Beam density	●	●		Ordinary
4	Strand moisture content	●			Ordinary
5	Billet moisture content	●			Ordinary
6	Beam moisture content	●	●		Weighted <sup>a</sup>
7	Void volume	●			Ordinary
8	Volumetric shrinkage	●			Ordinary
Mechanical Properties					
9	Modulus of elasticity (apparent)	●	●	●	Weighted
10	Modulus of elasticity (true)	●	●		Weighted
11	Shear modulus	●	●		Weighted
12	MOE true : Shear modulus ratio	●	●		Ordinary
13	Modulus of rupture	●	●	●	Weighted
14	Maximum shear strength (blocks)	●	●	●	Ordinary
15	Maximum shear strength (beams)	●	●		Ordinary

<sup>a</sup> Weighted method only used in three-way factorial

The one-way analysis was used in all cases as it allowed for ranking of treatments in order of performance. The three-way (2 x 2 x 2) factorial investigated the effects of the three main factors and was especially useful in looking at interactions. The two-way (2 x 2) factorial analyzed the non-lapped and lapped beam data separately. This allowed for determination of a theoretical best-performing strand type (without laps) followed by separate quantification of the best treatment type for possible production (with laps). Sections 5.3 and 5.4 look at the variables that were analyzed with either one-way or three-way analyses. If both

were employed, the three way analysis of variance table is shown, as this provides more information. The two way-analyses are presented in Section 5.5.

The least square method was determined by the equality of variance as described in Section 4.3.6. The weighted method was used only where: 1) The variances were unequal, 2) The weighted least square method found significant differences that varied from the ordinary least square method, and 3) Only for the 3-way factorial design as this was the only method that produced unequal variances (due to lap method).

In order to simplify presentation of the results, only selected statistical data are shown in the sections that follow. In the ANOVA tables, for example, individual F-tests are shown only with 'F' and 'Probability of > F' values, leaving out data such as sums of squares and mean squares. For multiple comparison tables, only the mean groupings are shown.

The results are presented in systematic fashion for each property, including:

1. A summary table of results by treatment, with sample size, mean, standard deviation and coefficient of variation (see Table 5.2). Minimum values are included for MOR and shear properties, which use lower 5<sup>th</sup> percentile exclusion limits (LEL) to derive design values.
2. A graphical representation of these summary results (see Figure 5.1). Error bars are +/- two times the standard error. The standard error was chosen as it allows for an estimation of the 95% confidence interval for the population, as opposed to the sample.
3. A summary of the F-values from the analysis of variance (see Table 5.3). The last column, entitled '<>' is used if a main effect is deemed significant, indicating which of the two levels was greater.
4. Tukey mean separation results, indicating if groups of treatment means belong to the same or different populations (see Table 5.4).

Physical properties are presented first, as they may have a direct effect on mechanical properties.

### 5.3. Physical Properties

Although all mechanical properties were adjusted for density and moisture content, results on these two variables are presented first as they explain some of the physical behavior of this product. Void volume is then investigated, a critical physical parameter due to the principle hypothesis of this experiment that it is reduced void volume which allows for the enhanced mechanical properties of triangular vs. square strand beams. Finally, volumetric shrinkage is covered, an important variable due to the fact that dimensional stability is a commonly referenced asset of many engineered wood products.

#### 5.3.1. Density

As mentioned in Chapter 3, density is a critical physical variable as it is known to be strongly correlated with mechanical properties of wood and wood composites. There are three types of density variation which were of concern: among strands, among billets and among beams. While strand and billet density are not truly response variables, as it is the density of the test beam which will influence mechanical properties, these are important in explaining any density differences among beams.

##### 5.3.1.1. Specific Gravity of Strands

Figure 5.1 and Table 5.2 show the means and relative variation of strand specific gravity for each treatment.

*Table 5.2 – Summary data for strand specific gravity by treatment*

TRT#	TRT Type	n <sup>a</sup>	Mean SG <sup>b</sup>	Std Dev	COV (%)
1	LS-L	60	0.524	0.0136	2.6
2	LS-NL	60	0.546	0.0156	2.8
	<b>LS</b>	<b>120</b>	<b>0.535</b>	<b>0.0185</b>	<b>3.5</b>
3	LT-L	60	0.542	0.0014	0.3
4	LT-NL	60	0.550	0.0047	0.9
	<b>LT</b>	<b>120</b>	<b>0.546</b>	<b>0.0053</b>	<b>1.0</b>
5	SS-L	60	0.546	0.0138	2.5
6	SS-NL	60	0.540	0.0160	3.0
	<b>SS</b>	<b>120</b>	<b>0.543</b>	<b>0.0142</b>	<b>2.6</b>
7	ST-L	60	0.529	0.0117	2.2
8	ST-NL	60	0.526	0.0104	2.0
	<b>ST</b>	<b>120</b>	<b>0.527</b>	<b>0.0104</b>	<b>2.0</b>
	<b>TOTALS</b>	<b>480</b>	<b>0.538</b>	<b>0.0138</b>	<b>2.6</b>

<sup>a</sup> 15 strands/billet \* 4 billets/treatment

<sup>b</sup> Oven dry weight, green volume basis

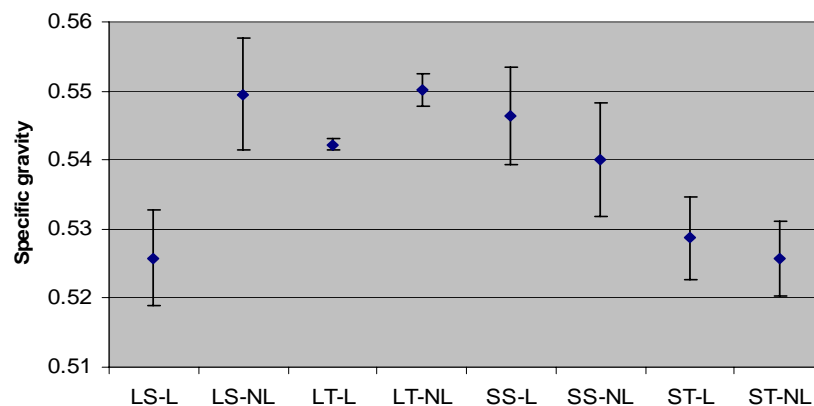


Figure 5.1 – Mean and standard error of strand specific gravity grouped by treatment

A one-way ANOVA was conducted showing that at least one significant difference existed among treatments (Table 5.3). Mean separation allows for determination of where the differences lie (Table 5.4).

Table 5.3 – One-way analysis of variance results for strand specific gravity

Source	DF	F Value	Prob > F
Model	7	5.05	<0.0001
Error	472		
Corrected Total	479		

Table 5.4 – Mean separation for strand specific gravity by treatment

Tukey Grouping <sup>a</sup>			Mean	n	TRT
	A		0.5503	60	LT-NL
	A				
B	A		0.5464	60	LS-NL
B	A				
B	A		0.5462	60	SS-L
B	A				
B	A	C	0.5422	60	LT-L
B	A	C			
B	A	C	0.5401	60	SS-NL
B		C			
B		C	0.5286	60	ST-L
		C			
		C	0.5257	60	ST-NL
		C			
		C	0.5244	60	LS-L

<sup>a</sup> minimum significant difference = 0.0196

Although significant differences did exist among treatments, there was quite a bit of overlap and no treatment stands out as grossly different. The low coefficients of variation indicate that although variation existed among treatments, there was little within treatments.

Comparisons against the means and coefficients of variation (COV) for specific gravity as reported in the Wood Handbook (USDA, 1999) are informative. The mean specific gravity of the 480 strands measured in this experiment (oven dry weight/green volume basis) was 0.54, higher than the reported value of 0.49. As the reported value is calculated as an average of many trees from many regions, this indicates that the average specific gravity of the red maple used in this experiment was higher than average. This may be true for the species in general throughout Maine, or may only be an indication of a higher-than-average specific gravity in the stand from which these trees were harvested. In terms of variation, the total COV of 2.6% was well below the reported average of 10%. It is assumed that such minor variation in strand specific gravity had little effect on the mechanical properties of the composite.

#### 5.3.1.2. Billet Density

Table 5.5 shows the mean out-of-press billet density by treatment. Note that the overall mean was close to the target density of 40.0 lbs/ft<sup>3</sup>, indicating that the calculations used to determine strand mass per billet (Table A.1) were fairly accurate. However, there was a large range of 39.0 (LS-NL) to 42.3 (ST-L). This variation was likely due primarily to uncontrolled and higher spread rates of the triangular treatments.

Table 5.5 – Summary data for out-of-press billet density

TRT#	TRT Type	n	Mean Density <sup>a</sup>	Std Dev	COV (%)
1	LS-L	4	40.2	0.4	1.0
2	LS-NL	4	39.0	0.0	0.1
	<b>LS</b>	<b>8</b>	<b>39.5</b>	<b>0.7</b>	<b>1.8</b>
3	LT-L	4	41.0	0.9	2.3
4	LT-NL	4	40.0	0.3	0.7
	<b>LT</b>	<b>8</b>	<b>40.5</b>	<b>0.8</b>	<b>2.0</b>
5	SS-L	4	40.5	0.5	1.2
6	SS-NL	4	39.5	1.1	2.9
	<b>SS</b>	<b>8</b>	<b>40.0</b>	<b>1.0</b>	<b>2.4</b>
7	ST-L	4	42.3	0.7	1.6
8	ST-NL	4	40.7	1.4	3.4
	<b>ST</b>	<b>8</b>	<b>41.5</b>	<b>1.3</b>	<b>3.2</b>
<b>TOTALS</b>		<b>32</b>	<b>40.4</b>	<b>1.2</b>	<b>2.9</b>

<sup>a</sup> lbs/ft<sup>3</sup> - weight adjusted to 12% MC/volume at MC out of press

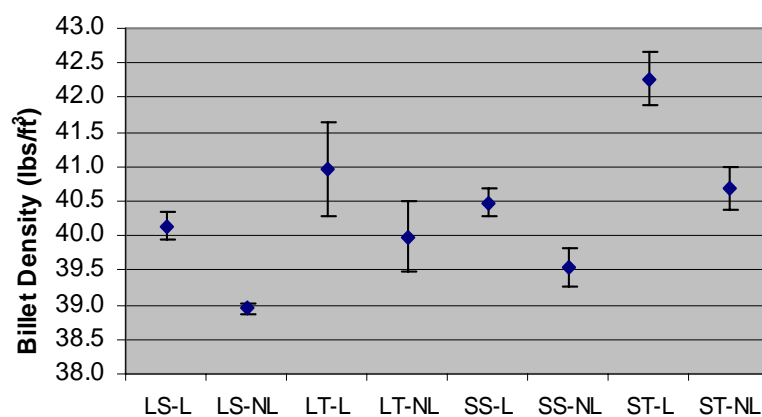


Figure 5.2 – Mean and standard error of billet density grouped by treatment

A one-way ANOVA (Table 5.6) and mean separation were conducted (Table 5.7) showing that significant differences in billet density did exist.

Table 5.6 – One-way analysis of variance results for billet density

Source	DF	F Value	Prob > F
Model	7	6.36	0.0003
Error	24		
Corrected Total	31		

Table 5.7 – Mean separation for billet density by treatment

Tukey Grouping <sup>a</sup>			Mean	n	TRT
	A		42.25	4	ST-L
	A				
B	A		40.95	4	LT-L
B	A				
B	A	C	40.68	4	ST-NL
B	A	C			
B	A	C	40.48	4	SS-L
B		C			
B		C	40.13	4	LS-L
B		C			
B		C	40.00	4	LT-NL
B		C			
B		C	39.53	4	SS-NL
		C			
		C	38.93	4	LS-NL

<sup>a</sup> minimum significant difference = 1.85

Table 5.7 indicates that three separate density populations existed. The large range of 3.4 lbs/ft<sup>3</sup> is alarming, and a more accurate method of quantifying actual spread rates will be needed in future research.

### 5.3.1.3. Beam Density

The previous section looked at density variation among billets, while this section looks at density variation within billets. Density differences among beams (Figure 5.3, Table 5.8) is of importance as any significant variation may confound the results of mechanical testing.

Table 5.8 – Summary data for beam density

TRT #	TRT	n	Mean Density <sup>a</sup>	Std Dev	COV (%)
1	LS-L	12	39.6	1.80	4.5
2	LS-NL	10	38.1	0.97	2.6
	<b>LS</b>	<b>22</b>	<b>38.9</b>	<b>1.63</b>	<b>4.2</b>
3	LT-L	12	39.7	0.76	1.9
4	LT-NL	12	38.9	1.00	2.6
	<b>LT</b>	<b>24</b>	<b>39.3</b>	<b>0.96</b>	<b>2.5</b>
5	SS-L	12	38.7	0.49	1.3
6	SS-NL	12	38.2	1.08	2.8
	<b>SS</b>	<b>24</b>	<b>38.5</b>	<b>0.87</b>	<b>2.3</b>
7	ST-L	12	41.0	0.98	2.4
8	ST-NL	11	39.6	1.28	3.2
	<b>ST</b>	<b>23</b>	<b>40.3</b>	<b>1.29</b>	<b>3.2</b>
	<b>TOTALS</b>	<b>93</b>	<b>39.3</b>	<b>1.38</b>	<b>3.5</b>

<sup>a</sup> lbs/ft<sup>3</sup> - Test weight/Volume @ test MC (~10%)

Theoretically, the mean billet density should equal that of beam density. Note, however, that in all cases the density of beams was less than that of billets, with the total mean being 1.1 lbs/ft<sup>3</sup> less. The principal reason for this difference is that the basis for density measurement changed from weight at 12% MC, volume out-of-press (approximately 12%/7%) for billets, to test weight/test volume (approximately 10%/10%) for beams. In the latter case, the numerator has decreased, while the denominator increased, both of which will lower the resulting calculation. The reason that two different measurement bases were employed is that in the case of billets, the out-of-press MC not only varied (see Section 5.3.2.2), but also was considered suspect as it was measured using a small sample which may not have been representative of the entire billet. An adjustment to a constant MC was therefore required to ensure that the target density was being reached. Beams, on the other hand, were predominantly equilibrated when tested (see Section 5.3.2.3), and actual density at the time of testing was considered most important.

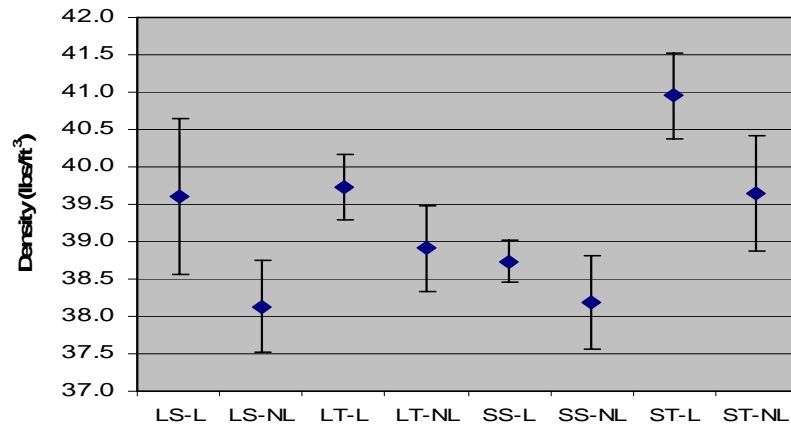


Figure 5.3 – Mean and standard error of beam density grouped by treatment

As seen in Table 5.9, the factorial analysis indicates no significant difference based on strand size, but one for both geometry (TRI>SQ) and lap type (L>NL). The significant F-test for geometry was likely due to the higher spread rate (and percent resin solids) of the triangular strands. For lap type, the difference was likely due to a more accurate calculation of the weight of strands required to achieve the target density (40 lbs/ft<sup>3</sup>) for the lapped beams. As shown in Table 5.8, lapped beam density averaged 39.75 lbs/ft<sup>3</sup>, while non-lapped was only 38.70 lbs/ft<sup>3</sup>. The significant interaction between strand size and geometry is likely due to the even higher spread rate of the small vs. large triangles. If this is true, it is likely that mean separation will show that the ST treatments belong to a higher density population than the LT (Table 5.10).

Table 5.9 – Three-way analysis of variance results for beam density

Source	DF	F Value	Prob > F	< >
Strand size	1	2.01	0.1689	
Geometry	1	37.59	<0.0001	TRI>SQ
Laptype	1	32.58	<0.0001	L>NL
Strand size * Geometry	1	14.51	0.0009	
Strand size * Laptype	1	0.21	0.6514	
Geometry * Laptype	1	0.08	0.7860	
Strand size * Geometry * Laptype	1	3.83	0.0622	

Table 5.10 – Mean separation for beam density by treatment

Tukey Grouping <sup>a</sup>		Mean	n	TRT
A		40.95	12	ST-L
B		39.73	12	LT-L
B				
B		39.65	11	ST-NL
B				
B		39.61	12	LS-L
B				
B	C	38.91	12	LT-NL
B	C			
B	C	38.73	12	SS-L
	C			
	C	38.18	12	SS-NL
	C			
	C	38.13	10	LS-NL

<sup>a</sup> minimum significant difference = 1.20

As predicted from the significant interaction term, the small triangular lapped beams belong to its own population, having significantly higher density than all other treatments. It is important to keep this in mind when interpreting the results of the mechanical properties that follow.

#### 5.3.1.4. Density Profile Among Beams Within Billets

Due to slight bowing of the press frame, along with pre-pressed mounding of the strands, there was concern regarding a potential density profile across the width of the billets (beam 3 being denser than 1 and 5). Table 5.11 shows that this was the case, with center beams being more than 1.5 lbs/ft<sup>3</sup> denser on average than the outer beams.

Table 5.11 – Mean separation for beam density by beam number

Tukey Grouping <sup>a</sup>		Mean	n	BEAM #
A		40.29	32	3
B		38.74	30	5
B				
B		38.69	31	1

<sup>a</sup> Minimum significant difference = 0.58

Although all mechanical properties were adjusted for density, the very significant nature of this variation raised concern that density could still confound the results of mechanical properties, with the center beam possessing significantly higher properties than the outer beams. ANOVA and mean separation for  $MOE_{app}$ , MOR and maximum shear strength (shear blocks) found no significant difference in properties among beams. This gives confidence in the conclusion that the density adjustment successfully prevented any confounding due to density variation. However, future production methods will need to be modified to address this problem.

### **5.3.2. Moisture Content**

As with density, moisture content is known to be strongly correlated with mechanical properties of wood and wood composites (USDA, 1999). However, while density is positively correlated, moisture content exhibits a negative correlation. It was therefore critical to quantify and adjust for any variation in moisture content. Strand and billet MC are not true response variables, as it is the MC of the beams which will influence mechanical properties. However, variation in strand and billet MC is a serious quality control issue, and knowledge of these parameters will allow for modifications to the manufacturing process.

#### **5.3.2.1. Strand Moisture Content**

The principal effect of differing strand moisture content is on pressing performance. Variable strand moisture content can affect the glass transition temperature, stiffness, the dielectric constant, as well as capacitance of the press charge. In all cases, uniformity is desired. Table 5.12 and Figure 5.4 show good uniformity, with all strands within the 6 – 7 % range. This indicates satisfactory kiln and conditioning chamber performance.

Table 5.12 – Summary data for moisture content of strands at time of lay-up

TRT#	TRT Type	n <sup>a</sup>	Mean (%)	Std Dev	COV (%)
1	LS-L	24	6.48	0.19	3.0
2	LS-NL	24	6.33	0.09	1.4
	<b>LS</b>	<b>48</b>	<b>6.41</b>	<b>0.16</b>	<b>2.5</b>
3	LT-L	24	6.04	0.68	11.3
4	LT-NL	24	6.19	0.51	8.3
	<b>LT</b>	<b>48</b>	<b>6.12</b>	<b>0.56</b>	<b>9.2</b>
5	SS-L	24	6.30	0.21	3.3
6	SS-NL	24	6.41	0.28	4.3
	<b>SS</b>	<b>48</b>	<b>6.36</b>	<b>0.23</b>	<b>3.7</b>
7	ST-L	24	6.04	0.39	6.4
8	ST-NL	24	6.41	0.30	4.7
	<b>ST</b>	<b>48</b>	<b>6.23</b>	<b>0.38</b>	<b>6.1</b>
	<b>TOTALS</b>	<b>192</b>	<b>6.28</b>	<b>0.37</b>	<b>5.86</b>

<sup>a</sup> 6 from each of 4 billets

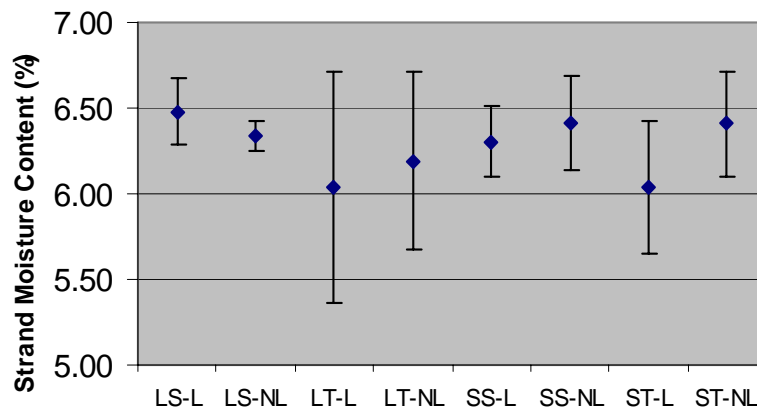


Figure 5.4 – Mean and standard error of strand moisture content grouped by treatment

Table 5.13 – One-way analysis of variance results for strand moisture content

Source	DF	F Value	Prob > F
Model	7	0.94	0.4917
Error	24		
Corrected Total	31		

The analysis of variance (Table 5.13) shows that no significant differences existed among treatments.

Mean separation was therefore not necessary.

### 5.3.2.2. Billet Moisture Content

Table 5.14 indicates that the out-of-press billet moisture content was slightly higher than that of the strands, indicating a net gain in moisture due to the resin.

Table 5.14 – Summary data for out-of-press billet moisture content

TRT#	TRT Type	n	Mean (%)	Std Dev	COV (%)
1	LS-L	4	7.35	0.29	4.0
2	LS-NL	4	7.02	0.21	2.9
	<b>LS</b>	<b>8</b>	<b>7.18</b>	<b>0.29</b>	<b>4.1</b>
3	LT-L	4	6.43	0.69	10.7
4	LT-NL	4	7.73	0.51	6.5
	<b>LT</b>	<b>8</b>	<b>7.08</b>	<b>0.89</b>	<b>12.6</b>
5	SS-L	4	6.21	0.41	6.6
6	SS-NL	4	6.91	0.55	7.9
	<b>SS</b>	<b>8</b>	<b>6.56</b>	<b>0.58</b>	<b>8.9</b>
7	ST-L	4	7.11	0.69	9.7
8	ST-NL	4	7.89	1.41	17.8
	<b>ST</b>	<b>8</b>	<b>7.50</b>	<b>1.11</b>	<b>14.8</b>
	<b>TOTALS</b>	<b>32</b>	<b>7.08</b>	<b>0.82</b>	<b>11.6</b>

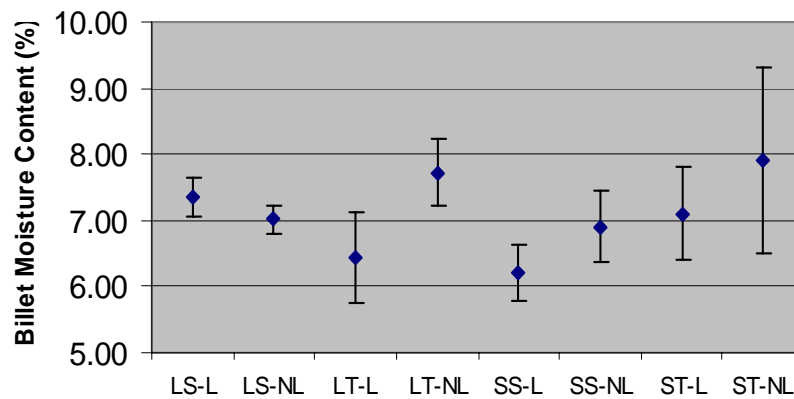


Figure 5.5 – Mean and standard error of billet moisture content grouped by treatment

The analysis of variance indicates that at least one significant difference existed.

Table 5.15 – One-way analysis of variance results for billet moisture content

Source	DF	F Value	Prob > F
Model	7	2.85	<b>0.0259</b>
Error	24		
Corrected Total	31		

A look at the mean separation (Table 5.16), however, indicates that the differences were slight.

*Table 5.16 – Mean separation for billet moisture content*

	<b>Tukey Grouping<sup>a</sup></b>	<b>Mean</b>	<b>n</b>	<b>TRT</b>
	A	7.89	4	ST-NL
	A			
B	A	7.72	4	LT-NL
B	A			
B	A	7.35	4	LS-L
B	A			
B	A	7.11	4	ST-L
B	A			
B	A	7.02	4	LS-NL
B	A			
B	A	6.91	4	SS-NL
B	A			
B	A	6.43	4	LT-L
B				
B		6.21	4	SS-L

<sup>a</sup> minimum significant difference = 1.61

These differences were not of great concern, as all billets were conditioned for a minimum 55 day period following fabrication (Table 5.17). As will be seen in the next section, billets in the chamber the longest did not necessarily have the highest final MC. It is suspected that this was due to differing void space volume by treatment, thereby affecting adsorption rates.

*Table 5.17 – Conditioning time and calculated moisture content of billets by treatment*

<b>Treatment</b>	<b>Days in chamber</b>	<b>Initial MC (%)</b>	<b>Final MC (%)</b>
SS-L	91	6.8	9.5
ST-L	85	7.7	9.5
SS-NL	78	7.3	10.1
ST-NL	76	9.8	10.6
LT-L	70	5.6	8.7
LT-NL	65	7.4	9.9
LS-NL	56	7.3	10.2
LS-L	55	7.2	9.6
<b>MEANS</b>	<b>72</b>	<b>7.4</b>	<b>9.8</b>

### 5.3.2.3. Beam Moisture Content

Following the approximate two month billet conditioning period, beams were ripped and allowed to condition further. It was anticipated that the mean MC of all beams would be fairly uniform. As seen in Table 5.18, this was the case with a full range difference of less than 2%.

Table 5.18 – Summary data for beam moisture content

TRT#	TRT Type	n	Mean (%)	Std Dev	COV (%)
1	LS-L	12	9.18	0.33	3.6
2	LS-NL	10	9.21	0.27	3.0
	<b>LS</b>	<b>22</b>	<b>9.20</b>	<b>0.30</b>	<b>3.3</b>
3	LT-L	12	9.09	0.52	5.2
4	LT-NL	12	10.27	0.21	2.0
	<b>LT</b>	<b>24</b>	<b>9.68</b>	<b>0.72</b>	<b>7.4</b>
5	SS-L	12	9.91	0.43	4.4
6	SS-NL	12	9.86	0.25	2.5
	<b>SS</b>	<b>24</b>	<b>9.88</b>	<b>0.35</b>	<b>3.5</b>
7	ST-L	12	10.55	0.82	7.8
8	ST-NL	11	10.93	0.75	6.9
	<b>ST</b>	<b>23</b>	<b>10.73</b>	<b>0.79</b>	<b>7.4</b>
	<b>TOTALS</b>	<b>93</b>	<b>9.88</b>	<b>0.78</b>	<b>7.9</b>

Figure 5.6, however, shows that small triangles had significantly higher variance than the other treatment groups.

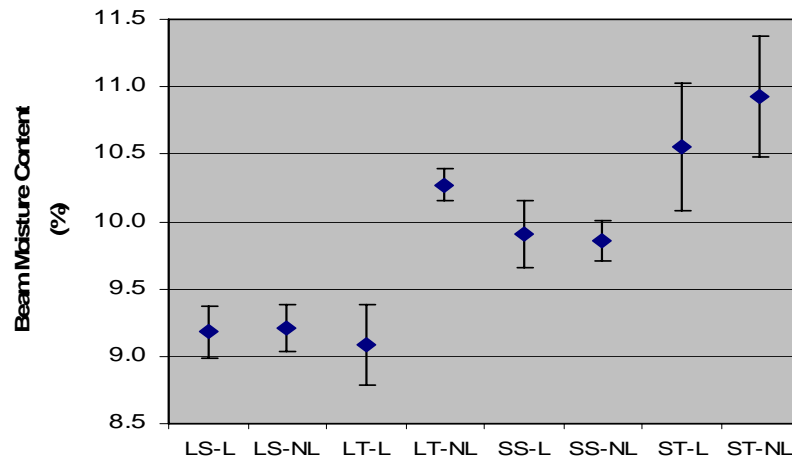


Figure 5.6 – Mean and standard error of beam moisture content grouped by treatment

As seen in Table 5.19 and 5.20, significant differences did exist for strand size and geometry. As expected SM>LG and TRI>SM. Again, this is likely a reflection of the significantly higher spread rate of the small, triangular strands.

Table 5.19 – Three-way analysis of variance results for beam moisture content

Source	DF	F Value	Prob > F	< >
Strand size	1	20.59	<b>0.0001</b>	<b>SM&gt;LG</b>
Geometry	1	12.07	<b>0.0020</b>	<b>TRI&gt;SQ</b>
Laptype	1	3.94	0.0588	
Strand size * Geometry	1	0.92	0.3465	
Strand size * Laptype	1	1.35	0.2564	
Geometry * Laptype	1	4.19	0.0518	
Strand size * Geometry * Laptype	1	0.92	0.3460	

Table 5.20 - Mean separation for beam moisture content by treatment

Tukey Grouping <sup>a</sup>			Mean	n	TRT
	A		10.93	11	ST-NL
	A				
B	A		10.55	12	ST-L
B	A				
B	A		10.27	12	LT-NL
B	A				
B	A	C	9.91	12	SS-L
B		C			
B		C	9.86	12	SS-NL
		C			
		C	9.21	10	LS-NL
		C			
		C	9.18	12	LS-L
		C			
		C	9.09	12	LT-L

<sup>a</sup> minimum significant difference = 1.03

As properties were adjusted for MC, these differences were not considered problematic. Also note that adjustments all fall within the acceptable 5% range required in ASTM D2915 (ASTM, 1998) of the final value of 12%, giving some confidence in the accuracy of the MC adjusted values.

The specimens for shear testing were in the conditioning chamber for approximately two weeks longer than the flexural specimens reported above. As these specimens were much smaller, and conditioned for longer, moisture content uniformity was assumed to be good. Although statistical analysis of the moisture contents of shear specimens is not included, results from Table 5.21 support this assumption. Note that the mean

MC for the shear blocks was exactly the same as the flexural beams, indicating that the latter were equilibrated at the time of testing.

*Table 5.21 – Summary data for moisture content of shear samples*

TRT#	TRT Type	Mean (%)	Std Dev	COV (%)	Mean (%)	Std Dev	COV (%)
Shear blocks				Short-Span Shear Beams			
1	LS-L	9.17	0.27	2.9	9.08	0.24	2.6
2	LS-NL	9.47	0.25	2.6	9.11	0.29	3.2
3	LT-L	9.48	0.42	4.5	9.31	0.26	2.8
4	LT-NL	9.99	0.35	3.5	10.01	0.22	2.2
5	SS-L	9.84	0.32	3.2	9.75	0.20	2.1
6	SS-NL	9.76	0.35	3.6	9.65	0.27	2.8
7	ST-L	10.74	0.62	5.8	10.50	0.70	6.7
8	ST-NL	10.62	0.73	6.9	10.51	0.75	7.2
<b>TOTALS</b>		<b>9.88</b>	<b>0.65</b>	<b>6.6</b>	<b>9.75</b>	<b>0.65</b>	<b>6.7</b>

### 5.3.3. Void Volume

Although an in-depth investigation of packing theory is beyond the scope of this thesis, the principal hypothesis throughout has been that the triangular strands would consolidate better than squares, and therefore have reduced inter-particle void volume. Theoretically, it would also be anticipated that smaller elements would pack better than large and therefore have reduced inter-particle void volume.

Figures 5.9 and 5.10 show a cross section of the four strand types and allow for qualitative confirmation of these assumptions. Keeping in mind the reservations behind the quantification of void volume employed (Section 4.2.4.2), Table 5.22, 5.23 and Figure 5.7 confirm that on a percentage basis, triangles indeed have less void volume than squares, small less than large. Mean separation (Table 5.24) indicates that each of the four strand types belongs to a separate population.

*Table 5.22 – Summary data for void volume*

TRT#	TRT	n	% Void Volume*	Stdev	COV (%)
1	LS-L	12	15.2	1.9	12.3
3	LT-L	12	7.5	2.3	31.1
5	SS-L	12	11.8	2.0	16.8
7	ST-L	12	3.1	1.4	43.4

\*  $(\text{Green volume}_{\text{caliper}} - \text{green volume}_{\text{H20 immersion}}) / \text{Green volume}_{\text{caliper}}$

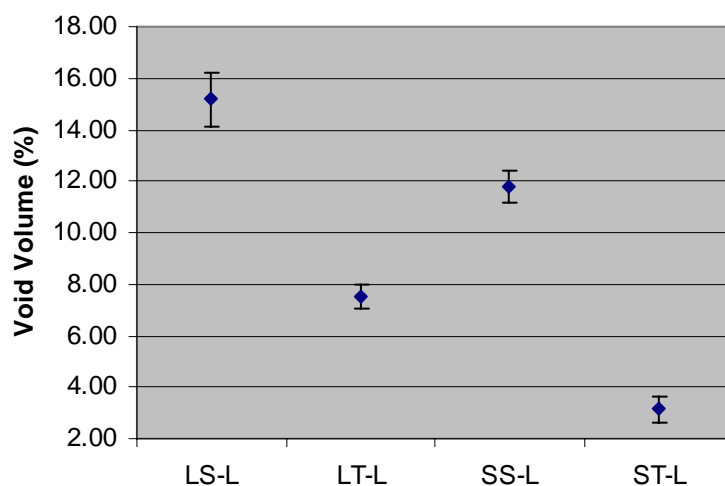


Figure 5.7 – Mean and standard error of void volume grouped by treatment

Note, however, the significantly higher COVs for the triangular treatments. As COV is measured as a percentage of the mean, care must be taken in interpreting and comparing COVs when the means are of significantly different magnitudes (as is the case here, but not for other properties). The ST-L treatment, for example, has by far the largest COV, but also the lowest standard deviation. When this standard deviation is put on a percentage basis of a very small mean, the calculated value is correspondingly high.

Table 5.23 – One-way analysis of variance results for void volume

Source	DF	F Value	Prob > F
Model	3	89.98	<0.0001
Error	44		
Corrected Total	47		

Table 5.24 – Mean separation for void volume by treatment

Tukey Grouping <sup>a</sup>	Mean	n	TRT
A	15.20	12	LS-L
B	11.77	12	SS-L
C	7.53	12	LT-L
D	3.13	12	ST-L

<sup>a</sup> minimum significant difference = 2.08

### 5.3.4. Volumetric Shrinkage

Table 5.25 presents a summary of the volumetric shrinkage results from testing on the lapped beams.

Table 5.25 – Summary data for volumetric shrinkage

TRT #	TRT	n	Mean (%) <sup>a</sup>	Std Dev	COV (%)
1	LS-L	12	10.4	1.8	17.3
3	LT-L	12	12.0	0.8	6.9
5	SS-L	12	11.0	1.1	9.6
7	ST-L	12	11.5	0.9	7.4

<sup>a</sup>  $((\text{Green volume}_{\text{caliper}} - \text{OD volume}_{\text{caliper}}) / \text{Green volume}_{\text{caliper}}) * 100$

All mean values were lower than that reported for solid red maple (12.6%). Two possible explanations for the reduced volumetric shrinkage values for LSSCL include: (1) The 1% wax emulsion included in the resin affected the sorptive properties of the wood and 2) The LSSCL samples were put through a desorption-adsorption-desorption cycle whereas the solid wood only experienced desorption. It is known that once wood is dried, many of the void spaces among the microfibrils close permanently, and are therefore not available as bonding sites for water upon adsorption. This would lead to an anticipated reduced volumetric shrinkage of the previously-dried LSSCL specimens vs. that of specimens only subjected to desorption.

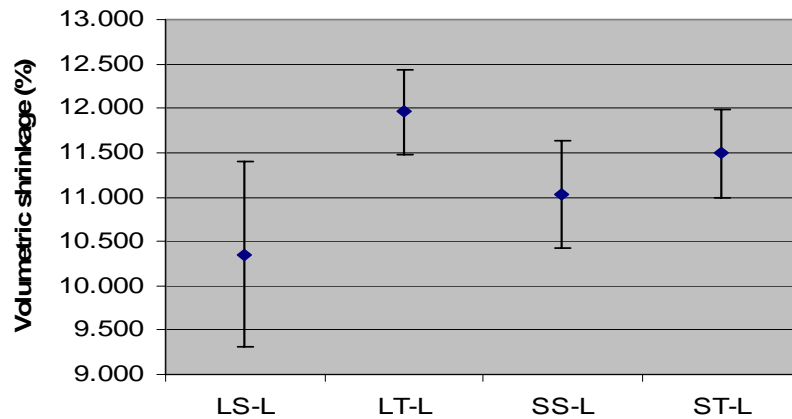


Figure 5.8 – Mean and standard error of volumetric shrinkage grouped by treatment

Note that although LS-L had the lowest mean, it also had significantly higher variability (Figure 5.8). Also note that triangles had larger shrinkage values than squares for a given strand size.

*Table 5.26 – One-way analysis of variance for volumetric shrinkage*

Source	DF	F Value	Prob > F
Model	3	3.85	0.0156
Error	44		
Corrected Total	47		

Mean separation allows for determination of where the differences lie (Table 5.27).

*Table 5.27 – Mean separation for volumetric shrinkage by treatment*

	Tukey Grouping <sup>a</sup>	Mean	n	TRT
	A	0.1196	12	LT-L
	A			
B	A	0.1149	12	ST-L
B	A			
B	A	0.1103	12	SS-L
B				
B		0.1035	12	LS-L

<sup>a</sup> minimum significant difference = 0.0132

Care must be taken in concluding that LS-L was the best performing treatment. The volumetric shrinkage values are based solely on one measurement of width, depth and length for each specimen (it is recommended for future experiments that 2 or 3 measurements of each be taken). As such, these values do not measure differential shrinkage within a specimen. As seen in Figure 5.9, although the LS-L treatment had the lowest volumetric shrinkage values, these specimens often distorted badly.

Comparing the results of void volume and volumetric shrinkage leads to a possible explanation for the distortion of the LS-L treatment (ignoring the possible effect of resin content differences). Since squares and triangles had roughly the same specific gravity, the amount of substance per unit volume is equal on a macro-level. Since void volume was significantly greater for the LS treatment, this must mean that the LS

strands have undergone greater average densification. Due to the variability in the size and location of the voids, with some being quite large, the densification was likely not uniform. It can be expected, then, that differential specific gravity throughout the cross section will lead to differential shrinkage and swelling.

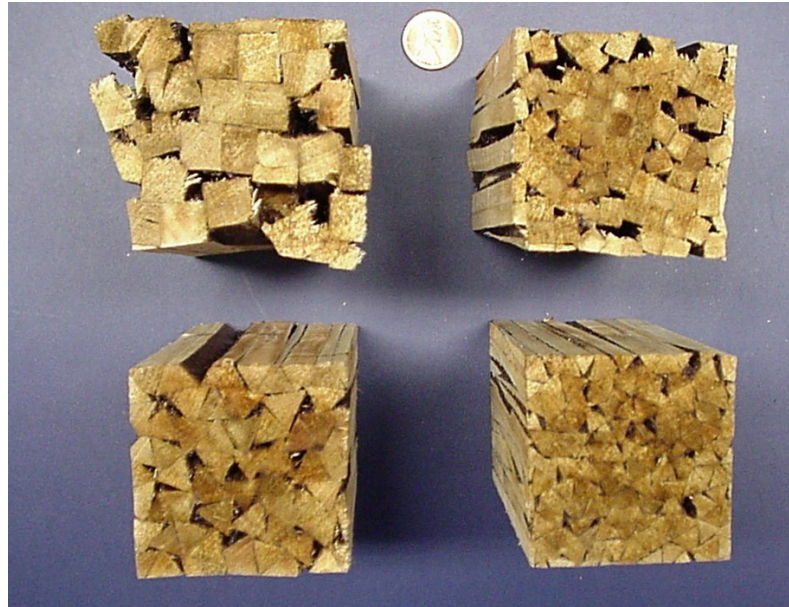


*Figure 5.9 – D1101 specimens showing typical distortion of the square strand treatments*

Future experiments may seek to quantify and predict this differential shrinkage and swelling by reducing the out-of-press composite back to strands and measuring their specific gravity. Based on the qualitative analysis provided herein, it would be predicted that the large square strands would exhibit considerable intra-strand specific gravity variation when compared with triangular strands.

### **5.3.5. Adhesive Joint Integrity**

The objective of ASTM standards D1101 and D2559 (ASTM, 1997, 2003) is to evaluate the performance of the adhesive bond of structural laminated wood products in exterior-use conditions. Both standards require quantification of the delamination present at the bondline. As previously mentioned, this type of calculation is not feasible for LSSCL, as the bondlines are too numerous and too small to accurately measure. It is also often the case, especially for the square strand beams, that an apparent bondline failure

is in fact not due to delamination, but rather a lack of intimate contact and bond formation in the first place (see the square specimens in Figures 5.9 and 5.10). In spite of these issues, a qualitative analysis of the bondline quality was deemed important to ensure integrity of the adhesive joints.

Figure 5.9 shows specimens cycled through D1101. No apparent adhesive failure was noticed, and all 48 specimens tested remained intact following the cycling.

Although similar, the two standards mentioned are different in terms of severity. While D1101 cycles specimens once, D2559 requires three separate cycles and adds an additional step of exposure to steam. As further confirmation of the general quality of the chosen adhesive in the ongoing application, a small sampling of specimens (2 from each of the lapped treatments) were cycled per ASTM D2559. The triangular treatments exhibited good overall quality in terms of both bondline integrity and distortion (Figure 5.10). Although not evident from the figure, the apparent bondline failures in the large, square treatment (upper left) were actually areas where the bondline was never formed, evidenced by the granular, dark purple surface of the strand when forced apart. Note, however, the significant distortion of this specimen.



*Figure 5.10 – D2559 specimens showing good bondline quality of the triangular treatments*

Although this qualitative analysis was useful in predicting satisfactory performance of the chosen adhesive with LSSCL, more accurate quantifications will be required. This can be accomplished by making test beams as prescribed in the two standards mentioned with the various species targeted for this product concept.

#### **5.4. Mechanical Properties**

Tests for all mechanical properties had a sample size of 12 per treatment, with the exception of the Large, Square, Non-Lapped (LS-NL) and Small, Triangle, Non-Lapped (ST-NL) treatments, which had 10 and 11 respectively. The reason for this is that two LS-NL and one ST-NL beams failed in shear during flexural testing. As the objective of the flexural testing was to determine flexural performance, data from these three beams were discarded. Although this data was discarded, tendency to fail in shear is an important consideration. An additional data point for LS-NL (giving a sample size of 9) was discarded for  $MOE_{true}$  and shear modulus, as it contained an unreasonable outlier.

##### **5.4.1. Modulus of Elasticity**

###### **5.4.1.1. Apparent Modulus of Elasticity ( $MOE_{app}$ )**

As SCL is available in larger sizes with considerably higher allowable bending stress than solid lumber, it is often used in long-span situations. Since deflection will often be the limiting design factor for long spans, MOE has increasing importance for SCL products. To compete with LVL and PSL, a  $MOE_{app}$  somewhere between 1,800,000 and 2,000,000 psi is desirable. When making comparisons, note that the length-to-depth ratio for competing SCL products is not indicated. However, as these products fall under AC47 (ICC, 2003), all must comply with the range of 17-21 prescribed in ASTM D5456 (ASTM, 2001). Results of  $MOE_{app}$  for LSSCL are presented in Table 5.28.

Table 5.28 – Summary data for  $MOE_{app}$  of beams

TRT#	TRT Type	n	Mean (psi) <sup>a</sup>	Std Dev	COV (%)
1	LS-L	12	1,779,806	69,890	3.9
2	LS-NL	10	1,848,641	41,341	2.2
	<b>LS</b>	<b>22</b>	<b>1,811,095</b>	<b>67,244</b>	<b>3.7</b>
3	LT-L	12	1,750,031	45,017	2.6
4	LT-NL	12	1,854,912	102,356	5.5
	<b>LT</b>	<b>24</b>	<b>1,802,472</b>	<b>94,071</b>	<b>5.2</b>
5	SS-L	12	1,671,777	49,300	2.9
6	SS-NL	12	1,751,253	38,550	2.2
	<b>SS</b>	<b>24</b>	<b>1,711,515</b>	<b>59,338</b>	<b>3.5</b>
7	ST-L	12	1,618,138	73,359	4.5
8	ST-NL	11	1,650,263	75,572	4.6
	<b>ST</b>	<b>23</b>	<b>1,633,502</b>	<b>74,538</b>	<b>4.6</b>
<b>TOTALS</b>		<b>93</b>	<b>1,739,251</b>	<b>103385</b>	<b>5.9</b>

<sup>a</sup> Adjusted to the average density (39.3 lbs/ft<sup>3</sup>) and a MC (9.88%) of all beams

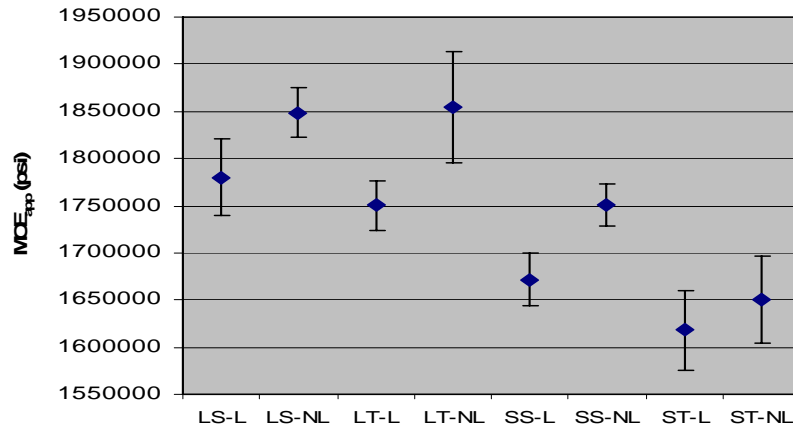


Figure 5.11 – Mean and standard error of  $MOE_{app}$  grouped by treatment

The graphical representation in Figure 5.11 shows two clear trends, one expected and the other not. It was expected that the lapped beams would have lower stiffness values than the non-lapped beams, due to the increased void volume and the negative effect of the lap joint. The non-lapped beams were 4.2% stiffer than the lapped beams, with the difference by strand type being 3.9% (LS), 6.0% (LT), 4.8% (SS) and 2.0% (ST). This indicates that the negative effect of the lap joint on stiffness was most pronounced with the large triangle treatment, and least so with the small triangle. The unexpected result was that larger strands were considerably stiffer than smaller, regardless of geometry. These trends are quantified in Table 5.29.

Table 5.29 – Three-way analysis of variance results for  $MOE_{app}$

Source	DF	F Value	Prob > F	< >
Strand size	1	24.78	<0.0001	LG>SM
Geometry	1	2.66	0.1158	
Laptype	1	6.96	0.0144	NL>L
Strand size * Geometry	1	1.42	0.2452	
Strand size * Laptype	1	0.32	0.5744	
Geometry * Laptype	1	0.01	0.9231	
Strand size * Geometry * Laptype	1	0.57	0.4592	

Table 5.30 – Mean separation for  $MOE_{app}$  by treatment

	Tukey Grouping *		Mean	n	TRT
	A		1,854,912	12	LT-NL
	A				
	A		1,848,641	10	LS-NL
	A				
B	A		1,779,806	12	LS-L
B	A				
B	A	C	1,751,253	12	SS-NL
B	A	C			
B	A	C	1,750,031	12	LT-L
B		C			
B	D	C	1,671,777	12	SS-L
	D	C			
	D	C	1,650,263	11	ST-NL
	D				
	D		1,618,138	12	ST-L

\*minimum significant difference = 122,638

Perhaps most surprising was that the small triangles, regardless of lap type, were the two lowest performing treatments. This was especially surprising since these treatments had significantly higher (more than 1 lb/ft<sup>3</sup>) beam density than any other treatment. Running an ANOVA and mean separation on  $MOE_{app}$  values unadjusted for density should have shown improved performance, as  $MOE_{app}$  is known to be positively correlated with density, everything else being equal. When this analysis was performed, the small triangular treatments were still the two lowest performers.

It was first postulated that this poor performance may be due to the high spread rate, and therefore thicker glue lines of these treatments, which may have had an adverse effect on the consistency and quality of the

bondline. A second hypothesis was that the small triangular strands were damaged upon sawing, causing cracks in the microstructure. As the 1/4" strands were cut on a table saw, with the blade angled at 30°, the distance between the blade and the fence was very small. Boards had to be pushed through with some force, and they could be seen vibrating back and forth upon clearing the blade. If these micro-fractures indeed existed, they may have been deep enough to worsen during pressing. The larger triangles, on the other hand, may have been large enough to avoid this problem. Even if micro-cracks were formed upon sawing, they may have been shallower as a percentage of strand thickness, and therefore not worsened upon pressing.

Both of these hypotheses are supported by Appendix X1.2.2 of ASTM D5456 (ASTM, 2001) which addresses the importance of controlling manufacturing induced defects in the microstructure of both the wood and the bondline. Of particular importance is the adverse affect that these defects may have in terms of sustained-load (creep-rupture) performance (Bledsoe et al., 1990). One study is quoted where two nearly identical aspen LSL beams (densified approximately 50%) were produced, one in a steam-injection press and the other in a conventional hot-platen press. The product made in the hot-platen press had significantly more failures over a six month sustained-load test, assumed to be caused by fractures in the microstructure due to insufficient plasticization during densification. Other suspected reasons were erratic bond quality and damage due to improperly controlled time/temperature cycles. Further research is clearly warranted on the reasons for the poor stiffness performance of the small triangular treatments, including optical investigation of the microstructure of both the wood and bondline, as well as quantifying the time/temperature behavior of the product during RF pressing in order to optimize plasticization.

It is encouraging, however, that the large treatments (both square and triangular) possess  $MOE_{app}$  values that approach or meet the desired minimum of 1,800,000 psi which may allow for competition against existing SCL products. Also promising was the average coefficient of variation value (5.9%), which was considerably lower than the average for solid, clear wood (22%) as reported in the Wood Handbook (USDA, 1999).

#### 5.4.1.2. True Modulus of Elasticity ( $MOE_{true}$ )

Figure 5.12 shows an example of the significantly steeper slope of the load vs. deflection curve for midspan deflection measured relative to the loadhead vs. relative to the reaction.

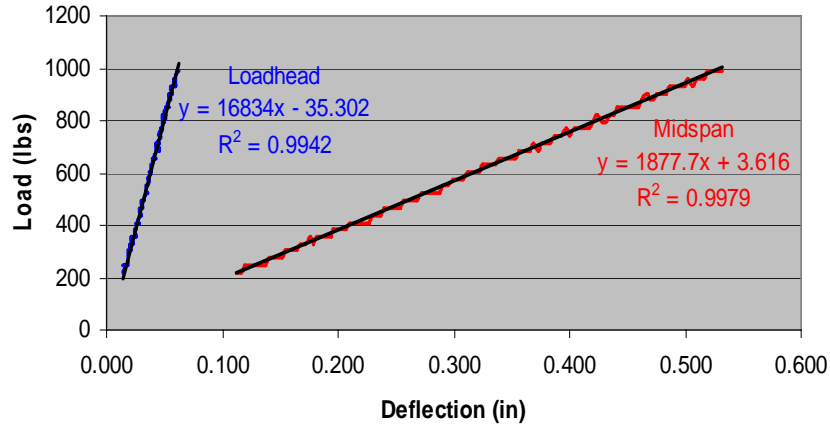


Figure 5.12 – Difference in slope of load-deflection curves recorded at load head and midspan

The reason this occurs is that deflection measured relative to the loadhead is caused solely by bending stress, as there is no shear stress present between the loadheads (Figure 4.18). On the other hand, deflection measured relative to the reactions contains deflection occurring in two zones, one in pure bending stress (between loadheads) and the other a combination of bending and shear stresses (between the loadhead and the reaction). Using only the deflection caused by bending stress allows for calculation of true modulus of elasticity. This is a useful property, as its calculation is not affected by other confounding variables such as varying span-to-depth ratios. Table 5.31 presents the results for  $MOE_{true}$ .

Table 5.31 – Summary data for  $MOE_{true}$  of beams

TRT#	TRT Type	n	Mean (psi) <sup>a</sup>	Std Dev	COV (%)
1	LS-L	12	2,134,706	108,173	5.1
2	LS-NL	9	2,200,809	127,258	5.8
	<b>LS</b>	<b>21</b>	<b>2,163,036</b>	<b>118,479</b>	<b>5.5</b>
3	LT-L	12	2,046,306	139,105	6.8
4	LT-NL	12	2,315,339	168,076	7.3
	<b>LT</b>	<b>24</b>	<b>2,180,823</b>	<b>204,074</b>	<b>9.4</b>
5	SS-L	12	1,962,266	137,255	7.0
6	SS-NL	12	2,105,354	92,206	4.4
	<b>SS</b>	<b>24</b>	<b>2,033,810</b>	<b>135,710</b>	<b>6.7</b>
7	ST-L	12	1,869,811	101,692	5.4
8	ST-NL	11	1,877,844	121,418	6.5
	<b>ST</b>	<b>23</b>	<b>1,873,653</b>	<b>109,035</b>	<b>5.8</b>
<b>TOTALS</b>		<b>92</b>	<b>2,061,619</b>	<b>192,113</b>	<b>9.3</b>

<sup>a</sup> Adjusted to the average density (39.3 lbs/ft<sup>3</sup>) and a MC (9.88%) of all beams

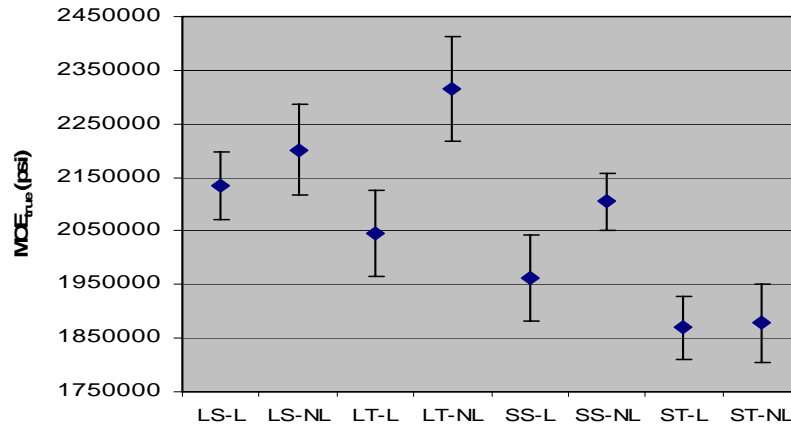


Figure 5.13 – Mean and standard error of  $MOE_{true}$  grouped by treatment

Table 5.32 indicates significant differences were caused by the same factors as for  $MOE_{app}$ .

Table 5.32 – Three-way analysis of variance results for  $MOE_{true}$

Source	DF	F Value	Prob > F	< >
Strand size	1	16.61	<b>0.0004</b>	<b>LG&gt;SM</b>
Geometry	1	1.89	0.1820	
Laptype	1	5.07	<b>0.0337</b>	<b>L&gt;NL</b>
Strand size * Geometry	1	2.47	0.1294	
Strand size * Laptype	1	0.76	0.3930	
Geometry * Laptype	1	0.08	0.7765	
Strand size * Geometry * Laptype	1	2.35	0.1383	

Table 5.33 – Mean separation for  $MOE_{true}$  by treatment

Tukey Grouping <sup>a</sup>			Mean	n	TRT
	A		2,315,339	12	LT-NL
	A				
B	A		2,200,809	9	LS-NL
B	A				
B	A	C	2,134,706	12	LS-L
B		C			
B		C	2,105,354	12	SS-NL
B		C			
B	D	C	2,046,306	12	LT-L
	D	C			
	D	C	1,962,266	12	SS-L
	D				
	D		1,877,845	11	ST-NL
	D				
	D		1,869,811	12	ST-L

<sup>a</sup> minimum significant difference = 201,168

Note that the order of treatments is the same as seen with  $MOE_{app}$ . This indicates that either the deflection caused by shear stress did not vary significantly among treatments, or that the effect of shear deflection is smaller than the treatment effect. If the shear deflection did not vary among treatments, it would be expected that no significant difference of shear modulus among treatments exists (this will be confirmed in the following section).

In terms of the negative effect of the lap joint on  $MOE_{true}$ , the non-lapped beams were 6.1% stiffer than the lapped beams, with the difference by strand type being 3.1% (LS), 13.1% (LT), 7.3% (SS) and 0.43% (ST). As with  $MOE_{app}$ , this indicates that the negative effect of the lap joint on stiffness is most pronounced with the large triangle treatment, and least so with the small triangle.

#### 5.4.2. Shear Modulus (G)

Shear modulus was determined both mathematically (back calculation) and empirically (flexural testing under varying length-to-depth ratios) according to ASTM D198 (ASTM, 1999).

#### 5.4.2.1. Mathematical Calculation of Shear Modulus

Table 5.34 presents a summary of the data for the back-calculated shear modulus.

Table 5.34 – Mathematically determined shear modulus of beams

TRT#	TRT Type	n	Mean (psi) <sup>a</sup>	Std Dev	COV (%)
1	LS-L	12	24,085	5,227	21.7
2	LS-NL	9	26,874	7,809	29.1
	<b>LS</b>	<b>21</b>	<b>25,280</b>	<b>6,435</b>	<b>25.5</b>
3	LT-L	12	32,070	18,155	56.6 <sup>b</sup>
4	LT-NL	12	20,560	4,979	24.2
	<b>LT</b>	<b>24</b>	<b>26,315</b>	<b>14,284</b>	<b>54.3</b>
5	SS-L	12	26,861	7,741	28.8
6	SS-NL	12	23,209	6,062	26.1
	<b>SS</b>	<b>24</b>	<b>25,035</b>	<b>7,051</b>	<b>28.2</b>
7	ST-L	12	27,988	8,507	30.4
8	ST-NL	11	30,478	9,389	30.8
	<b>ST</b>	<b>23</b>	<b>29,179</b>	<b>8,824</b>	<b>30.2</b>
	<b>TOTALS</b>	<b>92</b>	<b>26,461</b>	<b>9,738</b>	<b>36.8</b>

<sup>a</sup> Adjusted to the average density (39.3 lbs/ft<sup>3</sup>) and a MC (9.88%) of all beams

<sup>b</sup> Higher COV due to an outlier - 81,710 psi. If removed, COV would be 35%.

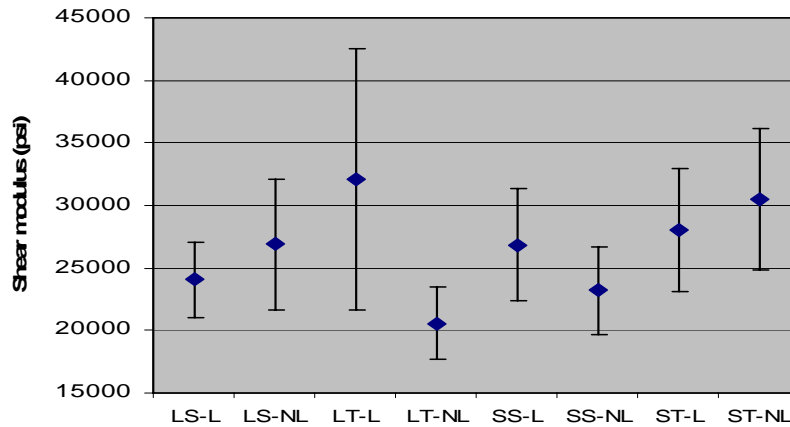


Figure 5.14 – Mean and standard error of shear modulus grouped by treatment

Note in Figure 5.14 that for two strand types (LT, SS) lapped beams had a higher modulus, while for the other two (LS, ST) non-lapped beams were higher. This seemingly indicates that the presence of laps has little if any effect on shear modulus. Also note the significantly higher COVs than those seen for other properties. This is likely due to sensitivity of the back-calculation method to error in the measurement of very small deflections.

Table 5.35 – Three-way analysis of variance results for shear modulus

Source	DF	F Value	Prob > F
Strand size	1	0.13	0.7266
Geometry	1	0.49	0.4925
Laptype	1	0.46	0.5033
Strand size * Geometry	1	0.19	0.6682
Strand size * Laptype	1	0.28	0.6018
Geometry * Laptype	1	0.28	0.6045
Strand size * Geometry * Laptype	1	1.83	0.1885

As no significant differences existed among treatments, mean separation was not necessary.

#### 5.4.2.2. Empirical Determination of Shear Modulus

Table 5.36 contains the results of the flexural testing of one sample beam. Note the very significant effect of the span-to-depth ( $l/d$ ) ratio on the calculation of  $MOE_{app}$ .

Table 5.36 – Empirically determined shear modulus of one beam

Span (in)	$l/d$	Load (lbs)	Def (in.)	$MOE_{app}$ (psi)	$1/MOE_{app}$ (psi)	$(h/L)^2$ (in <sup>2</sup> )
75.0	20	200	0.116	1,757,953	0.0000006	0.0024734
32.5	8.7	200	0.030	553,108	0.0000018	0.0131720
24.1	6.4	200	0.014	483,286	0.0000021	0.0239543
20.0	5.3	200	0.012	322,248	0.0000031	0.0347823

Figure 5.15 plots  $(h/L)^2$  vs.  $1/MOE_{app}$  to determine the slope of the least squares line.

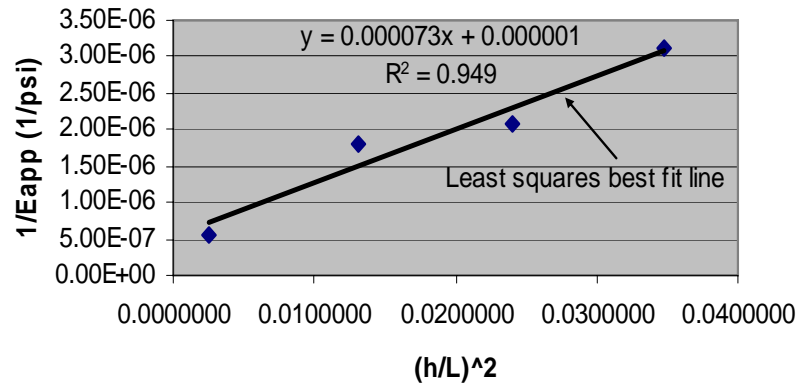


Figure 5.15 – Empirical determination of shear modulus

Shear modulus was then calculated as  $1.20/\text{slope}$  of the best-fit line, giving 16,439 psi for this beam. This is compared to the back-calculated G of 21,382 psi for this same beam, a value 30% higher than the empirical calculation.

Note that in all cases, the mathematical method produced significantly higher results than those derived empirically (Table 5.37). Caution should then be taken when analyzing the back-calculated G as significant error may be involved.

*Table 5.37 – Comparison of shear modulus depending on method*

TRT	n	Mathematical <sup>a</sup> (psi)	Empirical <sup>a</sup> (psi)	Difference (psi)	Difference <sup>b</sup> (%)
LS-L	1	21,382	16,439	4,943	30.0
SS-L	1	18,025	9,971	8,054	80.8
LT-L	1	52,916	21,907	31,009	141.5
ST-L	1	20,587	12,127	8,460	69.8

<sup>a</sup> Values unadjusted for density or MC

<sup>b</sup> Calculated as  $(\text{Mathematical}/\text{Empirical}) - 1 * 100$

Of perhaps greater importance is the fact that these values are all significantly lower than those published for SCL products. PSL, for example, publishes a shear modulus of 125,000 psi, a value 236% higher than the largest shear modulus reported in Table 5.37. The lower shear modulus of LSSCL may be due to poor bond performance or failures in the microstructure, and further investigation is warranted. As the MOE values of LSSCL tested in this experiment were similar to those of the SCL products mentioned (within ~15%), the low shear modulus of LSSCL will likely give high E/G ratios. A high E/G ratio would indicate a product susceptible to excessive shear deflections compared to products with lower ratios.

#### **5.4.3. E/G Ratio**

Mean E/G ( $\text{MOE}_{\text{true}} / \text{Back-calculated shear modulus}$ ) ratios by treatment are shown in Table 5.38. Note that the relatively high COVs are primarily due to variation in shear modulus rather than  $\text{MOE}_{\text{true}}$ .

Table 5.38 – Summary data for E/G ratio of beams

TRT#	TRT Type	n	Mean	Std Dev	COV (%)
1	LS-L	12	93	21	22.6
2	LS-NL	9	89	29	32.3
	<b>LS</b>	<b>21</b>	<b>91</b>	<b>24</b>	<b>26.4</b>
3	LT-L	12	77	29	37.8
4	LT-NL	12	119	34	28.5
	<b>LT</b>	<b>24</b>	<b>98</b>	<b>37</b>	<b>37.8</b>
5	SS-L	12	80	27	34.3
6	SS-NL	12	97	28	29.3
	<b>SS</b>	<b>24</b>	<b>89</b>	<b>29</b>	<b>32.6</b>
7	ST-L	12	72	19	27.0
8	ST-NL	11	67	19	28.4
	<b>ST</b>	<b>23</b>	<b>69</b>	<b>19</b>	<b>27.5</b>
<b>TOTALS</b>		<b>92</b>	<b>87</b>	<b>30</b>	<b>34.5</b>

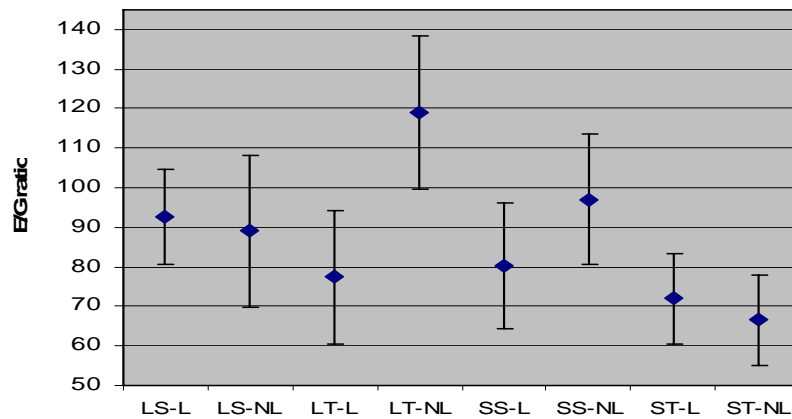


Figure 5.16 – Mean and standard error of E/G ratio grouped by treatment

Table 5.39 – Three-way analysis of variance results for E/G ratio

Source	DF	F Value	Prob > F	< >
Strand size	1	8.87	<b>0.0065</b>	<b>LG &gt; SM</b>
Geometry	1	1.39	0.2495	
Laptype	1	5.39	<b>0.0291</b>	<b>NL&gt;L</b>
Strand size * Geometry	1	6.02	<b>0.0218</b>	
Strand size * Laptype	1	1.68	0.2073	
Geometry * Laptype	1	0.96	0.3370	
Strand size * Geometry * Laptype	1	9.62	<b>0.0049</b>	

Table 5.39 indicates a significant difference due to both strand size (LG>SM) and laptype (NL>L). Geometry, however, had no significant impact on the E/G ratio. As no significant differences existed among shear modulus treatments, these differences are likely due solely to  $MOE_{true}$ . Mean separation (Table 5.40) indicates that without the significantly higher ratio for LT-NL all values would belong to the same population.

Table 5.40 – Mean separation for E/G ratio

	<b>Tukey Grouping<sup>a</sup></b>	<b>Mean</b>	<b>n</b>	<b>TRT</b>
	A	119	12	LT-NL
	A			
B	A	97	12	SS-NL
B	A			
B	A	93	12	LS-L
B	A			
B	A	89	9	LS-NL
B				
B		80	12	SS-L
B				
B		78	12	LT-L
B				
B		72	12	ST-L
B				
B		67	11	ST-NL

<sup>a</sup> minimum significant difference = 36

The most significant conclusion from these results is that LSSCL apparently has a considerably higher E/G ratio than both solid wood (~16) as well as existing SCL products (PSL = ~44), due primarily to a low shear modulus. Note again that the ratio is based on the back calculated shear modulus. If the empirically derived G were used, the ratio would be even higher.

#### 5.4.4. Modulus of Rupture

A summary of the data for MOR is presented in Table 5.41. Note that COVs are close to the 16% reported for clear, solid wood (USDA, 1999).

Table 5.41 – Summary data for modulus of rupture of beams

TRT#	TRT Type	n	Mean (psi) <sup>a</sup>	MIN (psi)	Std Dev	COV (%)
1	LS-L	12	8,133	6,808	975	12.0
2	LS-NL	10	10,294	8,978	1,025	10.0
	<b>LS</b>	<b>22</b>	<b>9,116</b>	<b>6,808</b>	<b>1,470</b>	<b>16.1</b>
3	LT-L	12	8,523	7,661	771	9.0
4	LT-NL	12	10,915	9,599	806	7.4
	<b>LT</b>	<b>24</b>	<b>9,719</b>	<b>7,661</b>	<b>1,445</b>	<b>14.9</b>
5	SS-L	12	8,699	6,681	913	10.5
6	SS-NL	12	10,788	9,256	833	7.7
	<b>SS</b>	<b>24</b>	<b>9,744</b>	<b>6,681</b>	<b>1,367</b>	<b>14.0</b>
7	ST-L	12	8,999	7,749	877	9.7
8	ST-NL	11	11,044	10,169	635	5.8
	<b>ST</b>	<b>23</b>	<b>9,977</b>	<b>7,749</b>	<b>1,288</b>	<b>12.9</b>
	<b>TOTALS</b>	<b>93</b>	<b>9647</b>	<b>6681</b>	<b>1404</b>	<b>14.6</b>

<sup>a</sup> Adjusted to the average density (39.3 lbs/ft<sup>3</sup>) and a MC (9.88%) of all beams

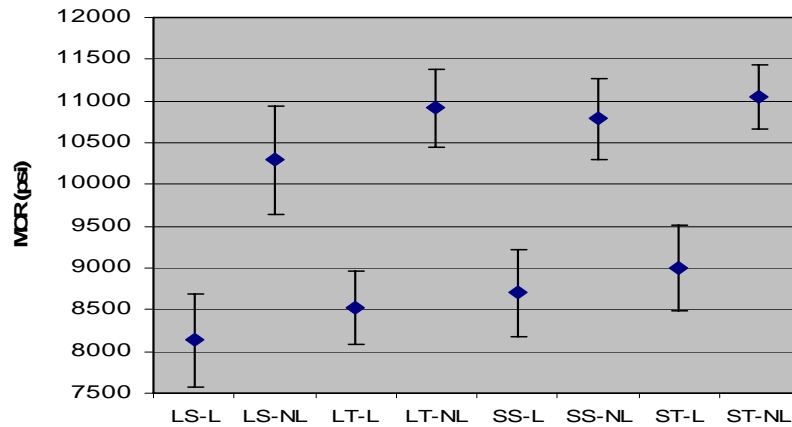


Figure 5.17 – Mean and standard error of MOR grouped by treatment

As might be expected, MOR is greatly affected by the presence of lap joints (Figure 5.17 and Table 5.42), with all non-lapped beams outperforming the lapped beams. The non-lapped beams were 25.3% stronger on average than the lapped beams, with the difference by strand type being 26.6% (LS), 28.1 % (LT), 24.0% (SS) and 22.7% (ST).

Surprisingly, geometry had no significant effect on MOR, refuting the hypothesis that triangular strands would produce stronger beams than square and that reduced void space improves bending strength. This very significant negative effect of lap joints behooves further research into modifying the lap method to improving bending strength.

Table 5.42 – Three-way analysis of variance results for MOR

Source	DF	F Value	Prob > F	< >
Strand size	1	2.15	0.1552	
Geometry	1	1.91	0.1795	
Laptype	1	55.81	<0.0001	NL>L
Strand size * Geometry	1	0.20	0.6580	
Strand size * Laptype	1	0.11	0.7393	
Geometry * Laptype	1	0.04	0.8521	
Strand size * Geometry * Laptype	1	0.09	0.7729	

Table 5.43 – Mean separation for MOR

Tukey Grouping <sup>a</sup>	Mean	n	TRT
A	11044	11	ST-NL
A			
A	10915	12	LT-NL
A			
A	10788	12	SS-NL
A			
A	10294	10	LS-NL
B	8999	12	ST-L
B			
B	8699	12	LT-L
B			
B	8523	12	SS-L
B			
B	8133	12	LS-L

<sup>a</sup> minimum significant difference = 1,284

Although mean values allow for ANOVA and mean separation, the minimum values are of greatest importance as allowable bending stress ( $F_b$ ) is based on the lower 5<sup>th</sup> percentile exclusion limit (LEL). As the sample size is less than 53, ASTM D2915 (ASTM, 1998) requires that the non-parametric LEL be used, which in this case is the minimum value. As beams of larger volume have been shown to more likely contain a critical defect, ASTM D5456 (ASTM, 2001) requires that the LEL value be adjusted for volume using equation 5.1:

$$K_d = \left( \frac{d_1}{d} \right)^{\frac{1}{m}} \left( \frac{L_1}{L} \right)^{\left( \frac{1}{m} \right)} \quad (5.1)$$

Where:

- $K_d$  = Factor applied to the design stress of the member of unit volume
- $d_1$  = Depth of unit volume member (2" non-lapped/3.75" lapped)
- $d$  = Depth of an application member (chosen as 12")
- $L_1$  = Length of unit volume member (3.67' non-lapped/6.67' lapped)
- $L$  = Length of an application member (chosen as 21')
- $m$  = A determined parameter. For  $COV < 0.15$ ,  $m=8$

The length (12") and depth (21') were chosen as these are required by the NDS (AF&PA, 1998) for glulam timbers. Unlike glulams, where width must also be adjusted to 5.125", ASTM D5456 does not require a width adjustment. In fact, the standard mentions that if anything, increasing width improves bending strength.

$K_d$  was calculated in this experiment as 0.642 for non-lapped and 0.749 for lapped beams. Having to reduce MOR values by these large amounts (35.8% and 25.1%) is very significant. The reduction factor is considered conservative and required to encourage the testing of larger members to accurately determine the volume effect for a given product. Future testing of larger specimens may, then, lead to a larger  $K_d$  and higher allowable bending stress values.

The minimum, volume adjusted MOR value was then divided by a safety factor of 2.1 to determine a projected  $F_b$  (Table 5.44) as prescribed by ASTM D5456.

*Table 5.44 – Projected allowable design bending stress by treatment*

TRT	TRT	Mean (psi) <sup>a</sup>	MIN (psi)	Volume adjusted MIN (psi)	$F_b$ (psi)
1	LS-L	8,133	6,808	5,099	2,428
2	LS-NL	10,294	8,978	5,764	2,745
3	LT-L	8,523	7,661	5,738	2,732
4	LT-NL	10,915	9,599	6,162	2,934
5	SS-L	8,699	6,681	5,004	2,383
6	SS-NL	10,788	9,256	5,942	2,830
7	ST-L	8,999	7,749	5,804	2,764
8	ST-NL	11,044	10,169	6,528	3,109

<sup>a</sup> Adjusted to the average density (39.3 lbs/ft<sup>3</sup>) and a MC (9.88%) of all beams

Note that these projected  $F_b$  values are likely an overestimation of the actual  $F_b$  that would be determined through full-scale testing. This is due to the small sample size used to determine MOR (12 vs. the 53 required by ASTM D5456) as well as a moisture content adjustment only to the average (9.88%) rather than the customary 12%.

Since only lapped beams would be used in production, a look at these is informative. The ranking was: ST (2,764), LT (2,732), LS (2,428) and SS (2,383). Here it is seen that while the average values were not affected by geometry, the minimum values (and therefore  $F_b$ ) were, with the triangular treatments outperforming the square by approximately 300 psi. The  $F_b$  values for the triangular treatments (~2,750 psi) approach the desired minimum of 2900 psi and may allow for competition in terms of  $F_b$  with existing SCL products.

#### 5.4.5. Maximum Shear Strength

##### 5.4.5.1. Shear Blocks

Table 5.45 is similar to the previous summary tables, but adds a column for allowable shear stress ( $F_v$ ).

Table 5.45 –Summary data for maximum shear strength of shear blocks

TRT#	TRT Type	n	Mean <sup>a, b</sup> (psi)	MIN (psi)	$F_v$ (psi)	Std Dev	COV (%)
1	LS-L	12	1,035	677	215	201	19.4
2	LS-NL	10	1,232	774	246	273	22.2
	<b>LS</b>	<b>22</b>	<b>1,124</b>	<b>677</b>	<b>215</b>	<b>251</b>	<b>22.3</b>
3	LT-L	12	1,151	805	256	228	19.8
4	LT-NL	12	1,112	738	234	313	28.1
	<b>LT</b>	<b>24</b>	<b>1,131</b>	<b>738</b>	<b>234</b>	<b>268</b>	<b>23.7</b>
5	SS-L	12	999	615	195	283	28.3
6	SS-NL	12	1,058	617	196	239	22.6
	<b>SS</b>	<b>24</b>	<b>1,028</b>	<b>615</b>	<b>195</b>	<b>258</b>	<b>25.1</b>
7	ST-L	12	1,297	1,085	344	198	15.3
8	ST-NL	11	1,392	1,075	341	205	14.7
	<b>ST</b>	<b>23</b>	<b>1,342</b>	<b>1,075</b>	<b>341</b>	<b>203</b>	<b>15.1</b>
	<b>TOTALS</b>	<b>93</b>	<b>1,155</b>	<b>615</b>	<b>195</b>	<b>263</b>	<b>22.8</b>

<sup>a</sup> Adjusted to the average density (39.3 lbs/ft<sup>3</sup>) and a MC (9.88%) of all beams

<sup>b</sup> Mean time to failure = 3.4 minutes

Allowable shear stress does not have a volume effect adjustment, and is therefore calculated as the minimum divided by the safety factor of 3.15 prescribed by ASTM D5456 (ASTM, 2001). Note again that due to the small sample size, the non-parametric LEL (minimum value) was used in determining  $F_v$ . Due to the fact that the sample size of 12 was less than the required 53, these  $F_v$  values are likely overestimations of the allowable design value that would be obtained through full-scale testing.

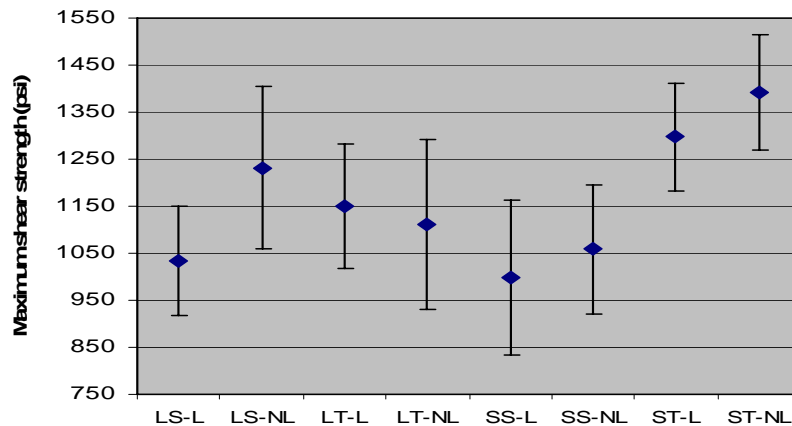


Figure 5.18 – Mean and standard error shear block results grouped by treatment

The graphical representation (Figure 5.18) shows that while the presence of lap joints continues to have a negative effect, it is less pronounced for shear strength than was the case for bending strength. The non-lapped beams were 6.9% stronger than the lapped beams, with the difference by strand type being 19.0% (LS), -3.5 % (LT), 5.9% (SS) and 7.3% (ST). ANOVA results (Table 5.46), however, show that these differences were not statistically significant.

The ANOVA also indicates that the triangular strands produce beams with significantly higher shear strengths than squares. These higher strengths are likely due to improved strand packing, reduced void volume and therefore larger shear areas for the triangular treatments. While the large and small triangular treatments belong to the same population (Table 5.47), the small triangular treatments were the only ones with projected design values that meet the desired minimum of 285 psi (they actually considerably exceed this value).

Table 5.46 – Three-way analysis of variance results for shear block maximum strength

Source	DF	F Value	Prob > F	< >
Strand size	1	1.31	0.2642	
Geometry	1	11.87	<b>0.0021</b>	<b>TRI&gt;SQ</b>
Laptype	1	2.95	0.0989	
Strand size * Geometry	1	12.49	<b>0.0017</b>	
Strand size * Laptype	1	0.01	0.9260	
Geometry * Laptype	1	1.44	0.2424	
Strand size * Geometry * Laptype	1	2.21	0.1498	

Table 5.47 – Mean separation for shear block maximum strength by treatment

Tukey Grouping <sup>a</sup>			Mean	n	TRT
	A		1,392	11	ST-NL
	A				
B	A		1,297	12	ST-L
B	A				
B	A	C	1,232	10	LS-NL
B	A	C			
B	A	C	1,151	12	LT-L
B	A	C			
B	A	C	1,112	12	LT-NL
B		C			
B		C	1,058	12	SS-NL
B		C			
B		C	1,035	12	LS-L
		C			
		C	999	12	SS-L

<sup>a</sup> minimum significant difference = 294

Note that the average COV of 22.8% is considerably higher than that reported for solid wood (14%). There are two hypothesized reasons for this increased variation:

1. As the samples were randomly cut from the beams, the location of the lap within the specimen varied. As the samples were only 2.5" high, it is possible that some samples from the lapped treatments did not contain a lap joint, as only 4" of every 6" of beam length were free of lap joints (Figure 3.4).
2. The size and location of void space along the shear plane varied from sample to sample (Figure 5.19). Specimens with large void spaces along the shear plane likely had lower strengths. Additionally, the

calculated shear strength of these specimens was likely an underestimation since the actual shear area was smaller than the nominal value measured by outside dimensions.

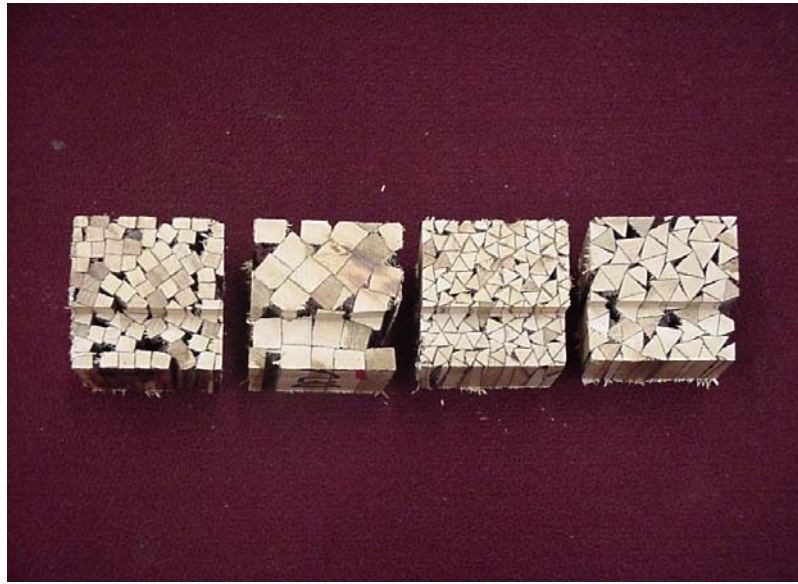


*Figure 5.19 – Void spaces along the shear plane of shear block samples*

These issues raise a concern regarding the use of small shear blocks to determine the allowable shear stress for LSSCL. The solution may involve a different testing protocol, subject to approval from the code agencies.

#### **5.4.5.2. Short-span Beams**

Results from the short-span shear testing are presented in Table 5.48. Note that the mean values for all strand types were lower for short-span beams than for shear blocks. In terms of variability, however, the short-span beams had a lower average coefficient of variation (18%) than that of shear blocks (22.8%), with most individual treatment COVs lower than that reported for solid wood (14%).

Table 5.48 – Summary data for maximum shear strength of short-span beams

TRT#	TRT Type	n	Mean <sup>a, b, c</sup> (psi)	MIN (psi)	F <sub>v</sub>	Std Dev	COV
1	LS-L	12	887	737	234	112	12.7
2	LS-NL	10	1,000	798	253	136	13.6
	<b>LS</b>	<b>22</b>	<b>938</b>	<b>737</b>	<b>234</b>	<b>136</b>	<b>14.5</b>
3	LT-L	12	936	667	212	192	20.6
4	LT-NL	12	1,085	951	302	113	10.5
	<b>LT</b>	<b>24</b>	<b>1,011</b>	<b>667</b>	<b>212</b>	<b>192</b>	<b>19.0</b>
5	SS-L	12	823	702	223	83	10.1
6	SS-NL	12	1,104	776	246	198	17.9
	<b>SS</b>	<b>24</b>	<b>964</b>	<b>702</b>	<b>223</b>	<b>198</b>	<b>20.5</b>
7	ST-L	12	979	780	248	126	12.9
8	ST-NL	11	1,210	1,012	321	168	13.9
	<b>ST</b>	<b>23</b>	<b>1,090</b>	<b>780</b>	<b>248</b>	<b>168</b>	<b>15.4</b>
	<b>TOTALS</b>	<b>93</b>	<b>1,001</b>	<b>667</b>	<b>212</b>	<b>180</b>	<b>18.0</b>

<sup>a</sup> Adjusted to the average density (39.3 lbs/ft<sup>3</sup>) and a MC (9.88%) of all beams

<sup>b</sup> Mean time to failure= 2:48 (lapped) and 2:36 (non-lapped)

<sup>c</sup> Length-to-depth ratio was 3.75 for all treatments

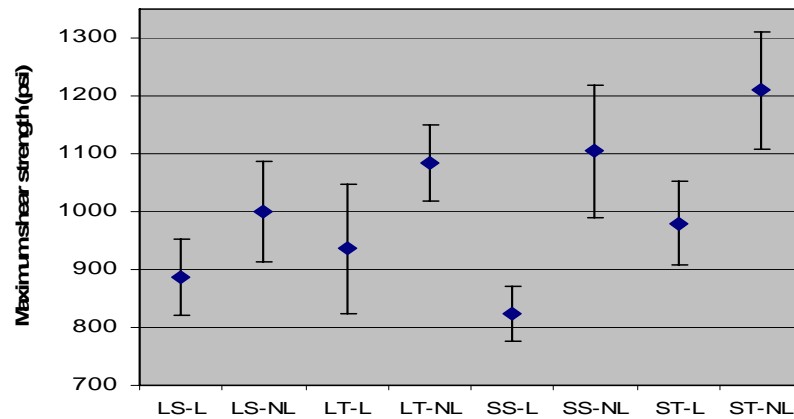


Figure 5.20 – Mean and standard error of short-span shear beam results grouped by treatment

As seen in Table 5.49, geometry again had a significant effect on performance with the triangular treatments outperforming the square. However, unlike the shear block results, the presence of laps did have a significantly negative effect on maximum shear strength. The non-lapped beams were 21.4% stronger than the lapped beams, with the difference by strand type being 12.7% (LS), 15.9 % (LT), 34.1% (SS) and 23.6% (ST). This makes sense as there are more lap joints in the longer short-span beams than the shear blocks.

Table 5.49 – Three-way analysis of variance for short-span maximum shear strength

Source	DF	F Value	Prob > F	< >
Strand size	1	1.93	0.1773	
Geometry	1	6.95	<b>0.0145</b>	<b>TRI&gt;SQ</b>
Laptype	1	25.55	<b>&lt;0.0001</b>	<b>L&gt;NL</b>
Strand size * Geometry	1	0.57	0.4581	
Strand size * Laptype	1	2.74	0.1110	
Geometry * Laptype	1	0.01	0.9214	
Strand size * Geometry * Laptype	1	0.46	0.5051	

Table 5.50 – Mean separation for short-span maximum shear strength

Tukey Grouping <sup>a</sup>			Mean	n	TRT
	A		1,210	11	ST-NL
	A				
B	A		1,104	12	SS-NL
B	A				
B	A		1,085	12	LT-NL
B	A				
B	A	C	1,000	10	LS-NL
B	A	C			
B	A	C	980	12	ST-L
B		C			
B		C	936	12	LT-L
B		C			
B		C	887	12	LS-L
		C			
		C	823	12	SS-L

<sup>a</sup> minimum significant difference = 248

As stated, the original purpose of testing shear strength using short-span beams was concern that shear blocks would give an excessively low allowable shear stress value due to the occasional presence of large voids along the shear plane. In comparing the results, however, it is seen that the mean shear strength determined was actually higher for shear blocks (1,115 psi) than for short-span beams (1,001). Minimum values were similar, with a difference of only 52 psi.

#### 5.4.6. Probability Results Summary for Factorial Analyses

Table 5.51 summarizes the results from the three-way factorial analyses conducted on the seven mechanical properties. It can quickly be seen which properties were significantly affected by the three main factors of the experiment.

Table 5.51 – Probability results summary for the three-way factorial analyses

Dependent Variable	Significant Differences (PROB > F)						
	STRSIZE	GEOMETRY	LAPTYPE	STRSIZE * GEOMETRY	STRSIZE * LAPTYPE	GEOMETRY * LAPTYPE	STRSIZE * GEOMETRY * LAPTYPE
MOE <sub>app</sub>	<b>&lt;0.0001</b>	0.1158	<b>0.0144</b>	0.2452	0.5774	0.9231	0.4592
MOE <sub>True</sub>	<b>0.0004</b>	0.1820	<b>0.0337</b>	0.1294	0.3930	0.7765	0.1383
Shear Modulus	0.7266	0.4925	0.5033	0.6682	0.6018	0.6045	0.1885
E/G	<b>0.0474</b>	0.4155	0.1162	0.0979	0.3720	0.4982	<b>0.0396</b>
MOR	0.1552	0.1795	<b>&lt;0.0001</b>	0.6580	0.7393	0.8521	0.7729
Short-Span Shear	0.1773	<b>0.0145</b>	<b>&lt;0.0001</b>	0.4581	0.1110	0.9214	0.5051
Shear Blocks	0.2642	<b>0.0021</b>	0.0989	<b>0.0017</b>	0.9260	0.2424	0.1498

**Bold** = Significant Pr < 0.05

Several conclusions can be made:

1. Strand size has the greatest effect on MOE. The larger strand size clearly gave higher stiffness values than the small.
2. In terms of geometry, the only clear significant advantage of the triangular strands is in terms of maximum shear strength.
3. The presence of the lap has a significantly negative effect on MOE, MOR and maximum shear strength.
4. Very few significant interaction terms are present (3 of 36). This is favorable in the sense that if triangular strands are chosen, changing strand size should not significantly affect any of the properties listed, with the (important) exception of shear blocks.

### **5.5. Two-way Statistical Analyses - Analysis by Lap Type**

As the presence of laps had a significantly negative effect on the performance of most properties, it was decided to analyze the lapped and non-lapped beams separately. This was done for two reasons: 1) Evaluation of the non-lapped beams allowed for determination of a best performing strand size and geometry without the complicated effects of the lap joint on mechanical properties, useful information if further research on the effects of strand size and geometry of LSSCL are conducted, and 2) The lapped beam data is perhaps more pertinent to the recommendation of a best performing combination for potential production, one of the key objectives of this experiment.

The lapped and non-lapped data could not be simply pulled out of the 3-way factorial analyses performed above, as the degrees of freedom change which affects both the ANOVA and mean separation. For that reason, the analyses that follow used a 2 x 2 full factorial design, looking at effects of strand size, strand geometry and any interaction between the two. Subsampling and error terms remained as previously described. All properties in the 2-way analysis had normally distributed residuals and equality of variance, indicating that the inequality of variance seen in the 3-way factorial was due primarily to the lap factor. ANOVA and multiple comparison tables are presented in Appendix C.

In terms of comparison with existing SCL products, MOE,  $F_b$  and  $F_v$  are the critical properties and are therefore the only values presented in the following sections. Two caveats must be repeated as these values are likely overestimations of the values that would be obtained during full-scale testing:

1. The values are based on a sample size of only 12. ASTM D2915 (ASTM, 1998) requires a minimum sample size of 53, allowing for use of the non-parametric lower tolerance limit (LTL) to be used (second to last value when ranked according to performance).
2. The moisture content values were adjusted only to the average of all beams (9.88%). Customarily, values are adjusted to 12%.

### 5.5.1. Projected Design Values of the Non-lapped Treatments

Table 5.52 presents the projected design values for the non-lapped treatments.

Table 5.52 – Projected design values by treatment for non-lapped beams <sup>a</sup>

TRT	MOE <sub>app</sub> (psi)	F <sub>b</sub> (psi)	F <sub>v</sub> (psi)
LS-NL	<b>1,848,641<sup>b</sup></b>	2,745	246
LT-NL	<b>1,854,912</b>	<b>2,934</b>	234
SS-NL	1,751,253	2,830	196
ST-NL	1,650,263	3,109	<b>341</b>

<sup>a</sup> All values adjusted to the average density (39.3 lbs/ft<sup>3</sup>) and a MC (9.88%) of all beams

<sup>b</sup> Bolded values exceed the desired minimums

In terms of design values, the large triangle (LT-NL) is the top performing treatment. Both MOE and F<sub>b</sub> meet the desired minimum values, with shear strength being the one exception. Although the large square treatment (LS-NL) appears to be the second best performing treatment, note that had the two beams that failed in shear been included, this treatment would have had a much lower F<sub>b</sub>.

### 5.5.2. Projected Design Values of the Lapped Treatments

As seen in Table 5.53, the small triangular (ST-L) treatment is the only one that had any values that met the desired minimums. However, short of a modification to improve its stiffness performance, the low MOE values of this treatment precludes its use. When all values are considered, the overall best performing treatment is the large triangle (LT-L). More discussion on this treatment will be given in Chapter 6.

Table 5.53 – Projected design values by treatment for lapped beams <sup>a</sup>

TRT	MOE <sub>app</sub> (psi)	F <sub>b</sub> (psi)	F <sub>v</sub> (psi)
LS-L	1,779,806	2,428	215
LT-L	1,750,031	2,732	256
SS-L	1,671,777	2,283	195
ST-L	1,618,138	2,764	<b>344<sup>b</sup></b>

<sup>a</sup> All values adjusted to the average density (39.3 lbs/ft<sup>3</sup>) and a MC (9.88%) of all beams

<sup>b</sup> Bolded values exceed the desired minimums

## Chapter 6

### CONCLUSIONS AND RECOMMENDATIONS

The objective of this chapter is to make conclusions regarding the experiment as well as recommendations for future research. The hypotheses are first reviewed and either confirmed or refuted. The best performing treatment is then indicated, and recommendations given to improve on the properties of that treatment. Recommendations for future research are then offered. Finally, a review of the objectives of the experiment is presented.

#### 6.1 Conclusions

##### 6.1.1 Review of Hypotheses

The hypotheses of the experiment are restated and investigated one by one.

1. *The triangular strand beams will have significantly less void space than square strand beams.* This hypothesis was confirmed, with triangular strand beams having less than half the void volume of the square strand beams at a given strand size (LS= 15.2%, SS=11.8%, LT=7.5%, ST=3.1%).
2. *The triangular strands will produce stronger and stiffer beams than those made from square strands.*  
In addition to the triangular shape causing better consolidation and reduced void space, it was found that where the strands did not align perfectly, the tips of the (high density) triangles served as wedges, embedding themselves in the adjacent strand. This wedging effect reduced void space even further and increased densification, both of which have a positive impact on strength properties. Figure 6.1 illustrates this effect.

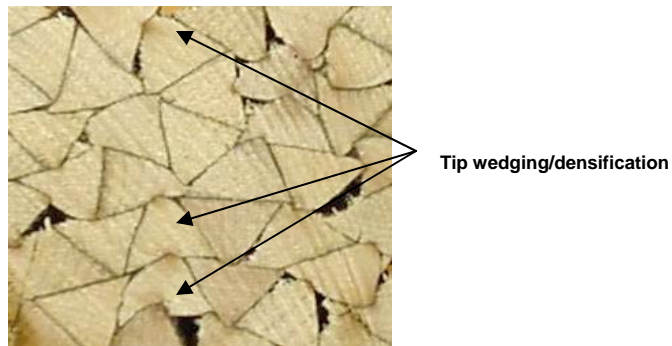


Figure 6.1 – Tip wedging and densification of the triangular strands

The hypothesis that the triangular strand beams were stronger than square was generally confirmed. Although triangles were no stronger than squares in terms of MOR, values for  $F_b$  were approximately 300 psi higher for both lapped and non-lapped beams. In terms of shear strength, the results confirm that triangles were stronger than squares, especially small triangles. Both of these results were likely due to the presence of large voids in areas of critical stress with the use of square strands.

In terms of stiffness, the hypothesis was refuted. The results show that it was not strand geometry, but rather size that had an effect on stiffness. Larger strands were significantly stiffer than small, with no difference between large triangle and small.

3. *The large triangular strands will produce stronger and stiffer beams than the small triangular strands.*

For strength, this hypothesis was flatly refuted. The only significant strength difference seen between the LT and ST treatments was a higher maximum shear strength for the small triangular strand beams (non-lapped only). In terms of stiffness, however, LT did outperform ST. However, this was not due to geometry, but rather solely strand size.

4. *Non-lapped beams will be both stronger and stiffer than lapped beams.* Although of no surprise, the lap had a clear, significant negative impact on all mechanical properties. The usefulness of this data will be to compare other lap methods to see if the negative impact can be lessened.

## **6.1.2 Best Performing Treatment**

### **6.1.2.1 Square vs. Triangular Strand Geometry**

In general, the triangular strands produced beams with higher mean values as well as lower coefficients of variation. The square strand beams, while achieving comparable properties in some categories, also possess undesirable properties such as differential volumetric shrinkage/swelling, tendency to fail in shear and relatively high coefficients of variation.

### 6.1.2.2 Large vs. Small Triangular Strand Size

In terms of large vs. small triangles, the stiffness values are the deciding factor. If the stiffness of the small triangular strand had been higher, it would have been the highest performing treatment. The significantly higher shear values of the small triangular beams would make it attractive in terms of competing against LSL, which possess high design values in shear. It is not clear from this experiment why the small strands had significantly lower stiffness than the large, and manufacturing modifications may allow for improved stiffness of beams made from small strands. However, as pointed out earlier, it is generally desirable to use the largest strand size to achieve the minimum values required. Larger strand size increases yields and reduces energy consumption.

## 6.2 Recommendations

### 6.2.1 Recommended Strand Size and Geometry

Overall, the large triangular (LT) strands were the best performers and are recommended for future testing and production. Table 6.1 shows a comparison between the desired minimum design values stated at the outset vs. those obtained in this experiment for the LT-L treatment. The caveats mentioned in Section 5.5 again apply.

*Table 6.1 – Comparison between desired minimum design values and treatment LT-L*

	MOE <sub>app</sub> (psi)	F <sub>b</sub> (psi)	F <sub>v</sub> (psi)
<b>Desired minimum</b>	1,800,000	2,900	285
<b>LT-L treatment</b>	1,750,031	2,732	256

Although the LT-L beams did not meet the desired minimums, the values were quite close, within 3%, 6% and 11% of the desired minimums for MOE<sub>app</sub>, F<sub>b</sub> and F<sub>v</sub> respectively. Several potential modifications may allow this treatment to meet the desired minimums. Among these are:

1. Increase density from 40 lbs/ft<sup>3</sup> to 43 lbs/ft<sup>3</sup>. There are two methods to estimate the increase in properties with a corresponding increase in density. The first is to use the Wood Handbook (USDA, 1999) values described earlier. The second is to use a regression equation calculated

from plots of density vs. various mechanical properties from the actual data of this experiment. This was done for the 12 beams of the LT-L treatment (Figures 6.2 – 6.5). The values used are adjusted for moisture content, but not density.

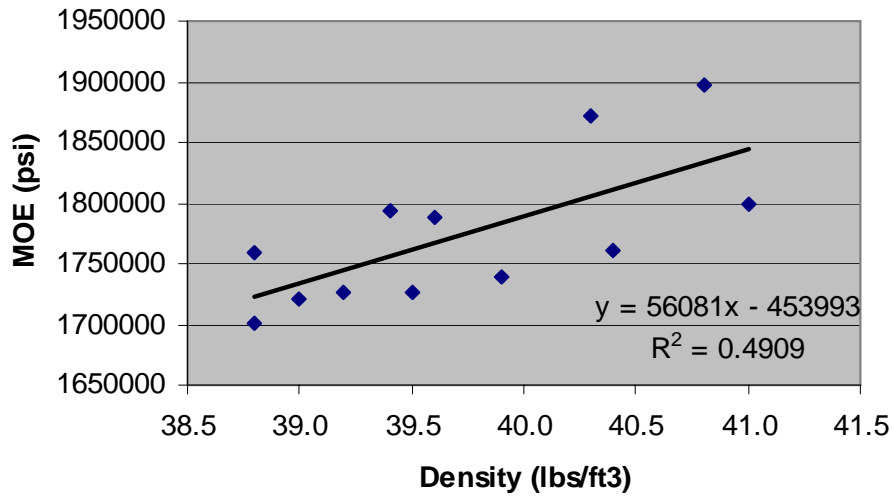


Figure 6.2 – Density vs. MOE for LT-L

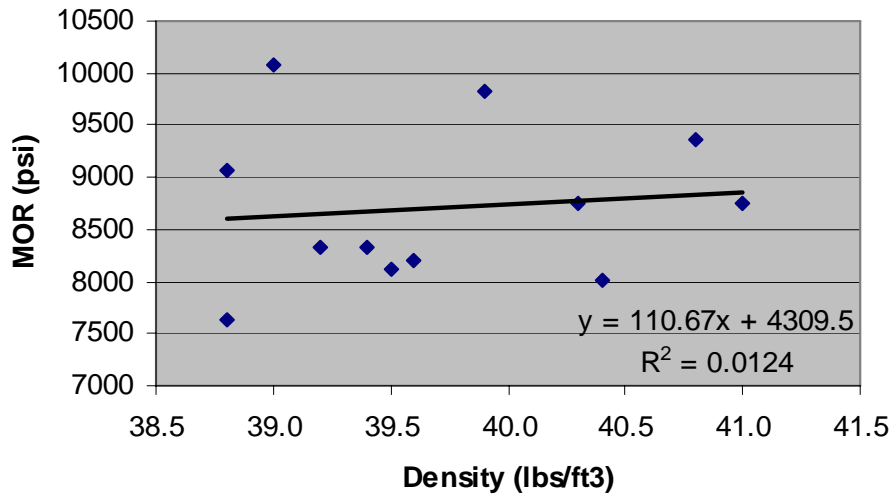


Figure 6.3 – Density vs. MOR for LT-L

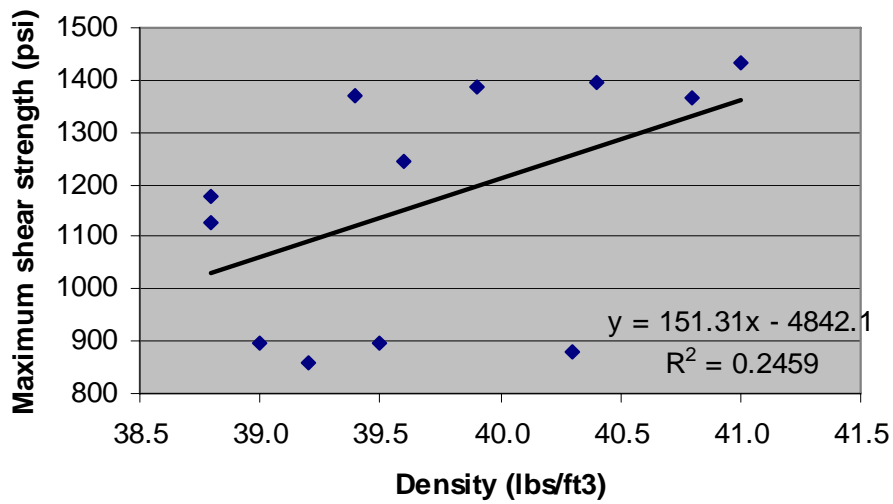


Figure 6.4 – Density vs. maximum shear strength for LT-L

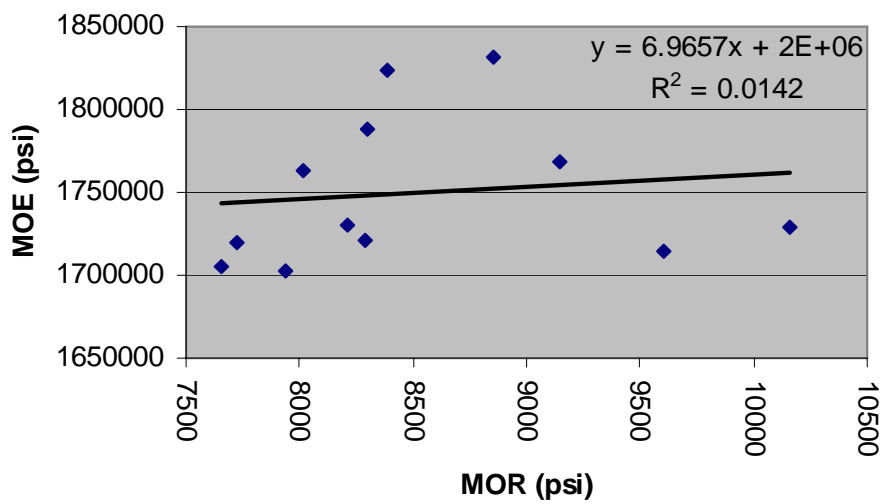


Figure 6.5 – MOE vs. MOR for LT-L

Note that density of the LT-L treatment is positively correlated with MOE and shear, but not so with MOR. Modifications other than increased density may need to be investigated to increase allowable bending stress. Also note that the correlation coefficients are very low ( $< 0.50$  in all cases). For this reason, little confidence can be placed in predicting mechanical properties based on differing densities using these equations.

Table 6.2 shows the expected increase in properties using the equations from the Wood Handbook.

*Table 6.2 – Expected design values at 43 lbs/ft<sup>3</sup>*

<b>Property</b>	<b>Current Values</b>	<b>Adjusted Values</b>
Density (lbs/ft <sup>3</sup> )	39.7	43
MOE <sub>app</sub> (psi)	1,750,031	1,850,633
F <sub>b</sub> (psi)	2,732	2,990
F <sub>v</sub> (psi)	256	280

Note that the calculated values at 43 lbs/ft<sup>3</sup> meet the desired minimum design values in all categories.

2. Test larger specimens, thereby increasing the unit volume used to determine the reduction for the volume effect ( $K_d$ ). The reduction in this experiment seen in section 5.4.1 was 25.1%. This has a significant negative impact on  $F_b$ . Larger specimens *may* lead to a decreased  $K_d$ .
3. Use a mix of northeastern hardwoods, including sugar maple, yellow birch and beech, all of which have higher specific gravities than red maple.
4. Modify the lap method. There exists a potential problem with the overlap method used in this experiment. When the strands at the 2" lap are pressed, often a strand from an adjacent layer will wedge itself between two strands from the other layer. This wedging action causes a large void space to open upstream (Figure 6.6).

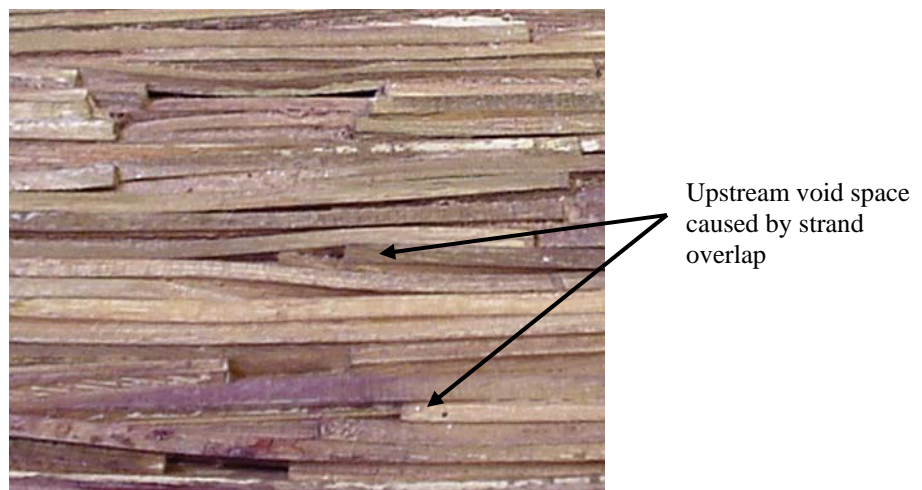


*Figure 6.6 – Void space created by strand overlap*

Note that the photo is of a billet made with small square strands (SS-L). The problem is made worse with triangular strands which serve as perfect wedges. Butt-joints or scarfed strands may alleviate this problem and further testing will need to be conducted to evaluate this issue.

## **6.2.2 Recommendations for Future Research**

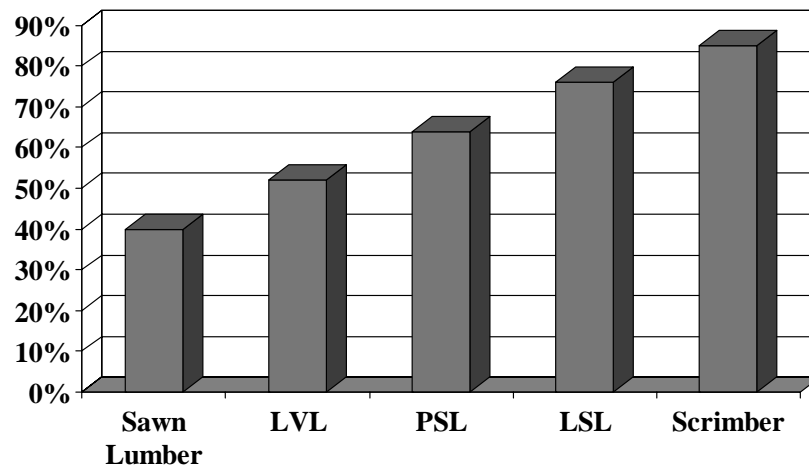
As this experiment was limited in scope, several avenues for future research are recommended.

1. Determine other critical mechanical properties such as tension parallel to grain, compression both parallel and perpendicular to grain, and nail withdrawal.
2. Investigate why the small strands had such lower stiffness values. This might include looking at the small triangular strands under a microscope to determine if failures in the microstructure were produced during strand breakdown.
3. Determine why LSSCL has such a low shear modulus in comparison with other SCL products. Improvements in this area will improve  $MOE_{app}$  as well as lower the excessively high E/G ratios.
4. Confirm and quantify the transverse isotropic behavior of LSSCL. This can be done by edgewise and flatwise bending tests, as well as shear block testing in both the LX and LY planes.
5. Try different lap techniques, including butt joints and scarfed strands to reduce void space at the lap joint. This would likely improve mechanical properties as well as improve the product's aesthetic appeal.
6. Modify the laboratory production procedure to eliminate the density profile across the width of the billet.
7. Using fiber optic thermocouples, plot billet temperature vs. time throughout the press cycle. Especially critical is determination of the point at which the wood is above its glass transition temperature, but below the curing temperature of the resin. This will allow for maximum plasticization of the wood furnish prior to use of high pressures.
8. In production, it is unlikely that strands can be aligned along the longitudinal axis of the member to the extent that was done with hand lay-up used in this experiment. It would be useful to know

the effect on mechanical properties of different levels of strand misalignment. This information could be used when designing lay-up equipment.

9. Try a mix of different size triangular strands. As with concrete, where sizes are mixed to maximize compaction, the same may hold true for LSSCL. However, producing various sizes may be untenable in a manufacturing setting.
10. Conduct creep-rupture tests, known to be a problematic area for SCL products.
11. Determine nailability/workability at different product densities.
12. Determine yields (percent of log used) for varying triangular strand sizes and breakdown methods. These can be compared to the yields of existing SCL products (Figure 6.7) and used to determine comparative resource costs.

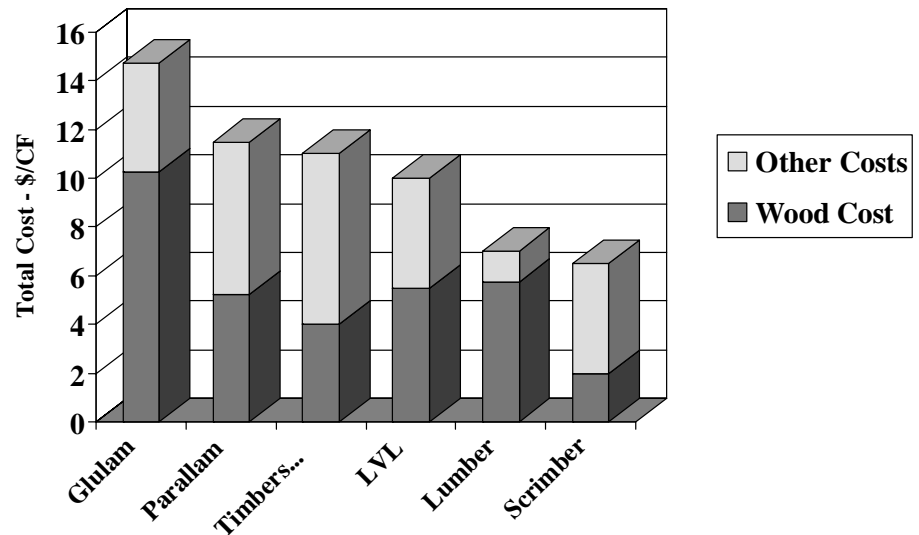
*Figure 6.7 – Comparison of yields for various SCL products*



Source: Nelson (1997) and Scrimber International

13. Determine raw material and manufacturing costs compared to existing SCL products (Figure 6.8). This information will be critical in highlighting the potential competitive advantages of LSSCL during the development of a business plan.

Figure 6.8 – Comparison of resource and manufacturing costs of existing SCL products



Source: Jarck and Sanderson, 2000.

### 6.3 Review of Objectives

All objectives of the ongoing research have been met. First, a unique, symmetrical strand geometry has been identified, allowing for the use of larger strand sizes as well as diffuse porous, high density hardwoods. Equipment and production methods were put in place to allow for laboratory-scale production and testing. Testing was conducted on a wide variety of physical and mechanical properties, allowing for broad evaluation of the performance potential of LSSCL. A best performing treatment (LT-L) was identified and recommendations made for modifications allowing for the minimum desired properties to be met.

## REFERENCES

1. American Society for Testing and Materials. 2000. ASTM D143-00 Standard Test Methods for Small Clear Specimens of Timber. Annual Book of ASTM Standards. ASTM, West Conshohocken, PA.
2. \_\_\_\_\_. 1999. ASTM D198-99 Standard Test Methods of Static Tests of Lumber in Structural Sizes. Annual Book of ASTM Standards. ASTM, West Conshohocken, PA.
3. \_\_\_\_\_. 1997. ASTM D1101-97a Standard Test Methods for Integrity of Adhesive Joints in Structural Laminated Wood Products for Exterior Use. Annual Book of ASTM Standards. ASTM, West Conshohocken, PA.
4. \_\_\_\_\_. 2000. ASTM D2344/D 2344M-00 Standard Test Method for Short-Beam Strength of Polymer Matrix Composite Materials and Their Laminates. Annual Book of ASTM Standards. ASTM, West Conshohocken, PA.
5. \_\_\_\_\_. 2002. ASTM D2395-02 Standard Test Methods for Specific Gravity of Wood and Wood-Based Materials. Annual Book of ASTM Standards. ASTM, West Conshohocken, PA.
6. \_\_\_\_\_. 1998. ASTM D2915-98a Standard Practice for Evaluating Allowable Properties for Grades of Structural Lumber. Annual Book of ASTM Standards. ASTM, West Conshohocken, PA.
7. \_\_\_\_\_. 2003. ASTM D2559-03 Standard Specification for Adhesives for Structural Laminated Wood Products for Use Under Exterior (Wet Use) Exposure Conditions. Annual Book of ASTM Standards. ASTM, West Conshohocken, PA.
8. \_\_\_\_\_. 1999. ASTM D4933-99 Standard Guide for Moisture Conditioning of Wood and Wood-Based Materials. Annual Book of ASTM Standards. ASTM, West Conshohocken, PA.
9. \_\_\_\_\_. 2001. ASTM D5456-01a Standard Specification for Evaluation of Structural Composite Lumber Products. Annual Book of ASTM Standards. ASTM, West Conshohocken, PA.
10. \_\_\_\_\_. 2001. ASTM D6027-03 Standard Practice for Calibrating Linear Displacement Transducers for Geotechnical Purposes. Annual Book of ASTM Standards. ASTM, West Conshohocken, PA.
11. Anonymous. 1975. Fundamentals of High Frequency Dielectric Heating. Chemetron Corporation – Votator Division.
12. APA: The Engineered Wood Association. 2000. Regional Production and Market Outlook for Structural Panels and Other Engineered Wood Products 2000-2005. APA, Tacoma, WA.
13. Barnes, Derek. 2002. A Model of the Effect of Strand Angle and Grain Angle on the Strength Properties of Oriented Veneer and Strand Wood Composites. Forest Prod. J. 52(4):39-47.
14. \_\_\_\_\_. 2001. A Model of the Effect of Strand Length and Strand Thickness on the Strength Properties of Oriented Wood Composites. Forest Prod. J. 51(2):36-46.

15. \_\_\_\_\_. 2000. An Integrated Model of the Effect of Processing Parameters on the Strength Properties of Oriented Strand Wood Products. *Forest Prod. J.* 50(11/12):33-42.
16. Bledsoe, J.M., et al. 1990. Creep Rupture Testing - A Necessary Part of Structural Composite Lumber Development. 24<sup>th</sup> International Particleboard/Composite Materials Symposium, Pullman, Washington.
17. Bodig, J., B Jayne. 1982. *Mechanics of Wood and Wood Composites*. Van Norstrand Reinhold Company Inc., New York, NY.
18. Bogdan, Zoltan. 1996. *Fundamentals of Dielectric Heating*. Publisher unknown.
19. Day, Robert F. 1974. Fiberization of Sugar Maple using the TVA Log Fiberizer. Thesis presented to the Department of Wood Science & Technology, University of Massachusetts.
20. Edgar, R.A., S. Shaler, H. Dagher, J. Fiutak. 2003. U.S. Provisional Patent for Long Strand Structural Composite Lumber. Serial No. 60/484,068.
21. Fiutak, J., S.M. Shaler, H.J. Dagher. 2001. Feasibility of "Long-Strand" Structural Composite Lumber from Northeastern Wood Species. 2001 New England Wood Research. University of Maine.
22. Geimer, R.L., R. J. Mahoney, S.P. Loehnertz, R.W. Meyer. 1985. Influence of Processing Induced Damage on Strength of Flakes and Flakeboards. Res. Pap. FPL 463. Madison, WI: U.S.D.A., Forest Service, Forest Products Laboratory.
23. Haygreen, J.G, J.L. Boyer. 1996. *Forest Products and Wood Science – An Introduction*. Third Edition. Iowa State University Press, Ames, IA.
24. Hoadley, R. B. 1980. *Understanding Wood*. The Taunton Press, Inc. Newtown, CT.
25. Hutchings, B. F., R.H. Leicester. 1988. Scrimber. 1988 International Conference on Timber Engineering at Washington State University. Editor, R. Itani. Forest Products Research Society. Madison, WI.
26. International Code Council, Evaluation Services, Acceptance Criteria 47, Interim Criteria for Structural Composite Lumber. Whittier, CA.
27. Jaffe, A.J., Herbert F. Spirer. 1987. *Misused Statistics, Straight Talk for Twisted Numbers*. Marcel Dekker, INC., New York, NY.
28. Janowiak, J. J., D. Hindman, H. Manbeck. 2001. Orthotropic Behavior of Lumber Composite Materials. *Wood and Fiber Science*, 33(4). pp. 580-594.
29. Jarck, W., G. Sanderson. 2000. Scrimber Born Again. *Timber Processing*, Nov. 2000.
30. Kamke, F.A., L.J. Casey. 1988. Fundamentals of Flakeboard Manufacture: Internal Mat Conditions. *Forest Prod. J.* 38(6):38-44.
31. Knudson, R.M. 1992. PSL 300 LSL: The Challenge of a New Product. Proceedings of the Twenty-Sixth Washington State University International Particleboard/Composite Materials Symposium. Pullman, WA.

32. Lin, R.T. 1967. Review of the Dielectric Properties of Wood and Cellulose. *Forest Products Journal*. 17(7):61.
33. Maine Forest Service. 1999. State of the Forest and Recommendations for Forest Sustainability Standards. Final report to the Joint Standing Committee of the 119<sup>th</sup> Legislature on Agriculture, Conservation and Forestry. Department of Conservation. Augusta, ME.
34. Mark, H. F., N. Bikales, C. Overberger, G. Menges. 1986. *Encyclopedia of Polymer Science and Engineering*, Vol. 5. John Wiley & Sons, New York, NY.
35. Marra, Alan A. 1992. *Technology of Wood Bonding – Principles in Practice*. Van Nostrand Reinhold, New York, NY.
36. Marra, Alan A, W. Hausknecht, R. Day. 1975. *Low Density Composites from High Density Hardwoods*. University of Massachusetts – Massachusetts Agriculture Experiment Station.
37. National Design Specification for Wood Construction. 1999. American Wood Council, American Forest and Paper Association. Washington, DC.
38. Nelson, S. 1997. Structural Composite Lumber. In: Smulski, S. (Editor) 1997. *Engineered Wood Products – A Guide for Specifiers, Designers and Users*. PFS Research Foundation, Madison, WI.
39. Pitcher, Kent. 1998. Bonding with Radio Frequency Heating. [Woodweb.com](http://Woodweb.com).
40. SAS System for Windows V8, Release 8.01. SAS Institute Inc., Cary, NC.
41. Shaler, S.M. 1986. The Usefulness of Selected Polymer Composite Theories to Predict the Elastic Moduli of Oriented Flakeboard. Ph.D. Thesis, The Pennsylvania State University.
42. Sheriff, D.W. 1998. Productivity and Economic Assessment of Hardwood Species for Scrimber Production. A Report for the Rural Industries Research and Development Corporation – RIRDC Publication No 98/4. CSIRO, Australia.
43. Schuler, A., C. Adair. 1999. Engineered Wood Products – Production, Trade, Consumption and Outlook. ECE/FAO Forest Products Annual Market Review, 1999-2000 – Chpt. 11.
44. Schuler, A., C. Adair, E. Elias. 2000. World Trends in EWP. Presentation to Joint ECE Timber Committee & FAO European Forestry Commission, October 2000, Rome, Italy.
45. Shigo, A.L., W.E. Hillis, 1973. Heartwood, Discolored Wood, and Microorganisms in Living Trees. *Annual Review of Phytopathology* 11:197-222.
46. Shigo, A.L., E. Larson, 1969. A Photo Guide to the Patterns of Discolorations and Decay in Living Northern Hardwood Trees. USDA Forest Service Research Paper NE-127, Northeastern Forest Experiment Station, Upper Darby, PA.
47. Smulski, S. (Editor). 1997. *Engineered Wood Products – A Guide for Specifiers, Designers and Users*. PFS Research Foundation, Madison, WI.
48. Steel, R. G. D., J. Torrie, D. Dickey. 1997. *Principles and Procedures of Statistics, A Biometrical Approach*. 3<sup>rd</sup> edition. WCB/McGraw-Hill. Boston, MA.
49. Stofko, Jan. 1960. The Effect of Geometrical Dimensions of the Chip on the Mechanical Properties of the Material Produced from Wood Chips. *Drevarsky Vyskum*. 5(2):241-261.

50. Timtek. 2001. Partnership with Mississippi State University. Press releases from MSU website: <http://www.cfr.msstate.edu/timtek>.
51. USDA. 1999. Wood Handbook – Wood as an Engineering Material. United States Department of Agriculture, U.S. Forest Service, Forest Products Laboratory, Madison, WI.
52. USDA. 1995. 1995 Forest Inventory and Analysis. USDA Forest Service, Northeastern Research Station. Newtown Square, PA.
53. Vlosky, R.P., P.M. Smith, P.R. Blankenhorn, M.P. Haas. 1994. Laminated Veneer Lumber: A United States Market Overview. Wood and Fiber Science, 26(4):456-466.
54. Wolcott, M.P., F.A. Kamke, D.A. Dillard. 1990. Fundamentals of Flakeboard Manufacture: Viscoelastic Behavior of the Wood Component. Wood and Fiber Science, 22(4):345-361.
55. Zabel, R.A., J. J. Morrell. 1992. Wood Microbiology – Decay and its Prevention. Academic Press Inc., New York, NY.
56. Zombori, B.G., F.A. Kamke, L.T. Watson. 2002. Simulation of the Internal Conditions During the Hot-Pressing Process. Wood and Fiber Science, 35(1):2-23.

## APPENDICES

## APPENDIX A

### Production and Testing Data

*Table A.1 – Calculation of weight of strands used per layer*

Line #	Description	Result	Calculation
<b>Lbs. of strands needed for each billet</b>			
A1	Billet Length (in)	84	—
A2	Billet Width (in)	14	—
A3	Billet Thickness (in)	2.1	—
A4	Billet Volume (ft <sup>3</sup> )	1.43	A1*A2*A3
A5	Target Density (lbs/ft <sup>3</sup> )	40	—
A6	Wt. of resin & strands needed at final billet MC of 12% (lbs)	57.2	A4*A5
A7	~Wt. of resin & strands needed at final billet MC of 0% (lbs)	51.0	A6/1.12
A8	~Wt. of resin & strands needed at final billet MC of 5% (lbs)	53.6	A7*1.05
A9	Ave. wt. of one strand (lbs) - Average of 6 sample strands	0.108	—
A10	MC of these strands (%) - Average of 6 sample strands	6	—
A11	Ave. OD wt. of one strand (lbs)	0.1019	A9/(1+(A10/100))
A12	Ave wt. of one strand at 5% MC (lbs)	0.107	A11*1.05
A13	~ # of strands/billet	501	A8/A12
A14	Surface area of one strand (ft <sup>2</sup> )	0.438	—
A15	Surface area of these strands (ft <sup>2</sup> )	219	A13*A14
A16	Spread rate (lbs/MSGL) - double glue line	43	—
A17	Spread rate (lbs/MSGL) - single glue line	21.5	A16/2
A18	Weight of wet resin (lbs)	4.72	(A17*A15)/1000
A19	Solids content	0.5	—
A20	Weight of dry resin (lbs)	2.36	A18*A19
A21	Wt. of strands needed @ 12% MC (lbs)	54.81	A6-A20
A22	Wt. of strands needed @ 0% MC (lbs)	48.94	A21/1.12
A23	Wt. of strands needed @ 5% MC (lbs)	51.38	A22*1.05
<b>For lapped billets:</b>			
A24	Overlap length (in)	2	—
A25	% of each layer with overlap	4.2	(A24/48)*100
A26	Wt. of strands needed @ 5% MC (lbs)	49.24	(A23*(1-(A25/100)))
A27	Amount of end trim (in)	1.5	—
A28	Length of untrimmed billet (in)	89	—
A29	% of billet trimmed	1.7	(A27/A28)*100
A30	Wt. of strands needed @ 5% MC (lbs)	50.07	A26*(1+(A29/100))
A31	Layers of strands/billet	9	—
A32	Lbs. of strands needed per layer	5.56	A30/A31
A33	Lbs. of strands needed per 1' layer	0.795	A32/(A1/12)
A34	Lbs. of strands needed per 4' layer	3.18	A33*4





*Table A.3 continued*

[illegible]









Table A.5 – Preliminary test data summary

Strand Geometry	n (billets)	n (beams)	MC <sup>a</sup> (%)	Density <sup>b</sup> lbs/ft <sup>3</sup>	MEAN MOE (* 10 <sup>6</sup> ) (psi)	MEAN MOR <sup>c</sup> (psi)	MIN MOR <sup>c</sup> (psi)	F <sub>b</sub> <sup>d</sup> (psi)
Liquid resin only								
Small squares	2	10	7.8	40.7	1.80	8325	6979	3323
Small triangles	-	-	-	-	-	-	-	-
Large triangles	1	5	8.0	44.1	1.99	10953	10152	4834
Powder resin only								
Small squares	3	15	7.6	40.5	1.61	6774	5582	2658
Small triangles	1	3	3.8	42.1	1.78	9507	8298	3952
Large triangles	1	5	9.2	44.6	1.56	10545	8805	4193
Powder & liquid resin combined								
Small squares	5	25	7.7	40.6	1.68	7394	5582	2658
Small triangles	1	3	3.8	42.1	1.78	9507	8298	3952
Large triangles	2	10	8.6	44.4	1.77	10749	8805	4193
TOTAL MEANS								
	8	38	7.28	42.4	1.75	9221	7963	3792

<sup>a</sup> Values not adjusted for MC or density (note large differences)

<sup>b</sup> Test weight/test volume basis

<sup>c</sup> Adjusted for volume by  $MOR * (depth/12'')^{1/8}$ .

<sup>d</sup> Minimum, volume adjusted MOR / safety factor of 2.1

An analysis of variance was conducted on Powder & Liquid resin results showing:

**MOR (mean):** All three geometries differ significantly using Fisher's Protected LSD ( $\alpha=.05$ ) with large triangles giving the best results.

**MOE (mean):** No significant difference exists between geometries.

**Resin:** Liquid resin was found to give significantly higher values than powdered resin for both MOE and MOR.

## APPENDIX B

### Coding Used to Conduct Statistical Analyses in SAS

---

```
*3-way factorial using Weighted Least Squares;  
TITLE 'VARIANCE BY BILLET FOR FACTORIAL - WLS';  
PROC SORT; BY STRSIZE GEOMETRY LAPTYPE BILLETNO;  
PROC MEANS N MEAN VAR NOPRINT; BY STRSIZE GEOMETRY LAPTYPE BILLETNO;  
VAR MOEAPPADJ;  
OUTPUT OUT=VARBYBILLET VAR=VARIANCE;  
DATA MERGED;  
MERGE ALL VARBYBILLET; BY STRSIZE GEOMETRY LAPTYPE BILLETNO;  
DATA WLS;SET MERGED;  
TITLE 'MERGED DATA SET WITH VARIANCES & WEIGHTS - FACTORIAL';  
WT=1/VARIANCE;  
PROC GLM; CLASSES STRSIZE GEOMETRY LAPTYPE BILLETNO BEAMNO;  
TITLE 'ANOVA ON FACTORIAL WITH SUBSAMPLES AND WLS';  
WEIGHT WT;  
MODEL MOEAPPADJ=STRSIZE GEOMETRY LAPTYPE STRSIZE*GEOMETRY  
STRSIZE*LAPTYPE GEOMETRY*LAPTYPE STRSIZE*GEOMETRY*LAPTYPE  
BILLETNO*STRSIZE*GEOMETRY*LAPTYPE;  
test h=STRSIZE GEOMETRY LAPTYPE STRSIZE*GEOMETRY STRSIZE*LAPTYPE  
GEOMETRY*LAPTYPE STRSIZE*GEOMETRY*LAPTYPE  
e=billetno*strsize*geometry*laptype;  
LSMEANS STRSIZE GEOMETRY LAPTYPE;  
RUN;
```

---

---

```
*3-way factorial using Ordinary Least Squares;  
PROC GLM; CLASSES STRSIZE GEOMETRY LAPTYPE BILLETNO BEAMNO;  
TITLE 'ANOVA ON FACTORIAL WITH SUBSMAPLES';  
MODEL MOEAPPADJ=STRSIZE GEOMETRY LAPTYPE STRSIZE*GEOMETRY  
STRSIZE*LAPTYPE GEOMETRY*LAPTYPE STRSIZE*GEOMETRY*LAPTYPE  
BILLETNO*STRSIZE*GEOMETRY*LAPTYPE;  
test h=STRSIZE GEOMETRY LAPTYPE STRSIZE*GEOMETRY STRSIZE*LAPTYPE  
GEOMETRY*LAPTYPE STRSIZE*GEOMETRY*LAPTYPE  
e=billetno*strsize*geometry*laptype;  
MEANS STRSIZE GEOMETRY LAPTYPE STRSIZE*GEOMETRY STRSIZE*LAPTYPE  
GEOMETRY*LAPTYPE STRSIZE*GEOMETRY*LAPTYPE/TUKEY  
e=billetno*strsize*geometry*laptype;  
LSMEANS STRSIZE GEOMETRY LAPTYPE;
```

---

---

```

*2-way factorial (lapped billets only) using Ordinary Least Squares;
PROC GLM; CLASSES STRSIZE GEOMETRY BILLETNO BEAMNO;
TITLE 'ANOVA ON FACTORIAL WITH SUBSMAPLES';
MODEL MOEAPPADJ=STRSIZE GEOMETRY STRSIZE*GEOMETRY
BILLETNO*STRSIZE*GEOMETRY;
test h=STRSIZE GEOMETRY STRSIZE*GEOMETRY e=billetno*strsize*geometry;
MEANS STRSIZE GEOMETRY STRSIZE*GEOMETRY/TUKEY
e=billetno*strsize*geometry;
LSMEANS STRSIZE GEOMETRY;

```

---



---

```

*One-way with multiple comparisons;
DATA MULTCOMP; SET ALLBEAMS;
PROC GLM; CLASSES STRANDLAP BILLETNO BEAMNO;
MODEL MOEAPPADJ=STRANDLAP STRANDLAP*BILLETNO;
TEST h=STRANDLAP e=STRANDLAP*BILLETNO;
MEANS STRANDLAP/TUKEY LINES e=STRANDLAP*BILLETNO;
LSMEANS STRANDLAP;
OUTPUT OUT=NORMALITY PREDICTED=PRED RESIDUAL=RESID;
PROC UNIVARIATE PLOT NORMAL;
VAR RESID;
PROC PLOT; PLOT RESID*PRED='*' /VREF=0;
DATA LEVINES; SET NORMALITY;
ABSRESID=ABS(RESID);
PROC ANOVA; CLASS STRANDLAP BILLETNO;
MODEL ABSRESID=STRANDLAP BILLETNO STRANDLAP*BILLETNO;
RUN;

```

---

## APPENDIX C

### Two-Way Analyses by Lap Type

#### Non-lapped Beam $MOE_{app}$

Table C.1 – Factorial analysis for non-lapped  $MOE_{app}$

Source	DF	F Value	Prob > F	
Strand size	1	36.64	<0.0001	LG>SM
Geometry	1	3.57	0.0833	
Strand size * Geometry	1	4.50	0.0553	

Table C.2 – Mean separation for non-lapped  $MOE_{app}$

	Tukey Grouping *	Mean	N	TRT
	A	1,854,912	12	LT-NL
	A			
B	A	1,848,641	10	LS-NL
B				
B	C	1,751,253	12	SS-NL
	C			
	C	1,650,263	11	ST-NL

\*minimum significant difference = 103,490

#### Non-Lapped Beam MOR

Table C.3 – Factorial analysis for non-lapped MOR

Source	DF	F Value	Prob > F
Strand size	1	1.89	0.1942
Geometry	1	3.65	0.0802
Strand size * Geometry	1	0.81	0.3858

Table C.4 – Mean separation for non-lapped MOR

	Tukey Grouping *	Mean	N	TRT
	A	11044	11	ST-NL
	A			
	A	10915	12	LT-NL
	A			
	A	10788	12	SS-NL
	A			
	A	10294	10	LS-NL

\*minimum significant difference = 987

## Non-lapped Beam Shear Blocks

Table C.5 – Factorial analysis for non-lapped shear blocks

Source	DF	F Value	Prob > F
Strand size	1	0.68	0.4261
Geometry	1	3.11	0.1032
Strand size * Geometry	1	15.54	<b>0.0020</b>

Table C.6 – Mean separation for non-lapped shear blocks

Tukey Grouping *		Mean	N	TRT
A		1392	11	ST-NL
A				
A	B	1232	10	LS-NL
	B			
	B	1112	12	LT-NL
	B			
	B	1058	12	SS-NL

\*minimum significant difference = 236

## Lapped Beam MOE

Table C.7 – Factorial analysis for lapped  $MOE_{app}$

Source	DF	F Value	Prob > F	< >
Strand size	1	19.02	<b>0.0009</b>	<b>LG&gt;SM</b>
Geometry	1	2.30	0.1554	
Strand size * Geometry	1	0.19	0.6721	

Table C.8 – Mean separation for lapped  $MOE_{app}$

Tukey Grouping *		Mean	N	TRT
A		1,779,806	12	LS-L
A				
A		1,750,031	12	LT-L
A				
A	B	1,671,777	12	SS-L
	B			
	B	1,618,138	12	ST-L

\*minimum significant difference = 115,493

## Lapped Beam MOR

Table C.9 – Factorial analysis for lapped MOR

Source	DF	F Value	Prob > F
Strand size	1	2.90	0.1144
Geometry	1	1.27	0.2818
Strand size * Geometry	1	0.02	0.8852

Table C.10 – Mean separation for lapped MOR

Tukey Grouping *	Mean	N	TRT
A	8,999	12	ST-L
A			
A	8,699	12	SS-L
A			
A	8,523	12	LT-L
A			
A	8,134	12	LS-L

\*minimum significant difference = 1,284

## Lapped Beam Shear Blocks

Table C.11 – Factorial analysis for lapped shear blocks

Source	DF	F Value	Prob > F	< >
Strand size	1	0.65	0.4341	
Geometry	1	9.23	<b>0.0103</b>	<b>TRI&gt;SQ</b>
Strand size * Geometry	1	1.79	0.2056	

Table C.12 – Mean separation for lapped shear blocks

Tukey Grouping *	Mean	N	TRT
A	1,297	12	ST-L
A			
A B	1,151	12	LT-L
A B			
A B	1,035	12	LS-L
B			
B	999	12	SS-L

\*minimum significant difference = 286

## APPENDIX D

Marketing Concept for DeltaStrand Triangular Strand Lumber (TSL)

